

Rising Demand, Sinking Land

About How Groundwater Extraction For Drinking Water Affects Subsidence

O.F. Neijenhuis

Delft University of Technology

Cover photo: Subsiding peat meadow areas in the Netherlands (Antea Group, [2023](#)).

Rising Demand, Sinking Land

About How Groundwater Extraction For
Drinking Water Affects Subsidence

by

O.F. Neijenhuis

Born on 25 August 1999 in Zwolle, the Netherlands

In partial fulfilment of the requirements for the degree of

Master of Science
in Civil Engineering

at the Delft University of Technology,
to be defended publicly on Thursday 4 July 2024 at 03:00 PM.

Student number:	5617987	
Thesis duration:	11 September 2023 – 4 July 2024	
Committee:	Prof. Dr. Ir. F. C. (Femke) Vossepoel (chair),	TU Delft, CEG
	Dr. Ir. O. A. C. (Olivier) Hoes,	TU Delft, CEG
	Dr. Ir. F. (Rik) Bisschop,	Arcadis
	Ir. H. J. (Rianne) Boks,	Arcadis
	Ir. M. (Muriël) Houdé,	Vitens
	Dr. Ir. R. (Rogier) van der Velde,	Vitens

An electronic version of this thesis is available at <http://repository.tudelft.nl/>.



Preface

In front of you is my thesis 'Rising Demand, Sinking Land: *About How Groundwater Extraction For Drinking Water Affects Subsidence*'. This product is the final assignment of the Master Water Management at the Faculty of Civil Engineering of Delft University of Technology. Completing this thesis has been an incredible journey, and the six years at both TU Delft and UTwente have been enriching and fulfilling, providing me with unforgettable experiences and opportunities for both personal and professional growth. With pleasure I have researched this topic which I found to be very broad with many different disciplines involved. Finding subsidence-related articles in the newspapers during the time I have worked on my project has greatly encouraged me. With pleasure I have attended the Deltares iMOD Python user's day, National Subsidence Congress in Amsterdam, and the NWA-LOSS symposium in Utrecht. Subsidence is getting increasingly more attention and I believe that there is still much more to discover about the functionality, interaction, and modelling of different subsidence processes around the world.

In the past nine months, I have been conducting my research at Arcadis in cooperation with drinking water company Vitens. Firstly, thank you Muriël Houdé for this opportunity, for trusting in me and learning me how to "lean back". Also, I want to express my sincere gratitude to my daily supervisors, Rianne Boks and Rik Bisschop, for their supervision and support throughout the entire graduation period. They not only provided insightful feedback, but also motivated me to stay on track throughout the process. I am grateful for the many in-depth discussions we had. In addition to my external supervisors, I would like to thank Arcadis for their aid and, in particular, my colleagues in the "Water & Ruimte" and "Groundwater" departments for their help, friendliness and interest. My gratitude goes to SkyGeo for letting me use their Bodemdalingskaart tool, which helped me understand subsidence even more. Furthermore, I want to thank Henk Kooi and Gilles Erkens for their support from a subsidence expert view. In particular Henk, by learning me how to model in SUB-CR, despite it did not fully work out in the end. Also, my gratitude goes to Sofie ten Bosch for helping me bridge my knowledge gap in subsidence modelling. Finally, thank you Hans Mankor for the relevant data and intriguing discussion in the Province Hall of Utrecht.

From TU Delft, I am grateful for the guidance of Femke Vossepoel and Olivier Hoes as well. Besides valuable tips, discussions, and feedback, Femke and Olivier significantly improved the readability of this report, and their different backgrounds enriched the scientific content of my research. Also, I thank Maurits Ertsen for his insightful comments and in-depth discussions during our thesis progress meetings, which contributed to the scientific foundation of my research. Thanks to Mirte, Rodrigo, and Peer from the TU Writing Centre in organising the Thesis Boost days and the Technical Writing course, you have elevated my thesis writing to a new level.

Special thanks to Koen, Vittorio, Anja, and Max for proofreading my thesis and providing it with helpful feedback. A big thanks to my roommates from 't Duintje for their support during the most challenging parts of my thesis. Our cozy dinners together provided a much-needed break from work and kept me sane, this meant a lot to me. In addition, I cherish all the Dutch and foreign friends I have encountered during my student career, thank you for all the unforgettable moments together. Most importantly, my family has been a constant source of support and encouragement, celebrating milestones with me throughout my life and studies. Thank you Gardi, Harold, Oma Grada, Jil, and Deen for everything. Lastly, I want to thank Laura for always being there for me, planning fun activities together, and supporting me in everything I do.

Enjoy reading!

*'Unfortunately, soils are made by nature and not by man,
and the products of nature are always complex...'*

—Karl von Terzaghi

Den Haag, July 2024
Ole Neijenhuis

Abstract

Groundwater extraction could be a crucial driver of subsidence; a phenomenon that has had, and still has, implications for the landscape, infrastructure, and environment. Vitens, a Dutch drinking water company, expects an increase of 10% in drinking water demand in 2040 for the Netherlands. This may intensify Subsidence due to Groundwater Extraction (SGE) in the future. The objective of this research is to quantify the historical and future effects of groundwater extraction on subsidence at Vitens extraction site "Groenekan" in the Province of Utrecht.

In this thesis, a methodology is developed to assess whether Vitens can responsibly expand Groenekan groundwater extraction from 5.0 Mm³/yr to 10.0 Mm³/yr. The groundwater extraction is situated in a rural polder landscape where two subsidence-sensitive soil layers are present: a 1 m thick Holocene peat/clay top layer and a 12 m thick aquitard (Waalre clay) at a depth of -48 m NAP. Under this aquitard, Vitens currently extracts ~5.0 Mm³/yr of drinking water from the second aquifer. Next, a groundwater model is used to study the lowering of the groundwater level and hydraulic head due to the extraction. Subsequently, the effect of both lowerings has been quantified for four subsidence processes, 1) Biochemical Degradation of Organic Material (BDOM), 2) shrinkage, 3) consolidation, and 4) creep. Groundwater lowering affects all four processes, whereas head lowerings only affect consolidation and creep. Occurred subsidence from the start of the groundwater extraction and for eight future scenarios is calculated with the aid of the groundwater model output, analytical approaches and a 2D subsidence model. The cumulative subsidence of these four processes is labelled as SGE.

From 1961 to 2023, the groundwater level at Groenekan is lowered with 33 and 60 cm for 5.0 and 10.0 Mm³/yr extraction discharges respectively. In the second aquifer, hydraulic head lowerings of 1.5 to 2.9 m with a symmetrical influence circle are observed at Groenekan. In a radius of 500 m around Groenekan, significant groundwater level lowerings are found, which enforces compaction processes in the form of BDOM and shrinkage. For the period 1961 to 2023, assuming a 1 m thick clean peat Holocene top layer reveals ~16 cm of potential BDOM. However, potentially ~11 or ~18 cm of shrinkage would occur over the same period assuming a clean clay or organic clay Holocene soil type respectively.

Compression of the Holocene and Waalre layers due to consolidation and creep has contributed ~10 times less to SGE around Groenekan compared to compaction due to BDOM and shrinkage. Within a 500 m radius of Groenekan, SGE is noticeable; beyond that, SGE is negligible. The maximum total subsidence through compression is ~1.0 cm over a period of 62 years (from the start in 1961 to 2023). Generally, consolidation contributes 75% to the total subsidence due to compression, whereas creep is responsible for 25% of the compression. Sensitivity analyses reveal that the Holocene soil type and the thickness of the soft soils are the most sensitive parameters in calculating the final subsidence. Clean peat soil gives a high potential subsidence rate, whereas sand soils hardly subside. Variations in groundwater level and head lowerings are found to be least sensitive. Within the Groenekan system, the 1 metre Holocene thickness is the limiting factor in the groundwater level lowering, since no additional subsidence effects are found if the groundwater level drops below the Holocene layer.

The future scenario of 10.0 Mm³/yr + an extreme climate shows ~1.2 cm of consolidation and creep in the Holocene and Waalre layers over the period 1961 to 2100 (139 years). The base scenario of 5.0 Mm³/yr gives of ~0.9 cm of subsidence, which results in ~0.3 cm of additional subsidence. This extra subsidence value is negligible over a period of 139 years compared to other locations in the Netherlands with dozens of centimeters of subsidence. Though, BDOM and shrinkage can potentially cause centimetres of subsidence in the Holocene on the long-term due to groundwater level lowering. In conclusion, expansion of Groenekan from 5.0 to 10.0 Mm³/yr is considered to be responsible for a subsidence perspective as long as BDOM and shrinkage are exercised with extreme caution. Future studies on the effects of extended droughts and the surface water system on the groundwater level are suggested to better distinguish the total subsidence from SGE. Lastly, it is recommended to Vitens to extract groundwater from deep, confined aquifers with a sandy top layer for maximal SGE mitigation.

Keywords: *subsidence, settlement, groundwater extraction, drinking water, Groenekan, Province of Utrecht, Vitens, modelling, D-Settlement, MODFLOW, AZURE, iMOD, GIS.*

Samenvatting

Grondwaterwinning kan een cruciale factor zijn voor bodemdaling; een fenomeen dat gevolgen heeft gehad, en nog steeds heeft, voor het landschap, de infrastructuur en het milieu. Nederlands drinkwaterbedrijf Vitens verwacht een toename van 10% in drinkwatervraag in 2040 voor Nederland. Dit kan de Bodemdaling door Grondwateronttrekking (BGO) in de toekomst intensiveren. Het doel van dit onderzoek is om de historische en toekomstige effecten van grondwaterwinning op bodemdaling bij de Vitens grondwaterwinning "Groenekan" in de provincie Utrecht te kwantificeren.

In deze thesis wordt een methodologie ontwikkeld om te beoordelen of Vitens op een verantwoorde wijze de grondwaterwinning in Groenekan kan uitbreiden van $5.0 \text{ Mm}^3/\text{jr}$ naar $10.0 \text{ Mm}^3/\text{jr}$. De grondwaterwinning is gesitueerd in een landelijk polderlandschap waar twee grondlagen aanwezig zijn die gevoelig zijn voor bodemdaling: een 1 m dikke Holocene veen/klei toplaag en een 12 m dikke scheidende laag (Waalre klei) op een diepte van -48 m NAP. Onder deze scheidende laag wint Vitens momenteel $\sim 5.0 \text{ Mm}^3/\text{jr}$ aan drinkwater uit het tweede watervoerende pakket. Vervolgens wordt een grondwatermodel gebruikt om grondwaterpeil- en stijghoogteverlagingen te bestuderen als gevolg van de winning. Vervolgens zijn de effecten van beide verlagingen gekwantificeerd voor vier bodemdalingsprocessen: 1) oxidatie, 2) krimp, 3) consolidatie en 4) kruip. Grondwaterverlaging beïnvloedt alle vier de processen, terwijl stijghoogteverlagingen alleen consolidatie en kruip beïnvloeden. De opgetreden bodemdaling sinds de start van de grondwaterwinning en voor acht toekomstscenario's wordt berekend met behulp van de grondwatermodel output, analytische benaderingen en een 2D bodemdalingsmodel. De cumulatieve bodemdaling van deze vier processen wordt aangeduid als BGO.

Van 1961 tot 2023 is het grondwaterpeil bij Groenekan verlaagd met 33 en 60 cm voor debieten van respectievelijk 5.0 en $10.0 \text{ Mm}^3/\text{jr}$. In de tweede aquifer worden stijghoogteverlagingen van 1.5 tot 2.9 m met een symmetrische invloedscirkel waargenomen bij Groenekan. Binnen een straal van 500 m rond Groenekan worden significante grondwaterpeilverlagingen gevonden, die compactieprocessen zoals oxidatie en krimp versterken. Voor de periode 1961 tot 2023, leidt een aanname van een 1 m dikke schone veen Holocene toplaag tot ongeveer 16 cm oxidatie. Echter, mogelijk zou ~ 11 tot 18 cm krimp optreden in die periode, uitgaande van een Holocene bodemtype van schone of organische klei.

Compressie van de Holocene en Waalre lagen als gevolg van consolidatie en kruip heeft ~ 10 keer minder bijgedragen aan BGO rond Groenekan vergeleken met de compactie door oxidatie en krimp. Binnen een straal van 500 m rond Groenekan is BGO merkbaar; daarbuiten is BGO verwaarloosbaar. De maximale totale bodemdaling door compressie is ~ 1.0 cm over een periode van 62 jaar (van de start in 1961 tot 2023). Over het algemeen draagt consolidatie 75% bij aan de totale bodemdaling door compressie en kruip 25%. Gevoeligheidsanalyses tonen aan dat het Holocene bodemtype en de dikte van de slappe bodems de meest gevoelige parameters zijn bij het berekenen van de uiteindelijke bodemdaling. Schone veengrond geeft een hoge potentiële bodemdaling, terwijl zandgronden nauwelijks dalen. Variaties in grondwaterpeil en drukverlagingen blijken het minst gevoelig te zijn. Binnen het Groenekan systeem is de 1 meter Holocene dikte de beperkende factor in de grondwaterpeilverlaging, aangezien er geen extra bodemdalingseffecten worden gevonden als het grondwaterpeil onder het Holocene laag daalt.

Het toekomstscenario van $10.0 \text{ Mm}^3/\text{jr}$ + extreem klimaat toont ~ 1.2 cm consolidatie en kruip in het Holocene en in Waalre in de periode 1961 tot 2100 (139 jaar). Het basisscenario van $5.0 \text{ Mm}^3/\text{jr}$ geeft ~ 0.9 cm bodemdaling, wat resulteert in ~ 0.3 cm extra bodemdaling. Deze extra bodemdaling is verwaarloosbaar over 139 jaar vergeleken met andere locaties in Nederland met tientallen centimeters bodemdaling. Echter, oxidatie en krimp kunnen op lange termijn centimeters bodemdaling veroorzaken in het Holocene door grondwaterpeilverlaging. Concluderend wordt de uitbreiding van Groenekan van 5.0 naar $10.0 \text{ Mm}^3/\text{jr}$ als verantwoord beschouwd vanuit een bodemdalingsperspectief, mits oxidatie en krimp met zorg worden behandeld. Toekomstige studies naar de effecten van droogtes en het oppervlaktewatersysteem op het grondwaterpeil worden voorgesteld om de totale bodemdaling beter te kunnen onderscheiden van BGO. Ten slotte wordt Vitens aanbevolen om grondwater te winnen uit diepe, afgesloten watervoerende pakketten met een zand toplaag voor maximale mitigatie van BGO.

Trefwoorden: bodemdaling, zetting, grondwateronttrekking, drinkwater, Groenekan, Provincie Utrecht, Vitens, modelleren, D-Settlement, MODFLOW, AZURE, iMOD, GIS.

Contents

Preface	ii
Abstract	iii
Samenvatting	iv
List of Figures	ix
List of Tables	xi
Nomenclature	xii
List of Acronyms	xii
List of Definitions	xiii
List of Symbols	xv
1 Introduction	1
1.1 Problem Statement	2
1.2 Knowledge Gap	2
1.3 Objectives & Questions	3
1.4 Approach	3
1.5 Thesis Structure	4
2 Groundwater Extraction & Subsidence	5
2.1 Analytical Groundwater Flow Approaches	5
2.2 Subsidence Processes	6
2.3 Subsidence Drivers	11
2.4 SGE Literature Case Studies	13
2.5 Consolidation & Creep Calculations	14
3 Groenekan	17
3.1 System Analysis	17
3.2 Geohydrological Profile	18
3.3 Historical Groundwater Extraction Discharge	20
3.4 Surface Water System Polder Maartensdijk	21
3.5 Hypotheses	22
4 Data & Models	23
4.1 Bodemdalingskaart Measured Subsidence Data	23
4.2 AZURE Groundwater Model	24
4.3 Analytical BDOM & Shrinkage Calculations	24
4.4 D-Settlement Subsidence Model	25
4.5 Future Scenarios Groenekan	26
5 Results	28
5.1 Bodemdalingskaart	28
5.2 Groundwater Level & Hydraulic Head	29
5.3 Analytical BDOM & Shrinkage	30
5.4 Consolidation & Creep in Holocene and Waalre Layers	31
5.5 Modelled SGE & Bodemdalingskaart Validation	35
5.6 Future Scenarios	36
6 Discussion	38
6.1 Limitations of Methodologies	38
6.2 Interpretation of Results	40

7	Conclusions & Recommendations	43
7.1	Conclusions	43
7.2	Recommendations	45
	References	47
	Appendices	51
A	Background Figures & Maps	54
A.1	Explainer Maps	54
A.2	Groenekan Figures	56
B	Additional Theory	61
B.1	Stationary vs. Transient Groundwater Flow & Models	61
B.2	Tertiary Compression	62
B.3	Measuring Subsidence	62
C	Selection Procedures	64
C.1	Location Selection	64
C.2	Groundwater Model Selection	64
C.3	Subsidence Model Selection	65
D	Pastas Time Series Model Analysis	68
D.1	Piezometer Hydraulic Head Data	68
D.2	Methodology Piezometer Time Series Models	69
D.3	Results Piezometer Time Series Models	70
E	Other Historical Subsidence Data Analyses	73
E.1	Meetkundige Dienst vs. Actueel Hoogtebestand Nederland	73
E.2	Historical Peat Oxidation in Province of Utrecht	76
F	AZURE	78
F.1	AZURE Packages & Layers	78
F.2	AZURE Assumptions & Conditions	79
F.3	AZURE Result Tables	79
F.4	AZURE Maps	80
G	BDOM & Shrinkage	82
G.1	BDOM & Shrinkage Parameterisation & Assumptions	82
G.2	BDOM & Shrinkage Result Tables	82
H	D-Settlement	83
H.1	D-Settlement Structure of Western and Eastern Models	83
H.2	D-Settlement Layer Parameterisation	84
H.3	D-Settlement Base Scenario Assumptions & Conditions	85
H.4	Consolidation & Creep in Holocene and Waalre Result Tables	86
I	Python Scripts	88
I.1	Analytical Groundwater Flow Calculations: Glee & Hantush	88
I.2	Aerobic BDOM Calculation	90
I.3	Shrinkage Calculation	92

List of Figures

1.1	Expected subsidence [cm] in the Netherlands for 2100 with a high emission climate scenario (Erkens et al., 2021).	1
1.2	Schematic soil cross-section of (un)confined aquifers and an aquitard. A: No extraction equilibrium. B: Disruption of the equilibrium due to groundwater extraction causing compression of soft soils, resulting in subsidence (Guzy, 2020).	2
1.3	Thesis structure flowchart. Grey box illustrates the used theoretical frameworks. The steps in the orange and yellow boxes belong to the methodology and results respectively. The validation method of the results is given in blue. Lastly, the answers to sub-questions 1 and 2 are given in turquoise, sub-questions 3, 4, and 5 in green, and sub-questions 6 and 7 in red.	4
2.1	Analytical calculation of head lowering over distance r for Groenekan with $5.0 \text{ Mm}^3/\text{yr}$ extraction. Transient time steps in various colors (Hantush & Jacob, 1955) and stationary lowering in navy blue (De Glee, 1930).	6
2.2	Subsidence processes (Van Asselen et al., 2019). Research focuses on cyan sub-processes.	6
2.3	Settlement components over time curve.	7
2.4	Three stages of shrinkage (Bronswijk & Evers-Vermeer, 1987); regular, residual, and zero.	9
2.5	Subsidence rate [cm/10yrs] due to geological processes in the Netherlands from 1926 to 1987 (Kooi et al., 1998), with ten subsidence or uplift classes. Groenekan = cyan dot.	10
2.6	Subsidence drivers and processes (Minderhoud et al., 2015). Research focuses on drivers within cyan frame.	11
2.7	Four step cycle of 1) initial water level, 2) lower Target Level Decision, 3a) consolidation, 3b) drying and aeration of peat, 3c) oxidation of organic matter, 4) subsidence (Dieudonné, 2023).	12
2.8	SGE visualisation (USGS, 2018a).	12
2.9	9 metres of subsidence in California (Ireland, 2018).	13
2.10	Difference between linear and natural strain (Den Haan, 2007).	15
2.11	Comparison of effective stress diagrams in (a) Consolidation model (CM) and (b) Iso-tach model (IM).	15
3.1	Study area map with Vitens groundwater extractions and surface level height [m NAP] (Provincie Utrecht, 2023).	17
3.2	REGIS.II geohydrological profile of Groenekan from Bethunepolder in the north-west to Utrechtse Heuvelrug in the east (BRO, 2023b). It distinguishes three different aquifers and the Waalre clay aquitard (Wak1) by cyan horizontal lines, the extractions are shown by filled blue arrows and the major groundwater flows by blue dashed arrows.	18
3.3	GeoTOP geohydrological profile of top layer around Groenekan from Bethunepolder in the north-west to Utrechtse Heuvelrug in the east (BRO, 2023a). Between +2 and -3 m NAP, peat, clay, and sand are coloured in brown, green, and yellow respectively.	19
3.4	Resistance [days] of Waalre clay aquitard (Wak1) around Groenekan extraction (TNO, 2023a).	19
3.5	Groundwater streamline analysis of two different extraction scenarios for Groenekan (Arcadis, 2023). Left: $0.0 \text{ Mm}^3/\text{yr}$. Right: $5.0 \text{ Mm}^3/\text{yr}$. Differences highlighted in cyan circles.	20
3.6	Annual extraction and permitted discharges of location Groenekan (Vitens, 2023).	20
5.1	Distribution histogram of subsidence or uplift rates around Groenekan, divided over 19 bins. 0-subsidence line is plotted in red, mean μ in blue and the standard deviation σ in grey.	28
5.2	Subsidence and uplift data points [cm/10yrs] within three circles with 1, 2, and 3 km radii (SkyGeo, 2023).	28

5.3	5.0 vs. 0.0 Mm ³ /yr extraction: Differences in head for the GLG in AZURE model layers 1, 6, and 11.	29
5.4	Head lowerings in four geohydrological layers. Piezometer TSMs (x-axis) plotted against AZURE results (y-axis) for scenario 5.0 Mm ³ /yr (Artesia, 2023).	30
5.5	Aerobic BDOM graphs of Holocene peat top layer with four distances to Groenekan for period 1961 to 2100. The year 2023 is shown with a grey dotted vertical line and future BDOM is plotted in dashes from 2023 onwards.	30
5.6	Shrinkage graphs of the Holocene top layer with four distances to Groenekan for period 1961 to 2023.	31
5.7	Settlement-Time linear graphs: Base scenario west of Groenekan over the period 1961 to 2023. The six coloured graphs represent a different distance to Groenekan.	32
5.8	Settlement-Time linear graphs: Base scenario east of Groenekan over the period 1961 to 2023. The six coloured graphs represent a different distance to Groenekan.	32
5.9	Settlement-Time linear graphs: Sensitivity analysis groundwater level and head lowerings for Groenekan base scenario (grey dashed). The ten coloured graphs represent different lowering variations.	33
5.10	Settlement-Time linear graphs: Sensitivity analysis layer thickness for Groenekan base scenario (grey dashed). The eight coloured graphs represent different thickness variations for the Holocene (H) and Waalre (W) layers.	34
5.11	Settlement-Time linear graphs: Sensitivity analysis Holocene soil type for Groenekan base scenario (grey dashed), including 0.16 cm Waalre settlement. The five coloured graphs represent a different soil type for the Holocene top layer.	34
5.12	Results overview for base scenario of Groenekan over the period 2017 to 2022 on a 10 km west to east cross-section (bottom left). A) Schematic geohydrological profile of Groenekan including groundwater level and head lowerings. Note: the y-axis (m NAP) is not to scale. B) Subsidence rate [cm/10yrs] around Groenekan. All modelled subsidence processes are presented as cumulative plots and the measured Bodemdalingskaart data is given.	35
5.13	Settlement-Time linear graphs: Future scenarios at Groenekan over the period 1961 to 2100 (139 years or 50,000 days). The eight coloured graphs each represent a different future scenario from 2023 (day 23,000) onwards. The grey graph is the base scenario which is plotted until 2100 as a reference scenario.	37
A.1	Drinking water companies and their service area in the Netherlands (Aqua Assistance, 2018).	54
A.2	Global extent of subsidence due to groundwater extraction (Dinar et al., 2019, p5).	55
A.3	Isohypse map around extraction Groenekan (Geologische Dienst Nederland, 2023). Groenekan groundwater level is between -0.5 and 0.0 m NAP.	56
A.4	Measured groundwater level at Groenekan in piezometer B31H0794-001 (Geologische Dienst Nederland, 2023). GXG is -0.22 m NAP and GLG is -0.30 m NAP from 2012 to 2019.	56
A.5	Land use (BBG) around extraction Groenekan (CBS, 2017).	57
A.6	Ground drill tests until -120m NAP in a 1km radius around Groenekan extraction (TNO, 2023a).	57
A.7	Cone resistances from two independent CPT tests in Utrecht (TNO, 2023b). Holocene top layer is located from 0 to -1 m NAP. Waalre clay is located from -48 to -60 m NAP. Both layers are highlighted with pink and red circles respectively.	58
A.8	Resistance [days] of Sterksel clay aquitard (STk1) around Groenekan extraction (TNO, 2023a).	59
A.9	Analytical calculation of head lowering over distance r for Groenekan with 7.5 Mm ³ /yr extraction. Transient time steps in various colors (Hantush & Jacob, 1955) and stationary lowering in navy blue (De Glee, 1930).	59
A.10	Analytical calculation of head lowering over distance r for Groenekan with 10.0 Mm ³ /yr extraction. Transient time steps in various colors (Hantush & Jacob, 1955) and stationary lowering in navy blue (De Glee, 1930).	60
B.1	Time vs. strain plots, including tertiary compression (Edil & Dhowian, 1979)	62

B.2	Extensometer system with three anchor levels (Van Asselen et al., 2020).	62
B.3	Representation of a setup with seven measurement plates (Van Asselen et al., 2019).	63
B.4	InSAR measurements before and after subsidence, extra phase signal in red (SkyGeo, 2023).	63
C.1	AZURE model boundaries (H2O Waternetwerk, 2014).	65
C.2	(a) TLS. (b) Schematisation of a voxel stack for an individual cell. (c) Time discretisation through stress periods.	66
D.1	Daily extraction discharge per location (Vitens, 2023).	68
D.2	Locations of considered piezometers (grey), Vitens' drinking water extractions (blue), and measuring stations for precipitation (green) and evaporation (orange) (Artesia, 2023).	69
D.3	Time series model results for piezometer B32C0003-001 from 1968 till 2005 (Artesia, 2023).	71
D.4	The estimated head lowering due to Groenekan extraction of twelve Pastas time series models (Artesia, 2023). The size of the dots on the map represents the depth of the filter.	72
E.1	Distribution histogram of subsidence or uplift rates around Groenekan, divided over 17 bins. 0-subsidence line is plotted in red, mean μ in blue and the standard deviation σ in grey.	73
E.2	Subsidence or uplift data points [mm/yr] obtained by comparing MD with AHN4 data points around Groenekan and Bethunepolder from 1954 to 2020 (AHN, 2023; Mankor, 2023).	74
E.3	Subsidence or uplift data points [mm/yr] within three circles with 1, 2, and 3 km radii (AHN, 2023; Mankor, 2023).	74
E.4	Results overview for base scenario of Groenekan over the period 1961 to 2023 with a 2 km west to east cross-section.	75
E.5	Vulnerability to peat oxidation around Groenekan extraction (Provincie Utrecht, 2008).	76
E.6	Historical peat oxidation around Groenekan extraction (Provincie Utrecht, 2022b).	77
E.7	Historical peat oxidation around Groenekan extraction vs. AZURE 5.0 Mm ³ /yr in L1 (phreatic) (Provincie Utrecht, 2022b).	77
F.1	7.5 vs. 5.0 Mm ³ /yr extraction: Differences in head for the GLG & GHG in AZURE model layers 1, 6, and 11.	80
F.2	10.0 vs. 5.0 Mm ³ /yr extraction: Differences in head for the GLG & GHG in AZURE model layers 1, 6, and 11.	81
H.1	Visualisation of the westward D-Settlement model structure.	83
H.2	Visualisation of the eastward D-Settlement model structure.	83

List of Tables

2.1	NEN-Bjerrum model symbols in Roman and Greek alphabetical order, including units and descriptions.	16
3.1	Five historical “Waterstaatskaarten” and their corresponding target level decisions in summer (SL) and winter (WL), plus the incremental and total summer level TLD decrease (Rijkswaterstaat, 2023a).	21
4.1	Estimated values for the parameters of the BDOM and shrinkage equations for peat, organic clay, and clean clay (Fokker et al., 2019). Number in the brackets is the standard deviation in units of the last digit.	25
4.2	Fifteen layer D-Settlement model structure for base scenario Groenekan extraction. Including soil type, depth in NAP and geohydrology.	25
4.3	KNMI (2023a) HD and LW data for the Netherlands in the year 2100 compared to the climatology of 1991 to 2020.	26
5.1	Bodemdalingskaart data analysis around Groenekan (GK) in four areas increasing in size.	29
5.2	Measured Bodemdalingsskaart (BDK) subsidence rate vs. SGE results west (W) and (E) of Groenekan (GK) for period 2017 to 2022 in [cm/10yrs]. One column excluding and one including BDOM.	36
A.1	REGIS.II soil formation and geohydrology at Groenekan extraction (TNO, 2023a). . . .	58
C.1	Sensitivity to subsidence, expansion plans, and model availability per considered extraction location in the Provinces of Utrecht and Flevoland in alphabetical order. Chosen location Groenekan in cyan.	64
C.2	Overview of software packages used in the Netherlands to predict shallow subsidence through compression, oxidation, and/or shrinkage (Van Asselen et al., 2019).	66
D.1	Results of evaluation criteria for piezometer time series models (Artesia, 2023).	70
E.1	MD vs. AHN4 data analysis on four different distances from Groenekan (GK) extraction.	75
F.1	Active packages for each layer in the AZURE model.	78
F.2	REGIS II.2 layers linked to formations, soil types, and AZURE model layers (Arcadis, 2019; BRO, 2023b).	78
F.3	AZURE groundwater level and head lowerings [m] (drawdown cones) in the phreatic aquifer (Holocene) and second aquifer (Waalre) for six westward distances to Groenekan and three different extraction scenarios.	79
F.4	AZURE groundwater level and head lowerings [m] (drawdown cones) in the phreatic aquifer (Holocene) and second aquifer (Waalre) for six eastward distances to Groenekan and three different extraction scenarios.	79
G.1	Aerobic BDOM of clean peat results west (W) and (E) of Groenekan (GK) for periods 1961 to 2023 and 1961 to 2100.	82
G.2	Clean clay and organic clay shrinkage results west (W) and (E) of Groenekan (GK) for period 1961 to 2023.	82
H.1	D-Settlement model parameter values for the four soil layers in base scenario. (U) = undrained, (D) = drained.	84
H.2	Holocene top layer NEN-Bjerrum isotach parameter values for clay soil types (NEN, 2017).	84
H.3	Waalre aquitard NEN-Bjerrum isotach parameter values for loam and clay soil types (NEN, 2017).	85

H.4	Settlement (S) results: Base scenario over western distance to Groenekan (GK) in period 1961 to 2023.	86
H.5	Settlement (S) results: Base scenario over eastern distance to Groenekan (GK) in period 1961 to 2023.	86
H.6	Settlement (S) results of sensitivity analysis: Groundwater level (GWL) and head lowerings at Groenekan in period 1961 to 2023. Base scenario highlighted in cyan and a settlement difference (ΔS) in percentages is given.	86
H.7	Settlement (S) results of sensitivity analysis: Holocene (H) and Waalre (W) layer thicknesses at Groenekan in period 1961 to 2023. Base scenario highlighted in cyan and a settlement difference (ΔS) in percentages is given.	87
H.8	Settlement (S) results of sensitivity analysis: Five different Holocene soil types at Groenekan in period 1961 to 2023. The Holocene settlement excludes 0.16 cm of Waalre settlement. Base scenario highlighted in cyan and a settlement difference (ΔS) in percentages is given.	87
H.9	Settlement (S) results: Eight future scenarios at Groenekan (GK) in period 1961 to 2100. Base scenario is highlighted in cyan as a reference and a settlement difference (ΔS) in percentages is given.	87

Nomenclature

List of Acronyms

List of acronyms in alphabetical order, including meaning in English and, if required, in Dutch. The page number is the in-text location where the acronym is first mentioned.

a,b,c	a,b,c isotach model	15
AGV	Waterboard "Amstel, Gooi & Vecht"	17
AHN	"Actueel Hoogtebestand Nederland" Current Altitude the Netherlands	3
AZURE	"Actueel modelinstrumentarium voor de Zuiderzee Regio" Current groundwater modelling tools for the Dutch South Sea Region	3
BDOM	Biochemical Degradation of Organic Material Biochemische afbraak van organisch materiaal	iii
BROloket	"Basis Registratie Ondergrond loket" Basic Registration Subsurface	3
CM	Consolidation Model	14
CPT	Cone Penetration Test Geotechnisch sondeonderzoek	16
DINOloket	"Data en Informatie van de Nederlandse Ondergrond loket" Data and Information of Dutch Subsurface	3
D-Settlement	Deltares Settlement Subsidence Model	4
GIS	Geographic Information Systems	3
GHG	"Gemiddeld Hoogste Grondwaterstand" Average High Groundwater Level	24
GLG	"Gemiddeld Laagste Grondwaterstand" Average Low Groundwater Level	24
GVG	"Gemiddelde Voorjaars Grondwaterstand" Average Spring Groundwater Level	61
GXG	"Gemiddelde Grondwaterstand" Average Groundwater Level	61
HD	High emissions & Desiccation Hoge emissie & verdroging klimaatscenario	26
HDSR	Waterboard "Hoogheemraadschap De Stichtse Rijnlanden"	17
iMOD	Interactive Model for Dewatering and Groundwater Management	3
IM	Isotach Model	14
InSAR	Interferometric Synthetic Aperture Radar	13
KNMI	"Koninklijk Nederlands Meteorologisch Instituut" Royal Dutch Meteorological Institute	4
LHM	"Landelijk Hydrologisch Model" Dutch National Hydrological Model	64
LW	Low emissions & Wetter Lage emissie & vernatting klimaatscenario	26
MD	"Meetkundige Dienst" Dutch Survey Department	23
NAP	"Normaal Amsterdams Peil" Normal Amsterdam Level	1
NEN-Bjerrum	NEN-Bjerrum isotach model	15
OCR	Over-Consolidation Ratio Over-consolidatie Ratio	16
SGE	Subsidence due to Groundwater Extraction Bodemdaling veroorzaakt door grondwateronttrekking	iii
TLD	Target Level Decision Peilbesluit	3
TLS	Target Level Section Peilvak	12
TSM	Time Series Model Tijdreeksmodel	24
V&V	Waterboard "Vallei & Veluwe"	17

List of Definitions

Crucial definitions used in this thesis are summed in alphabetical order:

Aquifer (NL: *watervoerend pakket*): Aquifers are subsurface layers, usually consisting of sand, containing water which can be extracted through a well. Aquifers can either be confined or unconfined. A confined aquifer, also known as an artesian aquifer, is an aquifer that is bounded above and below by impermeable layers (aquitards), restricting the movement of water into or out of the aquifer. Unconfined, also known as a phreatic aquifer, is an aquifer where the water table (the upper surface of the saturated zone) is free to rise and fall.

Aquitard (NL: *scheidende laag*): Aquitards (or leaky/semi-confining layers) are impermeable or poorly permeable layers (usually clay or peat), present above or below an aquifer.

Biochemical degradation of organic material: Or "*Oxidation*" is a process in which peat undergoes a series of reactions when exposed to oxygen. This process leads to the breakdown of the organic material within the peat and the release of carbon dioxide (CO₂) and other by-products into the atmosphere. Peat oxidation is a natural process, but can be accelerated by human activities, such as drainage or peat extraction.

Compression (NL: *samendrukking*): The process of reduction of thickness of a ground layer related to the state of (vertical) effective stress experienced by that layer (Kooi et al., 2018). Compression is mainly caused by external loading. Creep is also considered to give rise to compression. Negative compression is usually referred to as expansion or swelling.

Consolidation (NL: *consolidatie*): Development of the compression of an aquitard after a "loading" event. Loading can either refer to application of a weight, or reduction of the pore pressure near the top and/or bottom of the layer (Kooi et al., 2018). The consolidation rate depends on the rate at which the pore water can drain to the top and/or bottom of the layer.

Creep (NL: *kruip*): Slow soil volume changes occurring on a longer time scale than consolidation, irrespective of the effective stress on the soil particles.

Drawdown (NL: *verlagingskegel*): In geohydrology, drawdown is the reduction in groundwater level or hydraulic head observed around a well in an aquifer, typically due to groundwater extraction. Subsequently, the "cone of depression" is the term used to describe the shape of the water table or head surface around a well in an aquifer.

D-Settlement: D-Settlement is a modelling tool for predicting soil settlements by external loading. It accurately models and quickly determines the direct settlement, consolidation and creep along verticals in a two-dimensional geometry.

Gully (NL: *geul*): An opening or interruption of the aquitard layers, causing the deeper aquifers to connect with the phreatic aquifer and possibly exchange groundwater.

Hydraulic head (NL: *stijghoogte*): The potential level of the groundwater table, measured from a certain level (e.g. NAP) in aquifer or aquitard.

Isostasy: Or *equal standstill* is the state of gravitational equilibrium between Earth's crust (or lithosphere) and mantle such that the crust 'floats' at an elevation that depends on its thickness and density.

Klink: The compression of soil by its own weight. The Dutch geotechnical definition of *klink* is used in this study, in contrast to the definition from the perspective of soil science, where it is used to define compression as a result of lowering the groundwater level due to shrinkage and oxidation and a loss of buoyancy that causes an additional load (Zuur, 1958).

MODFLOW (MF): USGS's Modular Finite-Difference Groundwater Flow Model is the modular hydrologic model and is considered an international standard for simulating and predicting groundwater conditions & interactions between groundwater and surface water.

iMOD: Deltares' iMOD (Interactive Model for Dewatering and Groundwater Management) is a fast and dedicated graphical user interface for groundwater model building and results analysis. Also, iMOD supports structured calculations with MF. It can be coupled with the unsaturated zone model MetaSWAP.

Organic Soil: A soil with an organic matter content greater than 20 m% (ISO, 2019).

Peat (NL: *veen*): A soil with an organic matter content greater than 75 m% (ISO, 2019).

Piezometer (NL: *peilbuis*): A device used to measure the pressure of groundwater at a specific point in the subsurface. It is designed to monitor the hydraulic head in an observation well, extraction, or borehole.

Recharge (NL: *grondwateraanvulling*): Recharge is a hydrological process in which water moves downward from surface water to groundwater. Recharge is the primary method through which water enters and replenishes an aquifer.

Seepage (NL: *kwel/wegzijging*): Flow of water through soils. Seepage occurs when there is a difference in water level or hydraulic head between two locations. Groundwater will flow from the location with a high head to a low head.

Seeps (NL: *wellen*): Locations where water, usually groundwater, reaches the earth's surface from an underground aquifer. This typically happens just behind the dikes at a river or in Dutch polders.

Settlement (NL: *zetting*): Subsidence caused by external stresses, such as the weight of a loading component, which induces compression of the subsoil. It should be noted that settlement refers to the vertical downward movement of the original ground surface level, also when the loading component is an embankment.

Shrinkage (NL: *krimp*): Compaction of the soil due to loss of moisture or water content.

Subsidence (NL: *bodemdaling*): The surface level, or a level in the subsurface, sinks in relation to a reference plane. Subsidence is caused by different processes (Section 2.2).

Swelling/uplift (NL: *bodemstijging/opbarsting/opzwellen*): The vertical upward movement of a point at surface level, compared to a defined date in the past.

Tectonics: Processes which have resulted in the structure and properties of the Earth's crust and its evolution through time.

List of Symbols

List of symbols in Roman and Greek alphabetical order, including unit and description in English and Dutch. Several symbols have a dimensionless unit and some an undefined unit, which differs per equation or circumstance, such as the hydraulic conductivity (length over time) and (specific) discharge (cubic length over time).

Symbol	Unit	Description	Beschrijving
c	[T]	Hydraulic resistance	Hydraulische weerstand
c_v	[m ² /s]	Consolidation coefficient	Consolidatiecoëfficiënt
E	[mm]	Evapotranspiration	Evapotranspiratie
e	[-]	Void ratio	Poriëngetal
g	9.81 ¹ [m ² s ⁻¹]	Gravitational acceleration	Valversnelling
H	[m]	Hydraulic head	Stijghoogte
k	[L/T]	Hydraulic conductivity	Doorlatendheid
m_v	[m ² kN ⁻¹]	Compressibility coefficient	Compressiecoëfficiënt
n	[-]	Porosity of the soil	Porositeit van de grond
OCR	[-]	Overconsolidation ratio	Overconsolidatie ratio
P	[mm]	Precipitation	Neerslag
Q	[L ³ /T]	Discharge	Debiet
p	[kN m ⁻²]	Pressure	Druk
R	[L/T]	Recharge/Percolation	Grondwateraanvulling
S	[cm]	Settlement/Subsidence	Zetting/Bodemdaling
S	[-]	Storativity	Bergingscoëfficiënt
t_{age}	[T]	Equivalent age	Equivalente ouderdom
u	[kN m ⁻²]	Pore water pressure	Waterspanning
W	[mm/d]	Well function Hantush	-
V	[m/s]	Velocity	Snelheid
z	[m]	Vertical elevation	Hoogte
γ	[kg m ⁻² s ⁻²]	Specific weight	Soortelijk gewicht
γ_w	[kg m ⁻² s ⁻²]	Specific weight pore water	Soortelijk gewicht poriewater
γ_s	[kg m ⁻² s ⁻²]	Saturated specific weight	Verzadigd soortelijk gewicht
κ	[m ²]	Intrinsic permeability	Intrinsieke permeabiliteit
ρ	[kg m ⁻³]	Density	Dichtheid
σ	[kg m ⁻¹ s ⁻²]	Total stress	Totale spanning
σ'	[kg m ⁻¹ s ⁻²]	Effective stress ²	Korrelspanning
σ'_p	[kg m ⁻¹ s ⁻²]	Pre-consolidation stress	Grensspanning
τ_0	[d]	Initial intrinsic time	Intrinsieke tijd

¹ Average gravitational acceleration in the Netherlands (Crombaghs et al., 2002)

² Terzaghi (1925)

Introduction

For centuries, the Netherlands has faced a persistent challenge: subsidence (NL: *bodemdaling*). Subsidence has serious implications for the Dutch landscape, infrastructure, and environment. For example, subsidence aggravates flood risk in low-lying areas (Fokker et al., 2018), it damages foundations, buildings and infrastructure (Hommes et al., 2023), it harms ecology (USGS, 2018a), and it enforces climate change by releasing greenhouse gasses (Temminck et al., 2023; Van den Akker et al., 2010).

Subsidence is the phenomenon by which the surface level, or a level in the subsurface, sinks in relation to a reference plane, for example the Dutch "Normaal Amsterdams Peil" (NAP) (Van Asselen et al., 2019). On the contrary, uplift or swelling of the soil (NL: *bodemstijging*) is the opposite (Ye et al., 2016). Locally, subsidence rates may differ significantly depending on, for example, the composition of the soil, the groundwater levels, the climate, and the land use (Van Asselen et al., 2020). Figure 1.1 displays a map of the expected subsidence [cm] in the Netherlands for the year 2100 with a high emission climate scenario (Erkens et al., 2021). It shows regions such as the Randstad, Flevoland, Friesland, and Groningen in purple with more than 60 cm of expected subsidence. This subsidence phenomenon is enforced by human activities such as construction work, artificially maintaining low groundwater levels, salt and gas mining, and groundwater extraction (Holzer & Galloway, 2005).

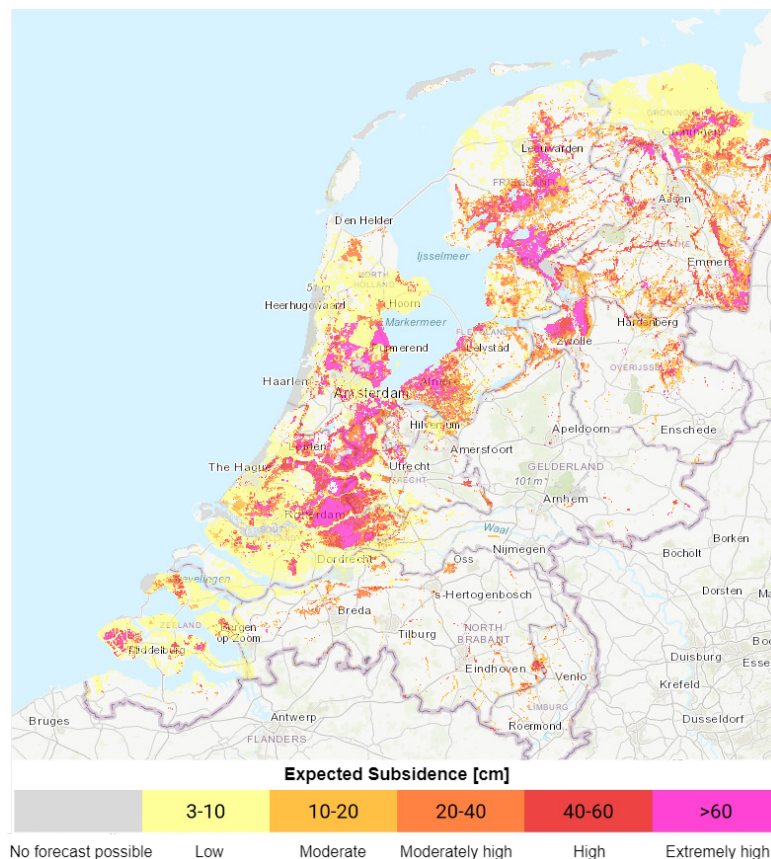


FIGURE 1.1: Expected subsidence [cm] in the Netherlands for 2100 with a high emission climate scenario (Erkens et al., 2021).

1.1. Problem Statement

One of the key drivers of subsidence is groundwater extraction (Syvitski et al., 2009). Besides the Netherlands, Dinar et al. (2019) shows that there are numerous global examples of groundwater extraction that have led to excessive settlement, damage, and flooding (Figure A.2). Vitens, a Dutch drinking water company, supplies water to 5.8 million customers in their service area (Figure A.1). They extract water from both groundwater and surface water sources and are one of the main drinking water producers in the Netherlands. Currently, Vitens faces an increase in water demand (RIVM, 2023) due to population growth, economic expansion, and increasing domestic and industrial water consumption. Additionally, hot and dry summers combined with extreme precipitation events have become a regular pattern in the Dutch climate in recent years (KNMI, 2023b). During these periods, lower surface water and groundwater levels occur more frequently while the evaporation and water demand is high. Consequently, Vitens is forced to increase their water production from groundwater sources to meet this demand. CBS (2023) shows that a 12% increase in total groundwater extraction by all Dutch drinking water companies is evident between 2014 and 2020 and Vitens expects the drinking water demand to increase with $\sim 10\%$ until 2040 (RIVM, 2023).

As a result, Subsidence due to Groundwater Extraction (SGE) has most likely played a role in historical subsidence and may intensify in the future if extractions are expanded. Figure 1.2 schematically explains SGE by comparing a “no extraction” equilibrium with a situation where the equilibrium is disrupted by groundwater extraction from a confined aquifer. Due to extraction, soft soils like peat and clay compress over time, resulting in subsidence. Since peat and clay is present around Groenekan groundwater extraction in the Province of Utrecht, Vitens aspires to know their contribution to the subsidence at this location. Currently, Groenekan extracts ~ 5.0 million (M) m^3/yr , but Vitens plans to expand to $10.0 \text{ Mm}^3/\text{yr}$ to ensure long-term availability of drinking water (RIVM, 2023). Such an expansion, however, raises concerns about increased subsidence and potential damage to surroundings. Unravelling these dynamics is crucial for sustainable water management and mitigating subsidence risks.

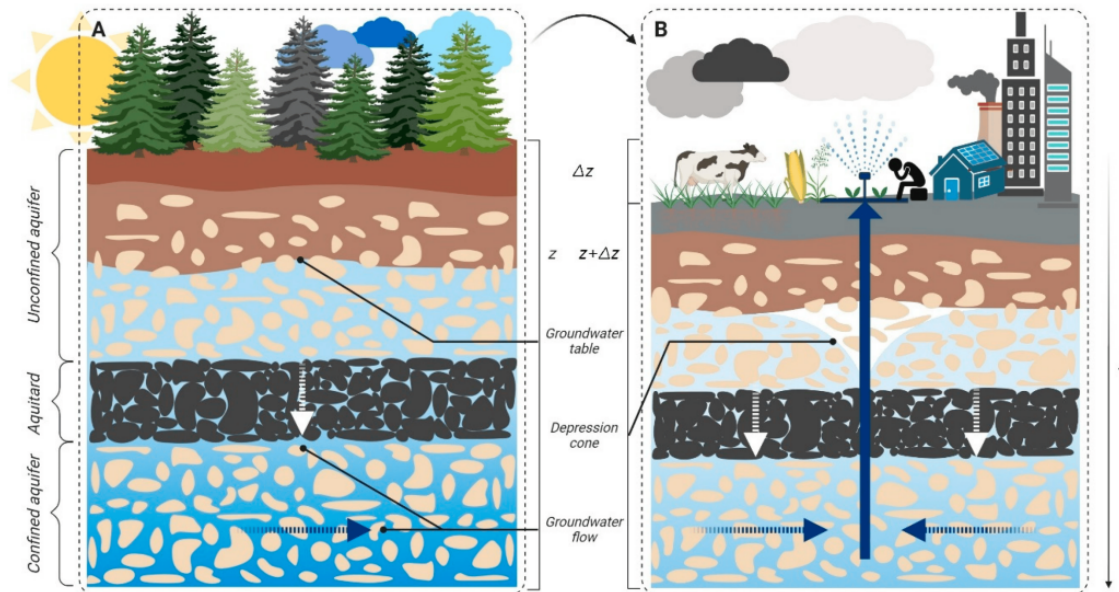


FIGURE 1.2: Schematic soil cross-section of (un)confined aquifers and an aquitard. A: No extraction equilibrium. B: Disruption of the equilibrium due to groundwater extraction causing compression of soft soils, resulting in subsidence (Guzy, 2020).

1.2. Knowledge Gap

Although extensive subsidence studies are abundant in the Netherlands (Bootsma et al., 2020; Erkens et al., 2021; Van Asselen et al., 2019), knowledge gaps remain, particularly in understanding the specific contributions and mechanisms of SGE in varying geological contexts. Although studies like those of Syvitski et al. (2009) and Dinar et al. (2019) provide an overview of subsidence phenomena globally, localised studies that account for unique geological and hydrological conditions, such as those found in the Netherlands, are limited. Specifically, the interaction between groundwater extraction

and subsidence in regions with peat and clay deposits, like Groenekan in the Province of Utrecht, requires further investigation. There is a lack of site-specific data on the rates and extents of subsidence directly attributable to varying levels of groundwater extraction. Furthermore, predictive models that incorporate the impacts of climate change are underdeveloped (Bootsma et al., 2020). The potential cumulative impacts of expanding Groenekan and a changing climate on subsidence rates are not fully understood. Addressing these gaps is essential for developing robust and sustainable water management strategies and mitigating the effects of subsidence on the environment and infrastructure. This study provides insight into the effects of groundwater extraction on subsidence and represents a step towards a reliable estimation of historical and future subsidence around groundwater extractions.

1.3. Objectives & Questions

In line with the problem statement and knowledge gap, this research aims to quantify the historical and future effects of groundwater extraction on subsidence at location Groenekan in the Province of Utrecht. As a result, the objective leads to the main research question:

From a subsidence perspective, can Vitens responsibly expand Groenekan groundwater extraction from 5.0 to 10.0 million m³/yr?

The research is divided into three themes: 1) Current situation overview, 2) Modelling of subsidence processes, 3) Future situation overview. Subsequently, the themes are translated to three sub-objectives in bold, containing seven sub-questions in total:

Analysis of geohydrological system and measured subsidence around Groenekan

1. What are the geohydrological details around extraction location Groenekan?
2. How much subsidence is measured through the Bodemdalingskaart around Groenekan over the period 2017 to 2023?

Quantification of SGE around Groenekan from 1961 to 2023

3. What is the temporal and spatial correlation between the groundwater level and hydraulic head lowerings and the extraction discharge of Groenekan?
4. How much SGE is modelled around Groenekan over the period 1961 to 2023?
5. How sensitive are the parameters that are used to quantify subsidence around Groenekan?

Future scenarios: Quantification of future SGE from 2023 to 2100

6. Which future climate and expansion scenarios should be considered for Groenekan?
7. How much SGE can be expected around Groenekan for the selected scenarios over the period 2023 to 2100?

1.4. Approach

In order to answer the research questions, the effects of (increased) groundwater extraction on subsidence around location Groenekan are modelled, mapped, and analysed. Data sources such as soil compositions and geotechnical information from "Data en Informatie van de Nederlandse Ondergrond loket" (DINOloket) and "Basis Registratie Ondergrond loket" (BROloket), surface level heights from "Actueel Hoogtebestand Nederland" (AHN), and extraction details from Provincie Utrecht (2023) and Vitens (2023) are essential in this research. For example, these data are used for the analysis of the geohydrological system, extraction discharge and Target Level Decision (TLD) of Groenekan. Also, measured subsidence data from Bodemdalingskaart (SkyGeo, 2023) is visualised and analysed in Geographic Information Systems (GIS).

Moreover, two separate models for groundwater flow and subsidence are used. The regional "Actueel modelinstrumentarium voor de Zuiderzee Regio" (AZURE) model (NHI, 2023a) is applied to calculate groundwater flows and hydraulic head variations. This model runs on MODFLOW2005 (Harbaugh, 2005), which is a numerical programme that simulates the flow of groundwater through finite elements. Visualisation of the output is done in Interactive Model for Dewatering and Groundwater Management (iMOD) version 5.5 (Deltares, 2023), which is a graphical user interface for running MODFLOW2005 calculations. Following, SGE is quantified in two separate steps. First, analytical equations

are adopted to calculate the potential **BDOM** and shrinkage. Second, two finite element Deltares Settlement (**D-Settlement**) models are built to quantify settlements in soft soil Holocene top layer and deeper aquitard (Visschedijk et al., 2009). Both steps are summed into a total value for **SGE**. This is then calculated for a "base scenario" of Groenekan, where the real extraction discharge is used and a time frame of 1961 (start of extraction) to 2023 is maintained, which is 62 years or $\sim 23,000$ days. Additionally, eight future scenario experiments quantify the total **SGE** from 1961 to 2100 (139 years or $\sim 50,000$ days). These eight scenarios are formed by combining four different extraction discharges (0.0, 5.0, 7.5, and 10.0 Mm^3/yr) and two "Koninklijk Nederlands Meteorologisch Instituut" (**KNMI**) climate scenarios for the year 2100.

1.5. Thesis Structure

First of all, Chapter 2 describes the theoretical background on groundwater extraction and subsidence. Next, Chapter 3 elaborates on extraction location Groenekan and in Chapter 4 the methodologies for the data analysis and models are presented. In Chapter 5, the modelled **SGE** results for **SGE** are examined and compared to the measured Bodemdalingskaart subsidence. Then, Chapter 6 discusses and interprets the thesis limitations, methods, and results. Finally, Chapter 7 summarises the conclusions and finalises with recommendations for future research and Viten.

This thesis is structured according to the flowchart in Figure 1.3. The grey box illustrates the used theoretical frameworks. The steps in the orange box belong to the methodology, whereas the steps in the yellow box are the results. The validation method of the results is given in blue. Lastly, the answers to sub-questions 1 and 2 are given in turquoise, sub-questions 3, 4, and 5 in green, and sub-questions 6 and 7 in red.

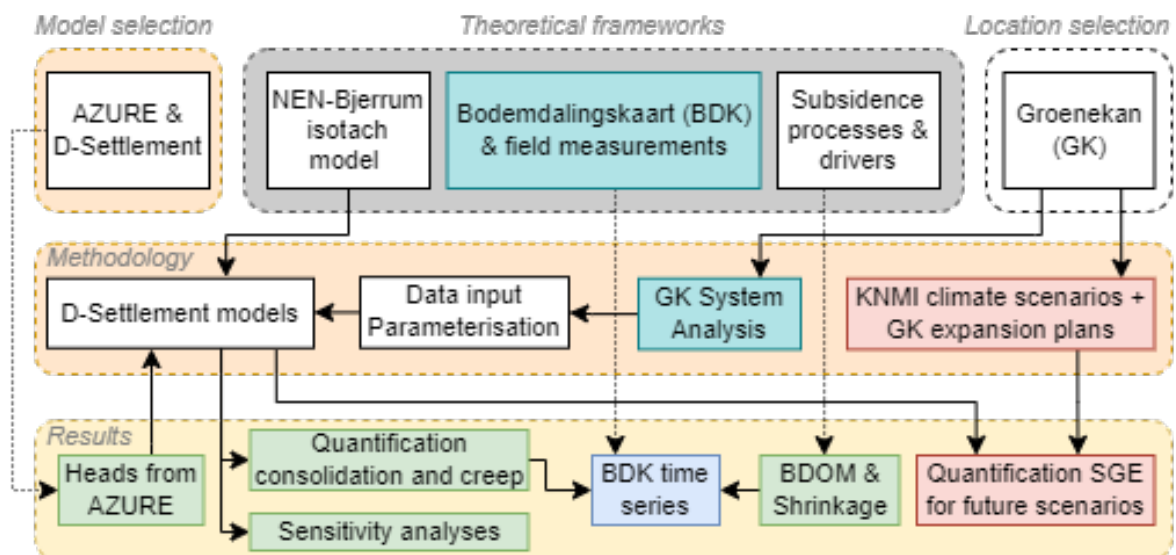


FIGURE 1.3: Thesis structure flowchart. Grey box illustrates the used theoretical frameworks. The steps in the orange and yellow boxes belong to the methodology and results respectively. The validation method of the results is given in blue. Lastly, the answers to sub-questions 1 and 2 are given in turquoise, sub-questions 3, 4, and 5 in green, and sub-questions 6 and 7 in red.

Groundwater Extraction & Subsidence

This chapter serves as the theoretical framework which is used as a foundation for understanding the (geohydrological) system around Groenekan in Chapter 3. Also, the data analysis and modelling work in Chapter 4 can be more effectively performed and better interpreted. First, Section 2.1 presents two analytical approaches relating groundwater flow and extraction and these approaches are directly applied to Groenekan. Sections 2.2 and 2.3 outline all subsidence processes and their drivers. Next, four global literature cases of SGE are listed in Section 2.4. Finally, in Section 2.5 the consolidation and isotach models that calculate subsidence are discussed.

2.1. Analytical Groundwater Flow Approaches

This section focuses on understanding two simple analytical approaches which represent the relation between groundwater flow and an extraction. There are two analytical equations for calculating the lowering of the hydraulic head, in the report referred to as head. One is for stationary (De Glee, 1930) and one for transient (Hantush & Jacob, 1955) calculations. A background on stationary vs. transient flows and models is presented in Appendix B.1.

De Glee (1930)

The equation of De Glee (1930) indicates a steady-state head lowering around an extraction with constant magnitude Q_0 [m³/d] in an aquifer of constant thickness D . Equation 2.1 is derived for the "Holland profile": A thick aquifer of Pleistocene sands confined by a clay aquitard and a Holocene top layer of clay and peat, in which a dense drainage system of permanent ditches (NL: *sloten*) is present.

$$H(r) = \frac{Q_0}{2\pi k D} K_0 \left(\frac{r}{\lambda} \right) \quad (2.1)$$

Where $H(r)$ [m] is the lowering of the head at distance r from the extraction well. k is the hydraulic conductivity or permeability of the aquifer [m/day] and D is the thickness of the aquifer [m]. The function K_0 has the shape of the draw-down cone caused by the extraction, for which the hyperbolic Bessel-function is used. The so-called spread length λ [m] is calculated as follows:

$$\lambda = \sqrt{k D c} \quad (2.2)$$

Where c is the hydraulic resistance of the aquitard in days. The spread length represents the spatial effect of the extraction. λ is shown in Equation 2.1 under the distance r : the greater λ , the greater the influence area. As a result, a large influence area means the lowering of the head is limited. The recharge of groundwater is, after all, spread over a larger area.

Hantush and Jacob (1955)

The equation of Hantush and Jacob (1955) calculates the transient head lowering around an extraction:

$$H(r, t) = \frac{Q_0}{4\pi k D} * W \left(\frac{r^2 S}{4k D t}, \frac{r}{\lambda} \right) \quad (2.3)$$

Where t represents the time from start of extraction [days], W is the "Well function of Hantush" (Hantush & Jacob, 1955), S is the elastic storativity [-] and the rest of the parameters are similar to Equations 2.1 and 2.2.

Both analytical groundwater flow approaches (Equations 2.1 and 2.3) are applied to the following parameters, specified for Groenekan:

- Extractions Q_0 of 5.0, 7.5, and 10.0 Mm^3/yr (Vitens, 2023);
- For the second aquifer; a hydraulic conductivity k of 50 m/day and a thickness D of 80 m are assumed, resulting in $kD = 4,000 \text{ m}^2/\text{day}$ (TNO, 2023a);
- Hydraulic resistance c of the Waalre clay is 2,500 days (Figure 3.4 (TNO, 2023a));
- Elastic storativity S of 0.001 (Allan Freeze & Cherry, 1979);
- Spread length λ of 3,162 m ($\sqrt{50 \cdot 80 \cdot 2500}$) (Verruijt, 2010);
- Horizontal distance r of 5,000 m to Groenekan, after that the influence area is assumed to be negligible.

Crucially, it is assumed that groundwater is extracted from a homogeneous, confined aquifer beneath an aquitard (Waalre clay) and a Holocene phreatic top layer with ditches. Solving Equations 2.1 and 2.3 with the parameters values, the stationary and transient head lowerings are plotted in Figure 2.1.

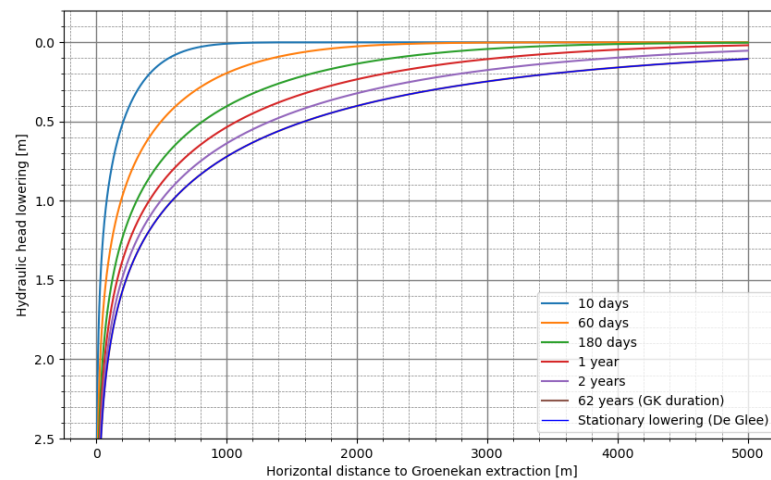


FIGURE 2.1: Analytical calculation of head lowering over distance r for Groenekan with 5.0 Mm^3/yr extraction. Transient time steps in various colors (Hantush & Jacob, 1955) and stationary lowering in navy blue (De Glee, 1930).

It is visible that the stationary head lowering by Equation 2.1 (navy blue graph) is instant. The transient approach (Equation 2.3) shows the gradual lowering of the head over time towards the stationary scenario. These results are used to obtain a better understanding of how the groundwater system of Groenekan works and are subsequently compared to the AZURE results in Section 5.2. Figures A.9 and A.10 present the head lowerings for 7.5 and 10.0 Mm^3/yr , which both only show a deeper drawdown cone. The Python code for creating the graphs is presented in Appendix I.1.

2.2. Subsidence Processes

Subsidence is the phenomenon by which the surface level sinks in relation to a reference plane, for example the Dutch NAP. In practice, the term subsidence often refers to the “vertical downward movement of the surface level” (NL: *maaiveld dalend*). Figure 2.2 shows that subsidence is induced by sub-surface deformation, which is caused by three main processes: compression, compaction, and geological processes (Van Asselen et al., 2019). In addition, erosion and excavation of the top soil layer lowers the surface level directly. However, this research focuses specifically on the sub-surface processes consolidation, creep, aerobic Biochemical Degradation of Organic Material (BDOM), and shrinkage (cyan blocks).

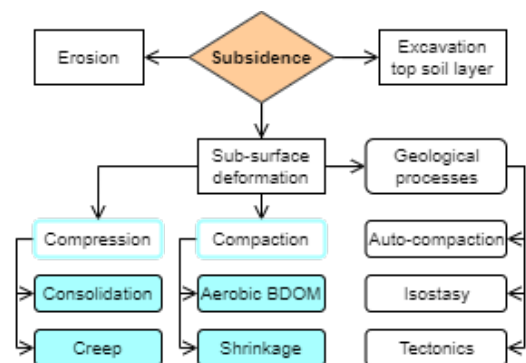


FIGURE 2.2: Subsidence processes (Van Asselen et al., 2019). Research focuses on cyan sub-processes.

2.2.1. Compression by Increasing the Effective Stress

Increased soil stresses may cause subsidence. This behaviour is time-dependent. Soil stresses exist due to its own load, soil water content, external stresses, and possible man-made structures on the surface. All loads combined define the soil's total stress. Part of this total weight is carried by water present in pores - called water pressure. In general, water pressure is zero at the phreatic level and increases linearly with depth. The remaining part of weight is carried by contact points in the granule structure - called effective stress (NL: *korrelspanning*). According to the effective stress principle of Terzaghi (1925), a change in effective stress σ' can either be caused by a change in the total stress component σ or by the pore water pressure u :

$$\sigma' = \sigma - u \quad (2.4)$$

Generally, there are two ways to intervene in the effective stress balance: by changing the pore water pressure u (groundwater levels, hydraulic heads, seepage/leakage, saturation degree) or by changing the total stress σ . For this research, a decrease in pore water pressure (lowering of the groundwater level and heads) is most relevant. An external stress, such as groundwater extraction, may potentially cause settlement in soft soil layers. The total settlement contributes to subsidence and can be written as the sum of four components:

$$S_t = S_i + S_{co} + S_{cr} + S_{te} \quad (2.5)$$

Where S_t is the total settlement [m], S_i is the immediate settlement [m], S_{co} is the consolidation settlement [m], S_{cr} is the creep settlement [m], and S_{te} is the tertiary settlement [m]. Since tertiary compression is a minor or non-existent component (Feng et al., 2021), it is considered to be outside the scope of this research. Thus, the first three components are discussed in the following paragraphs.

Initial Compression

The immediate settlement component S_i follows from the initial compression of the soil, caused by the elasticity of soil structure and by compression and expulsion of gas in the soil pores after initial increase of effective stress (Figure 2.3). This settlement component is usually a small portion of the total settlement.

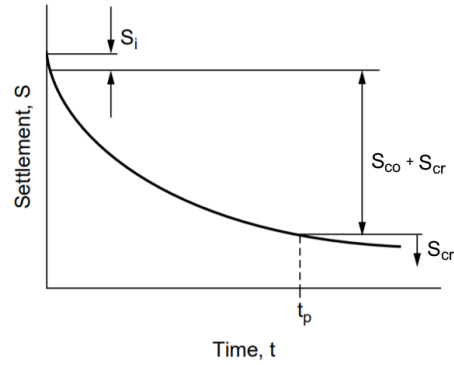


FIGURE 2.3: Settlement components over time curve.

Consolidation (Primary Compression)

Consolidation, or primary compression, is the development of the compression of an soil layer after a "loading" event. Loading can either refer to application of a weight, or reduction of the pore pressure near the top and/or bottom of the layer (Kooi et al., 2018). The rate of consolidation depends on the rate at which pore water can drain to the top and/or bottom of the layer. Consolidation is a slow process in which water is pressed out of pore spaces. The total elapsed time for this process in a layer, also called hydrodynamic period, is described by Terzaghi (1925):

$$t_p = \frac{m_v \gamma_w D^2}{2k} \quad (2.6)$$

Where t_p is the end of the hydrodynamic period [s], m_v is the compression constant [m^2/kN], γ_w is the density of water [kN/m^3], D is the thickness of the compressible layer [m], and k is the hydraulic conductivity of the soil [m/s].

Creep (Secondary Compression)

In general, the compression of soil layers is not limited to only the initial and primary compression, but occurs over a prolonged period of time following the loading, also known as creep or "secondary compression" (Keverling Buisman, 1936). The main reason for this delayed response is that the compression of a saturated soil layer can only proceed at the rate at which the pore water is expelled from the layer. In particular, for thick layers with a low hydraulic conductivity such as clay and peat, this

expulsion is slow and continues after dissipation of excess pore pressure, resulting in a (lower) creep rate (Kooi et al., 2018; Mesri, 1973).

Kooi et al. (2018) states that creep represents an active process that occurs irrespective of the effective stress conditions (constant, decreasing, increasing) and happens nonetheless. For constant effective stress (nominally constant head), for instance, the porous medium is actively ‘squeezed’ by the creep. Elastic (or ideal plastic) compression, in contrast, is passive in the sense that it is slave to effective stress change (i.e. no effective stress change, no elastic strain). In contrast, creep is a slow viscous strain of the soil, resulting in a downward movement of the ground surface.

Additionally, factors such as changes in soil moisture content or temperature can influence the rate of creep-induced subsidence. Creep is particularly notable in regions with organic material and clay-rich or unconsolidated soils, which are abundant in the Netherlands. Measurement of creep parameters is a standard practice in oedometer¹ and constant-rate-of-strain laboratory tests (ISO, 2004).

2.2.2. Compaction

Compaction is another process that plays a crucial role in the subsurface. Two sub-processes of compaction are described in the following two paragraphs.

Biochemical Degradation of Organic Material

An important factor directly driving subsidence is Biochemical Degradation of Organic Material (BDOM). In history, peatlands have been drained to create agricultural land. When organic soils are exposed to oxygen, the organic constituents decompose resulting in compaction. This effect not only affects the settlement of objects (foundations), but can also lead to biodiversity loss and alterations in the landscape (Bootsma et al., 2020).

Either aerobic or anaerobic BDOM could occur, based on the availability of oxygen. When BDOM under aerobic conditions is considered, for example due to the increased extent of aeration following the drainage of peatlands, often the term “oxidation” is used. The end product of aerobic oxidation is carbon dioxide trapped (CO_2) in the soil. Through the emission of these greenhouse gases, BDOM enforces global warming. Van den Akker et al. (2010) states that CO_2 emissions from aerobic degradation of peat soils in the Netherlands are about 4.2 million tonnes per year, which is approximately 3% of the total yearly emission of greenhouse gases in the Netherlands. Anaerobic BDOM is not taken into account in this study, since it is an ongoing process which is not caused by a groundwater extraction and it contributes minimally to overall BDOM (Ten Bosch, 2020).

Studies conducted in the Netherlands that focused on peat oxidation generally use a fixed annual oxidation rate with respect to the aerated part of a layer (Bootsma et al., 2020; Van der Meulen et al., 2006). In other words, it is assumed only the aerated part of the peat layer is oxidising if the phreatic groundwater level is situated within a peat layer. Because only the organic matter oxidises, a residual thickness representing admixed clastic sediments should ideally be taken into account. This is implemented in Equation 2.7 as a fraction of the original thickness, denoted as residual thickness λ_r (Fokker et al., 2019). If a layer is completely composed of organic matter, the fraction λ_r is 0. To calculate the thickness reduction of a dry layer during a time step Δt , the part h_{BDOM} of the layer that is susceptible to BDOM is first determined. This starts with $h_{BDOM}(t = 0) = h_0 - \lambda_{r,BDOM} \cdot h_0$ in which h_0 is the initial thickness. When part of the layer has already been oxidised, then $h_{BDOM}(t) = h(t) - \lambda_{r,BDOM} \cdot h_0$. Both the total thickness and the part that is excluded from oxidation is corrected for the wet part as follows:

$$\Delta h_{BDOM} = \left(1 - e^{(-V_{BDOM} \cdot \Delta t)}\right) \cdot (h_{exp} - h_{wet} - \lambda_{r,BDOM} \cdot [h_0 - h_{wet}]) \quad (2.7)$$

Where Δh_{BDOM} is the reduction of peat thickness above the phreatic water level through BDOM [m], V_{BDOM} is the BDOM velocity [m/m/yr], Δt is the time step [yr], h_{exp} and h_{wet} are the thickness of peat exposed to oxygen and below the phreatic groundwater level [m], $\lambda_{r,BDOM}$ is the fraction of the initial thickness that represents the residual thickness after BDOM [-], and h_0 is the initial thickness in [m].

¹Oedometer tests measure the consolidation properties of a soil by applying different loads to a soil sample and measuring the strain response.

Shrinkage

Compaction by shrinkage (NL: *krimp*) is also a significant contributor to subsidence in the Netherlands. Shrinkage is primarily observed in areas where organic soils as clay and peat are abundant. Dutch clay soils belong to the strongest swelling and shrinking soils of the world, with volume decreases being maximally 49% between a saturated and oven-dry state sample (Bronswijk & Evers-Vermeer, 1990).

When clay soils lose moisture content, they undergo desiccation, they compact, eventually resulting in shrinkage. More specifically, it is the contraction of soil layers above the water level, following the development of negative pore water pressures in the unsaturated zone of the soil. This process leads to a reduction in volume and higher density of the soil, causing subsidence. Prolonged drought conditions or human-induced activities such as superficial withdrawal of groundwater can accelerate the desiccation of these soils, intensifying shrinkage-induced subsidence. The loss of moisture weakens the soil structure, making it more susceptible to compaction, ultimately manifesting as subsidence.

Ten Bosch (2020) lists that loss of water can for example be caused by:

- Sum of evaporation and transpiration components is higher than precipitation;
- Soil sealing: the covering of soil with impermeable material (buildings, asphalt, pavements, parking lots, etc.), which limits infiltration of water in the soil;
- Dewatering: drainage of surface water, which keeps the groundwater level at a certain TLD;
- Excessive groundwater extraction: more groundwater is used than recharged.

Shrinkage curves illustrate the subsidence due to moisture loss. Figure 2.4 shows the relationship between the soil moisture number on the x-axis (volume of moisture over volume of solids) and on the y-axis the void ratio e (volume of pores over volume of solids) of a clay soil. Three shrinkage phases are distinguished:

1. **Regular shrinkage;** where decrease of soil volume is equal to decrease of water volume;
2. **Residual shrinkage;** where decrease of soil volume is less due to the entrance of air in pores;
3. **Zero shrinkage;** during which the soil volume remains constant due to decreasing water volume and increasing air volume in the pores.

Bronswijk and Evers-Vermeer (1987) states that shrinkage can be divided in a reversible (zero & residual) and a non-reversible (regular) component, which is essential for long-term subsidence considerations. Non-reversible shrinkage can be seen as a final process of soil structure forming processes. Often, initial dewatering holds the non-reversible shrinkage part, after which shrinkage and swelling become reversible. An important characteristic of soil shrinkage is that the ratio of shrinkage does not have to be similar in all directions. On a macroscopic level, total shrinkage shows in two ways, horizontally through shrinkage cracks and vertically through subsidence of the surface.

Fokker et al. (2019) considered subsidence by shrinkage in the Flevoland polder. It was expected that initial groundwater lowering could induce a non-reversible shrinkage mechanism. They chose to implement a relationship similar to Equation 2.7 for BDOM. Looking at the soil composition in Flevoland, Groenekan shows similarities and therefore Equation 2.8 may be applicable to this research. The height reduction due to shrinkage was calculated with:

$$\Delta h_{sh} = \left(1 - e^{(-V_{sh} \cdot \Delta t)}\right) \cdot (h_{exp} - h_{wet} - \lambda_{r,sh} \cdot [h_0 - h_{wet}]) \quad (2.8)$$

Δh_{sh} is the reduction of clay thickness above the phreatic water level through shrinkage [m], V_{sh} is the shrinkage velocity [m/m/yr], and $\lambda_{r,sh}$ is the fraction of the initial thickness that represents the residual thickness after shrinkage [-].

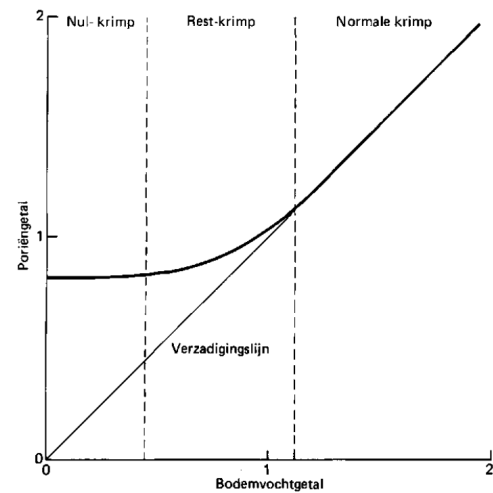


FIGURE 2.4: Three stages of shrinkage (Bronswijk & Evers-Vermeer, 1987); regular, residual, and zero.

2.2.3. Geological Processes

Geological processes are driven by the Earth's crustal movements and cannot be stopped. Subsidence calculations should therefore always consider geological processes. The underlying geological sub-processes are auto-compaction, isostasy, and tectonic movements (Kooi et al., 1998).

Auto-compaction

Auto-compaction is subsidence of shallow layers (up to 300 meters) due to mass of overlying young sediments. Compaction refers to vertical contraction of rock and sediments upon burial. Auto-compaction mainly increases towards coastal areas in the Netherlands, where more compactable organic soil is present. In the Netherlands, the mean rate of vertical surface level change at present due to auto-compaction is ~ -0.1 cm/10yrs.

Isostasy

Isostasy is the concept that Earth's lithosphere (crust and uppermost part of the mantle) is floating in gravitational balance on the denser, more fluid asthenosphere beneath it. The lithosphere adjusts vertically to maintain equilibrium based on variations in density and thickness. Isostatic adjustments may also contribute to subsidence. For instance, if there is a removal of material (such as sediment or ice) from the Earth's surface, the lithosphere responds by adjusting vertically ("tilting") to maintain equilibrium. The mean rate of vertical surface level change due to glacio- and hydro-isostasy in the Netherlands is -0.1 cm/10yrs with an error margin of 0.4 cm/10yrs.

Tectonics

Tectonics refers to the Earth's lithosphere and the interactions of tectonic plates. Subsidence may occur due to movement of tectonic plates. Tectonic ground motion across the Netherlands is hardly present since the Netherlands is not located on a fault line. Therefore, it seems that the only way to assess recent tectonic movements in the Netherlands is to correct the geodetic rates for isostasy and auto-compaction and to attribute the residuals, if significant, to short-term tectonic processes.

Groenekan

Figure 2.5 displays a contour map of regional subsidence due to the geological processes auto-compaction, isostasy, and tectonics in the Netherlands, created with a data set spanning from 1926 to 1987. Groenekan (cyan dot) and the Province of Utrecht are at the border of the green and orange categories, ranging from -0.4 to 0.0 cm/10yrs subsidence. Therefore, for Groenekan, a geological subsidence of 0.2 cm/10yrs is assumed. Standard deviations in the data range from 0.1 to 0.3 (Kooi et al., 1998).

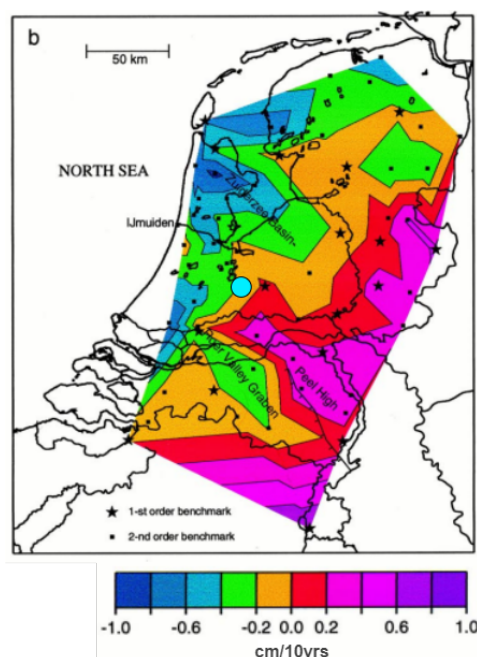


FIGURE 2.5: Subsidence rate [cm/10yrs] due to geological processes in the Netherlands from 1926 to 1987 (Kooi et al., 1998), with ten subsidence or uplift classes. Groenekan = cyan dot.

2.3. Subsidence Drivers

Next, the causes or “drivers” of the subsidence processes are explained in this section. Figure 2.6 shows a standard ground composition with aquifers and aquitards. Dutch geohydrological profiles might have an additional Holocene peat top layer and a deeper clay aquitard, resulting in a system with multiple (un)confined aquifers. The subsidence processes in Figure 2.2 are included within the cyan frame. In addition, both the natural (green) and anthropogenic, or human-induced (red) drivers of subsidence are visually presented.

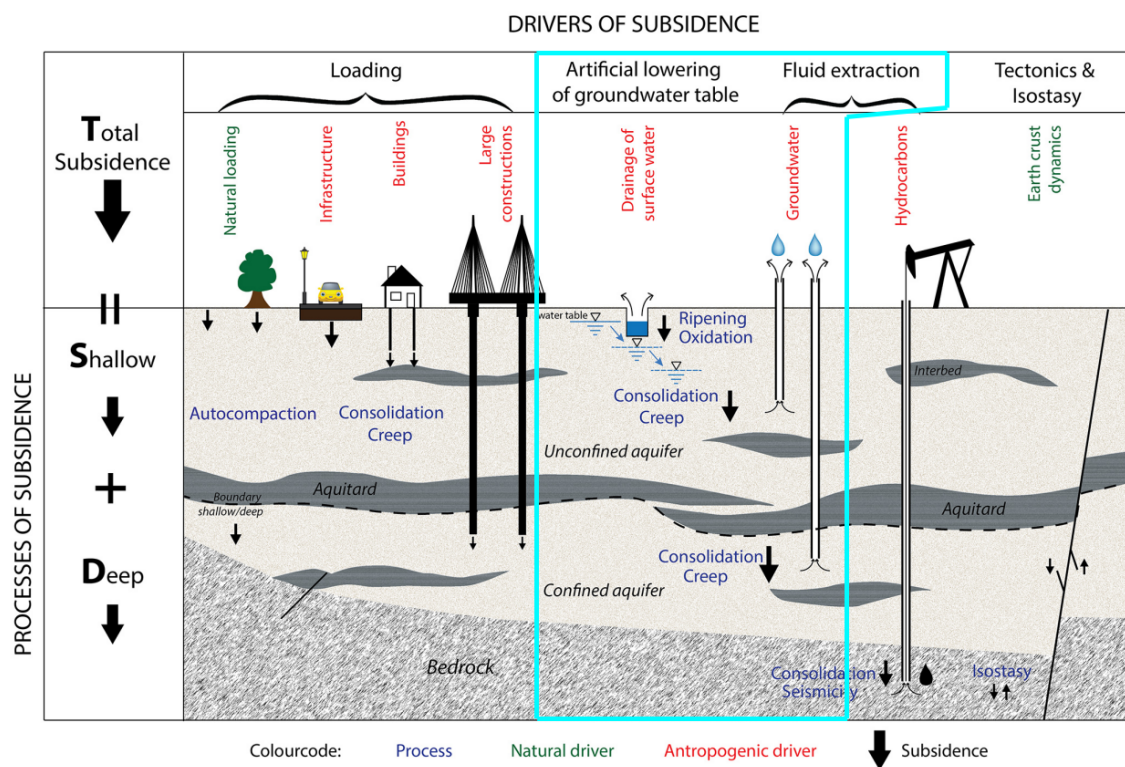


FIGURE 2.6: Subsidence drivers and processes (Minderhoud et al., 2015). Research focuses on drivers within cyan frame.

2.3.1. Increase in Loading

A primary driver of subsidence is the increase in the load on soil layers. An increase in load causes consolidation and creep. Load-induced subsidence often arises from the soil’s own weight and the weight of overlying natural material (soil, trees, forests, meadows, etc.), which leads to the compression of underlying soft soils, such as peat and clay. Natural loading is extensively documented in geotechnical studies (USGS, 2018a; Visschedijk et al., 2009), but is assumed to be negligible for the case of Groenekan. Furthermore, anthropogenic activities such as the construction of buildings, embankments, or infrastructure can cause load-induced subsidence. Over time, the soil layers gradually compress, resulting in a decrease in the elevation of the surface level. The direct surroundings of Groenekan are dominated by open agricultural fields and meadows (Figure A.5), thus subsidence by loading is not applicable to the case of Groenekan. Therefore, the analysis of load-induced subsidence is assumed to be redundant.

2.3.2. Lowering of Groundwater Level

Lowering of the groundwater level may cause subsidence through compression and compaction and is caused naturally by downward seepage, evaporation, and water uptake by roots. Moreover, there are anthropogenic actions that cause an artificial lowering of the groundwater level. Examples are maintaining certain surface water levels in ditches and canals or by groundwater extraction. A decrease in groundwater level causes an increase in effective stresses in the soil layers. Since the water pressure decreases and the total stress stays the same, the effective stress increases. In a “zero-situation” without extraction, the groundwater level, on average, shows a sinusoidal gradient with time (Ernst & Feddes, 1979). This time dependence can be explained by the fact that precipitation per month on average is fairly constant and evaporation (in conjunction with solar radiation) has a sinusoidal course over time.

Target Level Decision (NL: Peilbesluit)

A Target Level Decision (**TLD**) is a regional policy from Rijkswaterstaat and the Dutch water boards where the surface water bodies are set to a desired water level. The determined **TLDs** must be maintained as much as possible, taking into account different stakeholders (agriculture, nature, urban areas etc.) and seasonality (Rijkswaterstaat, 2023a). These **TLDs** are decided and revised by the water boards and each separate Target Level Section (**TLS**) or (NL: *peilvak/polder*) has its own **TLD**. Generally, separate summer and winter **TLDs** are made to counteract variable groundwater situations and needs in the low-lying polders, where the summer level, from April to September, is higher than the winter level, from October to March. This is done because there is usually more drought in summer and a precipitation surplus in winter. On top of that, more water is needed in spring and summer for the growth of plants and trees in nature and for agricultural crops (Unie van Waterschappen, 2023). On the contrary to nature organisations, the Dutch agriculture sector prefers low groundwater levels to work their land and have dry feet for their cattle to graze in the meadows. However, subsidence in the polders, usually peat oxidation or clay shrinkage, causes the dry board (NL: *ontwateringsdiepte*) to become smaller and the groundwater level to be closer to surface level. As a result, the top soil layer becomes wetter and unsuitable for tractors and cattle, which eventually may trigger a new **TLD** with lower summer and winter levels. Figure 2.7 illustrates a four-step cycle of 1) an initial **TLD** or surface water level, 2) a lower **TLD** causing 3a) consolidation, 3b) drying and aeration of the peat, 3c) **BDOM**, and eventually 4) subsidence, which in return triggers a new cycle. Section 3.4 elaborates on the historical and current **TLDs** of Groenekan.

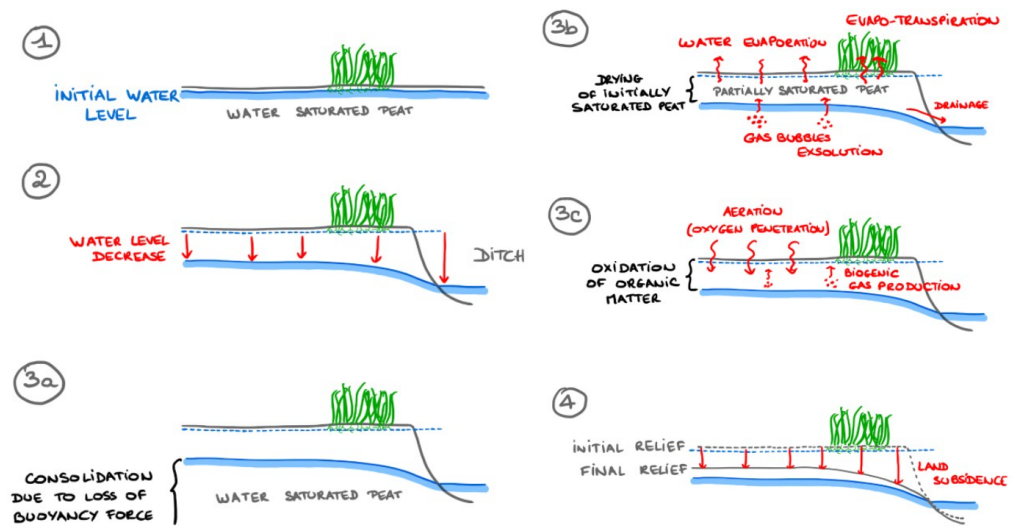


FIGURE 2.7: Four step cycle of 1) initial water level, 2) lower Target Level Decision, 3a) consolidation, 3b) drying and aeration of peat, 3c) oxidation of organic matter, 4) subsidence (Dieudonné, 2023).

2.3.3. Subsidence due to Groundwater Extraction

Another key driver of subsidence is groundwater extraction. This extraction is essential for drinking water supply, industry, and agriculture, but has an effect on the phreatic groundwater level and heads in deeper confined aquifers. Consequently, through long-term extraction, the clay and peat Holocene top layer and deeper aquitards may compress due an effective stress increase beyond the pre-consolidation stress (σ'_p). Figure 2.8 shows a visualisation of **SGE** through soil compression (Minderhoud et al., 2015; USGS, 2018a).

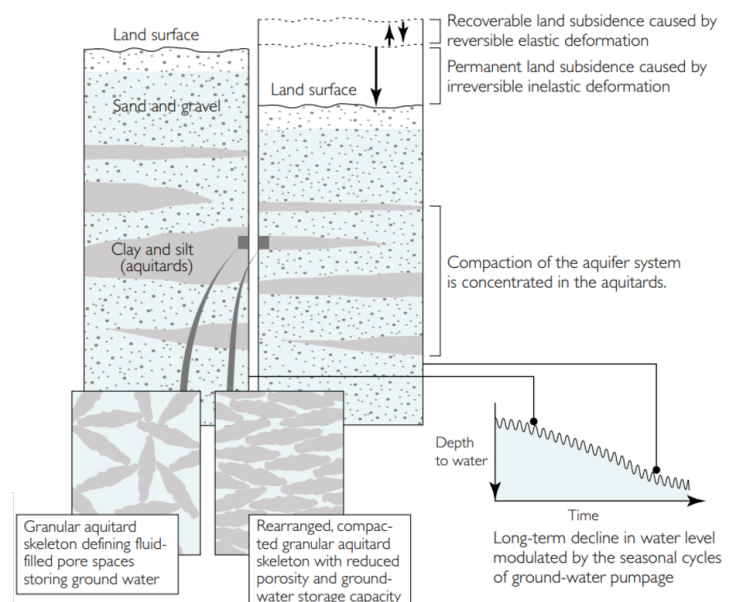


FIGURE 2.8: SGE visualisation (USGS, 2018a).

Furthermore, the groundwater level is possibly lowered due to an extraction if an aquitard is “leaky”, meaning its hydraulic resistance c is low or if the layer is interrupted by a gully (NL: *geul*). If an extraction lowers the phreatic groundwater level, SGE indirectly may influence processes as BDOM and shrinkage as well.

2.4. SGE Literature Case Studies

In this section, four global SGE case studies in California, USA, the Mekong Delta, Vietnam, Jakarta, Indonesia and DSM in Delft, the Netherlands are addressed to set the scope area of Groenekan into perspective and compare causes and consequences of SGE. Although these examples are different with respect to geohydrological profiles and extraction discharges, the common process of soil compression, BDOM and shrinkage could also be applied to soft soils around Groenekan.

California - United States of America

According to Holzer and Galloway (2005), the main causes of subsidence in the United States are anthropogenic, namely groundwater and petroleum extraction, mining of coal and minerals, drainage of organic soils, and diversion of sediment from marshes in the delta of the Mississippi River. The article notes that withdrawal of underground fluids from porous granular media is the most significant cause of subsidence in terms of affected area. Figure 2.9 shows the situation in the San Joaquin Valley, California, where the surface level subsided approximately 9 metres from 1925 to 1977 due to aquifer-system compression. Signs on the telephone pole indicate the former elevations of the land surface in 1925 and 1955 respectively. Similarly to the Netherlands, San Joaquin valley mainly consists of soft soils as clay and loam. Recently, several extensometers have been placed in the valley to help in understanding the subsidence rate, extent, and at what depths in the system subsidence is occurring (USGS, 2018b). An extensometer measures the one-dimensional (1D) change in thickness of a specified depth interval. In other words, it measures the compression and expansion of the aquifer system to a specific depth.



FIGURE 2.9: 9 metres of subsidence in California (Ireland, 2018).

Mekong Delta - Vietnam

Minderhoud et al. (2017) concludes that SGE is a major driver of subsidence in the Mekong Delta, Vietnam. The geohydrological system of the delta has been transformed from an almost undisturbed system into a human-impacted state with accelerated aquifer compression due to increased groundwater extraction in the past 25 years. The study estimates that a quarter-century of SGE caused the delta to sink on average by approximately 18 cm over the past 25 years, with specific areas subsiding even more than 30 cm. Currently, the average SGE rate in the delta is around 1.1 cm/yr, with local extremes over 2.5 cm/yr. Also, Minderhoud et al. (2015) highlights the urgent threat SGE can pose to low-lying deltas such as the Mekong delta, exacerbating flood vulnerability, saltwater intrusion, and coastal erosion. The same might hold for the Netherlands, which is also a low-lying delta.

Jakarta - Indonesia

Kooi and Yuherdha (2018) claim that the extraction of deep groundwater is the leading cause of subsidence that has occurred since the mid-1970s in Jakarta, up to about 4 metres in total. This is indicated by Interferometric Synthetic Aperture Radar (InSAR) observations and analyses as well (Abidin et al., 2011). Since 2015, Deltares is developing modelling-based subsidence forecasts in SUB-CR (Kooi et al., 2018) that first seek to explain the past subsidence, and then are extended to predict future development of subsidence. Three locations in Jakarta were investigated: Daan Mogot, Sunter, and Marunda. Subsidence was calculated for each location in three future groundwater extraction scenarios:

1. Business as usual (continued pumping and lowering of heads)
2. Reduced/controlled deep groundwater extraction (stabilised heads)
3. Stopped deep groundwater extraction (slow and fast recovery of heads)

In summary, the model output is consequent and validated through calculations in SUB-CR. For each location, the business as usual scenario would result in more than 1 metre of subsidence from 2018 to 2050. The stopped scenario with fast head recovery would mean that each location would swell upward, so uplift would occur instead of subsidence.

DSM, Delft - The Netherlands

Another example of subsidence and uplift/swelling is found around the industrial terrain of DSM in Delft. In the twentieth century, Delft and surrounding areas have experienced ~50 cm of subsidence due to the 12.5 Mm³/yr groundwater extraction in the first aquifer underneath a thick Holocene peat and clay top layer (Maas, 2018). In 2004, DSM wanted to completely terminate their groundwater extraction, but the expectation was that the soil would quickly swell after abrupt stopping. On the other hand, a positive effect of stopping the extraction is that subsidence due to BDOM and shrinkage was expected to decrease or even stop. Roelofsen et al. (2008) conducted a study in collaboration with the municipality of Delft and other stakeholders, and examined the effects of these changes. The study underscores the necessity for monitoring and a phased approach to avoid 8 to 16 cm of swelling. Therefore, the extraction is currently step-wise being reduced to zero to avoid swelling damage in the centre of Delft (Maas, 2018; Roelofsen et al., 2008).

2.5. Consolidation & Creep Calculations

Consolidation and creep play a major role in quantifying subsidence. Both processes are integrated in various models. In Subsection 2.5.1, the classical Consolidation Model (CM) by Terzaghi (1925) is discussed and in Subsection 2.5.2 this theory is extended to the Isotach Model (IM), which forms the theoretical support for the subsidence modelling in D-Settlement.

2.5.1. Consolidation Models

One dimensional consolidation models have been developed to quantify subsidence. 1D consolidation was first expressed by Terzaghi (1925) in Equation 2.9, which can be derived from the general three-dimensional consolidation equation using the following assumptions:

- Loading is one-dimensional
- Soil grains are non-deformable
- Hydraulic conductivity of the soil is constant
- Saturated flow
- Soil is uniform
- Flow is controlled by Darcy's law
- Fluid is incompressible
- Stiffness in the soil is constant
- Small strain hypothesis

$$\frac{\delta u}{\delta t} = c_v \frac{\delta^2 u}{\delta z^2} \quad (2.9)$$

Where u is the excess pore water pressure [kN/m²], c_v is the consolidation coefficient [m²/s], z is the vertical direction [m] and t is time [s]. The consolidation coefficient is defined as:

$$c_v = \frac{k_v}{\gamma_w \cdot m_v} = \frac{k \cdot E_{oed}}{\gamma_w} \quad (2.10)$$

Where k_v is the vertical permeability [m/s], γ_w is the unit weight of water [kN/m³] and $m_v (= 1/E_{oed})$ is the compressibility coefficient [m²/kN], where E_{oed} is the oedometer modulus in [kPa].

2.5.2. Isotach Models

Isotach models combine consolidation calculations with creep of a soil. Creep is a crucial factor in calculating subsidence rates on large time scales (Den Haan, 2007). In the past, the traditional Koppejan model was applied often due to its ease of use, the large amount of experience gained in using it, and the relatively simple and standardised methods of parameterisation. It combines theories from Terzaghi and Keverling-Buisman to describe overall settlement behaviour (Koppejan, 1948). However, nowadays two essential isotach models for the calculation of strain associated with consolidation of soft

soils are used: the NEN-Bjerrum isotach model (NEN-Bjerrum) (Bjerrum, 1967), and the a,b,c isotach model (a,b,c) (Den Haan, 1994). In this section, only the NEN-Bjerrum and a,b,c-models are discussed, since these are used in D-Settlement modelling. Also, Koppejan is only applicable to staged loading and has major limitations for time-dependent loads relevant to subsidence, such as creep (Van Asselen et al., 2019).

The NEN-Bjerrum model supports today's international standards for settlement prediction and is based on linear or Cauchy strain (Equation 2.11). The a,b,c-model is a comparable model that employs a natural or Hencky strain (Equation 2.12). The difference in strain is presented in Figure 2.10.

$$\epsilon^C = \frac{h_0 - h}{h_0} \quad (2.11)$$

$$\epsilon^H = -\ln\left(\frac{h}{h_0}\right) = -\ln(1 - \epsilon^C) \quad (2.12)$$

The a,b,c-model is superior for handling large strains (i.e. centimeters per year) and for cyclic change behavior of effective stress (Den Haan, 1994). However, the strain rates in Groenekan are expected to be small (millimeters per year), therefore NEN-Bjerrum suffices in calculating the subsidence and a,b,c is not further discussed.

Figure 2.11 shows the differences in effective stress diagrams in both a CM and IM. For CMs, the void ratio e is plotted against the effective stress σ'_p and goes from elastic to more severe plastic state when the pre-consolidation stress σ'_p is reached. Also, e becomes smaller, meaning there is less air present between the pores, resulting in a more compressed soil.

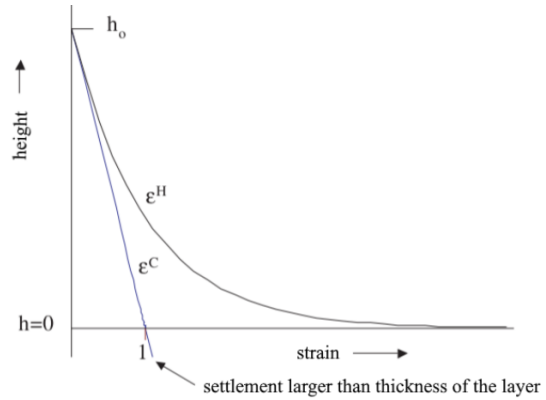


FIGURE 2.10: Difference between linear and natural strain (Den Haan, 2007).

On the other hand, IMs reach a viscous regime after σ'_p and follow strain ϵ over intrinsic time τ (red contour lines, also called isotaches). Each line represents an equal total creep strain, but with a ten times smaller creep strain rate $\dot{\epsilon}_{cr}$. The constant time t from a CM and isotach concepts were combined into an "equivalent time" to each rate of strain. Den Haan (1994) finally renamed equivalent time "intrinsic time" (τ). For example, the first isotach line would represent the creep after one day and the second after 10 days et cetera. Therefore, isotaches are plotted lower in the $\sigma'-\epsilon$ graph and correspond to lower creep rates.

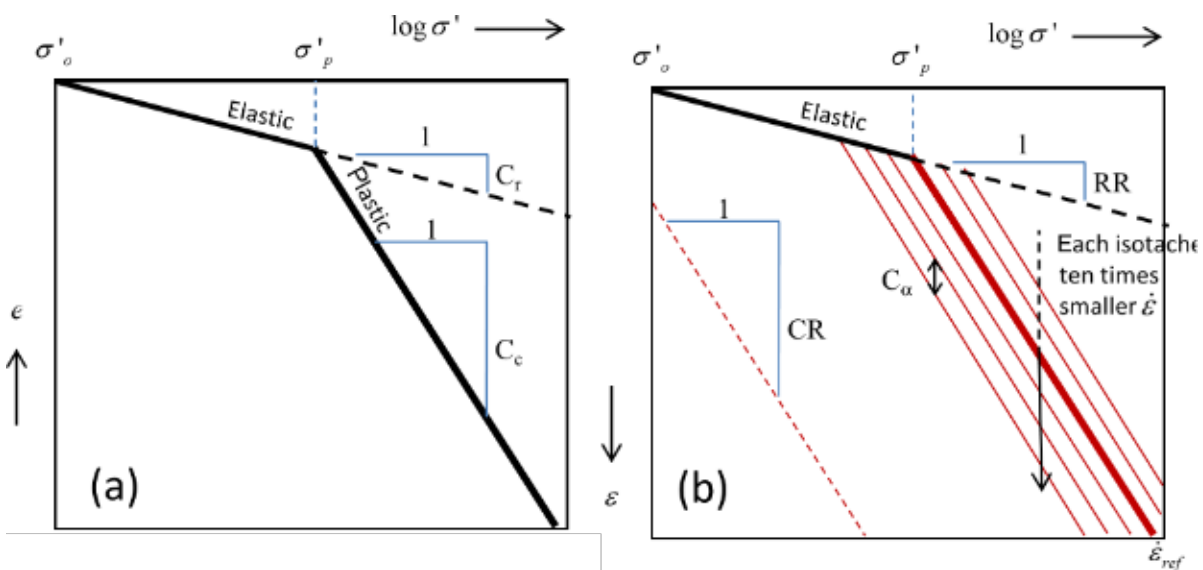


FIGURE 2.11: Comparison of effective stress diagrams in (a) Consolidation model (CM) and (b) Isotach model (IM).

NEN-Bjerrum model

Bjerrum (1967) implied that the creep rate increases by loading and reduces by unloading over time. Nowadays, **NEN-Bjerrum** is a significant conceptual framework used in geotechnical engineering to predict and understand subsidence phenomena. This model is based on the principle that the rate of subsidence of soil layers is proportional to the excess pore water pressure generated by the applied load. It considers the relationship between the rate of consolidation and the rate of dissipation of excess pore water pressure within the soil. Table 2.1 lists the relevant symbols for the **NEN-Bjerrum** model.

TABLE 2.1: NEN-Bjerrum model symbols in Roman and Greek alphabetical order, including units and descriptions.

Symbol	Unit	Description	Beschrijving
RR	[-]	Recompression or swelling Ratio	Recompressie Ratio
CR	[-]	Consolidation Ratio	Consolidatie Ratio
C_α	[-]	Creep ratio	Kruip ratio
OCR	[-]	Overconsolidation Ratio	Overconsolidatie Ratio
POP	[kNm ⁻²]	Pre-overburden pressure	Grensspanning - korrelspanning
e	[-]	Void ratio	Poriëngetal
ϵ	[-]	Strain	Rek
σ	[kNm ⁻²]	Total stress	Totale spanning
σ'	[kNm ⁻²]	Effective stress	Korrelspanning
σ'_p	[kNm ⁻²]	Pre-consolidation stress	Grensspanning
τ	[-]	Intrinsic time	Intrinsieke tijd

The **NEN-Bjerrum** relationship between strain, stress and intrinsic time is described by:

$$\epsilon = RR \cdot \log \left(\frac{\sigma'_p}{\sigma'_0} \right) + CR \cdot \log \left(\frac{\sigma'}{\sigma'_p} \right) + C_\alpha \cdot \log \left(\frac{\tau}{\tau_{ref}} \right) \quad (2.13)$$

From this main equation, the elastic and and creep strains dissected and are given:

$$\epsilon_e = RR \cdot \log \left(\frac{\sigma'_p}{\sigma'_0} \right) + RR \cdot \log \left(\frac{\sigma'}{\sigma'_p} \right) + RR \cdot \log \left(\frac{\sigma'}{\sigma'_0} \right) \quad (2.14)$$

$$\epsilon_{cr} = (CR - RR) \cdot \log \left(\frac{\sigma'}{\sigma'_p} \right) + C_\alpha \cdot \log \left(\frac{\tau}{\tau_{ref}} \right) \quad (2.15)$$

Subsequently, the intrinsic time τ and creep coefficient C_α define the creep strain rate $\dot{\epsilon}_{cr}$ through (Kooi et al., 2018). In Figure 2.11, each new isotach line represents a ten times smaller $\dot{\epsilon}_{cr}$.

$$\dot{\epsilon}_{cr} = \frac{\Delta \epsilon_{cr}}{\Delta t} = \frac{\log(e) \cdot C_\alpha}{\tau} \quad (2.16)$$

Input of initial over-consolidation in an **IM** is usually done via either an Over-Consolidation Ratio (**OCR**) value, which is the ratio between the pre-consolidation stress σ'_p and the effective stress σ' . Alternatively, it is calculated with the "pre-overburden pressure" value, which is the difference between σ'_p and σ' . Equation 2.17 calculates the equivalent age of a soil layer with the **OCR** and **NEN-Bjerrum** parameters (Visschedijk et al., 2009).

$$t_{age} = \tau_0 \cdot OCR^{\left(\frac{CR-RR}{C_\alpha} \right)} \quad (2.17)$$

Where τ_0 is the initial intrinsic time [days] of the concerning soil layer.

If the equivalent age of a soil is known and if the parameters of an **IM** are determined through a Cone Penetration Test (**CPT**), the **OCR** can be calculated. Parameterisation of the Groenekan case for **NEN-Bjerrum** parameters and the **OCR** is done in Section 4.4.

In this chapter, relevant information regarding Groenekan groundwater extraction is thoroughly discussed. In order to understand the process and effects of SGE at Groenekan, a system analysis is conducted in Section 3.1. In Section 3.2, the geohydrological profile of Groenekan is presented. Section 3.3 shows the historical extraction discharge and in Section 3.4 an explanation of the surface water system around Groenekan is given. Finally, this chapter provides the background to formulate six hypotheses, which are summed in Section 3.5 and further assessed in Chapters 5 and 6.

3.1. System Analysis

Groenekan is a Vitens drinking water extraction located 5 km north of Utrecht and was opened in 1961. Fourteen wells at a filter depth of -60 to -115 m NAP realise a current extraction discharge of approximately 5.0 Mm³/yr. For the argument of the available thesis time, Groenekan groundwater extraction was selected as the final scope location by weighing the following three criteria: 1) sensitivity to subsidence (based on geohydrological soil profile), 2) expansion plans, and 3) model availability. Appendix C.1 summarises the steps taken in selecting Groenekan. Figure 3.1 presents a map of the study area in the Province of Utrecht in the Netherlands, bounded within a 16x16 km area.

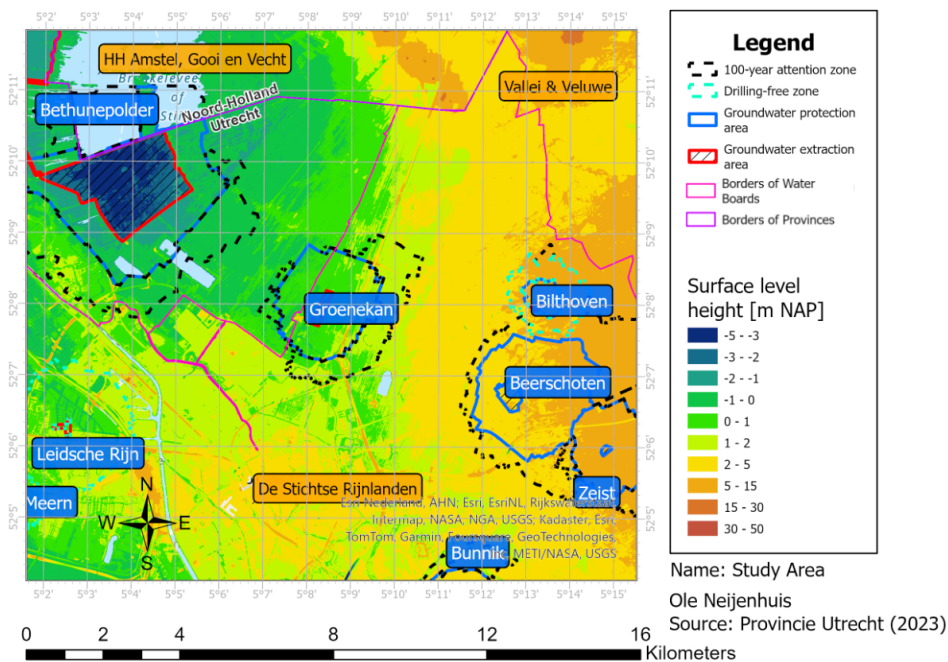


FIGURE 3.1: Study area map with Vitens groundwater extractions and surface level height [m NAP] (Provincie Utrecht, 2023).

The border to the Province of Noord-Holland in the north is coloured purple. In pink, the borders of Waterboard "Vallei & Veluwe" (V&V) in the north-east, Waterboard "Hoogheemraadschap De Stichtse Rijnlanden" (HDSR) in the south and Waterboard "Amstel, Gooi & Vecht" (AGV) in the north-west are given. Groenekan extraction is displayed in the centre, along with other surrounding extractions plus their corresponding protection areas and 100-year attention zones, where groundwater is less than 100 years en route to the extraction well (Provincie Utrecht, 2023). The surface level height varies from +10 m NAP in the east at Bilthoven to -3 m NAP in the west at the Bethunepolder. The region is divided

into several polders that each strive to keep water levels at a fixed Target Level Decision (TLD) (NL: *peilbesluit*) with a complex system of ditches, canals, weirs, and pumping stations, see Sub-section 2.3.2 for detailed explanation. Land use is given by the Bestand Bodemgebruik (CBS, 2017) and is a mixture of agriculture in rural polders, nature in the Utrechtse Heuvelrug and around the river Vecht, and urban environments such as Utrecht and Zeist (Figure A.5).

It is clearly visible that the surface level height varies from +30 m NAP in the east (Utrechtse Heuvelrug) to -3 m NAP in the west (Bethunepolder). Groenekan extraction is located at 0 m NAP. The groundwater level naturally follows the gradual change in surface level height from the elevated Utrechtse Heuvelrug (east) to the low-lying peatland area of the Bethunepolder (west), which is clearly recognisable in the isohypses in Figure A.3. The low groundwater levels in this polder have a strong suction effect on the groundwater in the vicinity of the polder, due to the low hydraulic heads. Also, Groenekan extraction creates a strong seepage effect toward the wells in deeper aquifers and a drawdown cone from the phreatic aquifer. The phreatic groundwater level is located at approximately -0.5 m NAP, thus half a metre below the surface level. Figure A.5 shows the land use for the study area, which is dominated primarily by agriculture.

3.2. Geohydrological Profile

Figure 3.2 shows the geohydrological profile of Groenekan and its surrounding extractions Bethunepolder and Beerschoten, which pump 30.0 and 8.0 Mm³/yr respectively (Provincie Utrecht, 2023). Similar to Groenekan, Beerschoten extracts its groundwater from the second aquifer. On the contrary, the Bethunepolder extracts from surface water and is continuously drained (NL: *bemaling*), causing seeps (NL: *wellen*) due to a head difference between the second aquifer and the phreatic aquifer above. To the east of Groenekan lies the propagated Ice Age deposit (code DTc in DINoloket) of the Utrechtse Heuvelrug. The upper layer of the lateral moraine (NL: *stuwwal*), the so-called “sliding surface”, has a high resistance *c* of approximately 10,000 days. On top of that, there is no surface water drainage system (NL: *poldersysteem*) present. Therefore, the infiltration to deeper layers is low, causing the precipitation surplus to drain laterally towards the west. Besides the superficial flow, deeper groundwater flows towards the west via the second aquifer. Figure 3.2 distinguishes the three different aquifers and the Waalre clay aquitard (Wak1) by cyan horizontal lines, the extractions are shown by filled blue arrows and the major groundwater flows by blue dashed arrows. In Appendix A.2, Figure A.6 shows two local ground drill (NL: *grondboring*) tests which confirm Figure 3.2. Furthermore, Table A.1 presents the various REGIS.II soil formations at Groenekan.

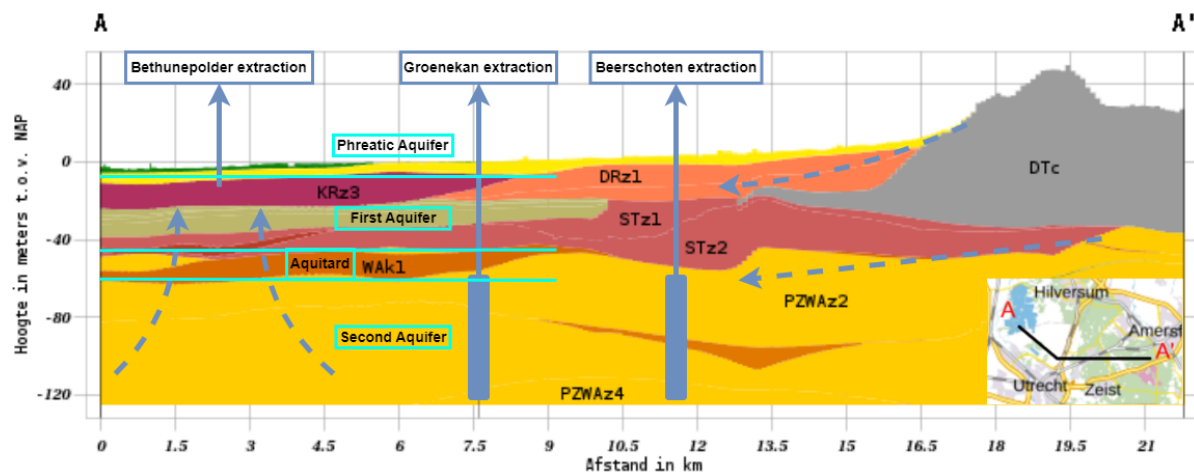


FIGURE 3.2: REGIS.II geohydrological profile of Groenekan from Bethunepolder in the north-west to Utrechtse Heuvelrug in the east (BRO, 2023b). It distinguishes three different aquifers and the Waalre clay aquitard (Wak1) by cyan horizontal lines, the extractions are shown by filled blue arrows and the major groundwater flows by blue dashed arrows.

Figure 3.3 illustrates a detailed cross-section of the top layer from +2 to -3 m NAP (TNO, 2023a). The peat (brown) and clay (green) Holocene top layer can evidently be distinguished, becoming thicker towards the west at the Bethunepolder and fading towards the east in the Utrechtse Heuvelrug.

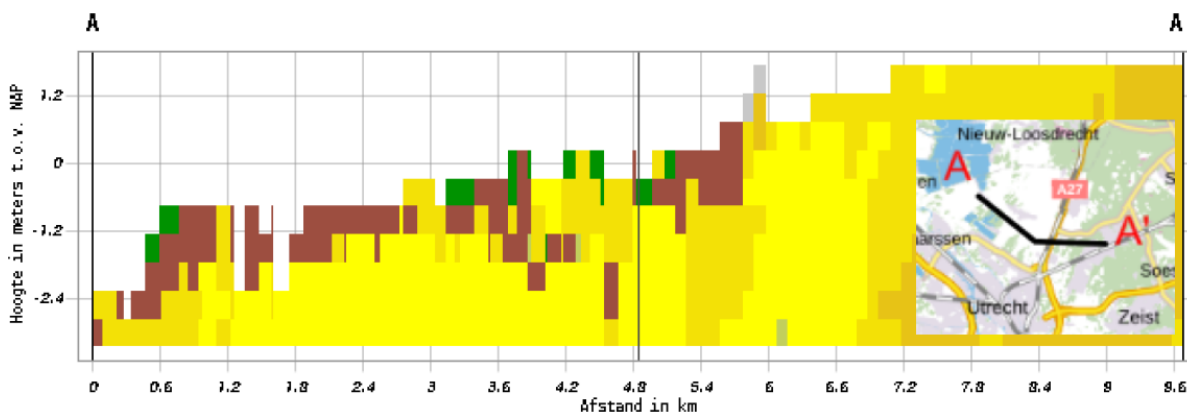


FIGURE 3.3: GeoTOP geohydrological profile of top layer around Groenekan from Bethunepolder in the north-west to Utrechtse Heuvelrug in the east (BRO, 2023a). Between +2 and -3 m NAP, peat, clay, and sand are coloured in brown, green, and yellow respectively.

Overall, Figures 3.2 and 3.3 show that four subsidence processes that should be considered for Groenekan. First, **SGE** through 1) consolidation and 2) creep of the Holocene top layer and Waalre aquitard is most likely to occur. Additionally, 3) **BDOM** and 4) shrinkage may play a role in the Holocene top layer. Geological processes should always be included, but are not considered the be part of **SGE**, since they are driven by the Earth's crustal movements. Compression by loading is almost negligible in the rural area of Groenekan, except to the south (urban area of Utrecht) and to the east (A27 highway).

Waalre & Sterksel Aquitards

The Waalre (WAK1) and Sterksel (STK1) deeper clay layers are aquitards in the geohydrological system of Groenekan. In Figure 3.4, the resistance of the Waalre clay layer is displayed. The Waalre clay is a thick clay layer at a depth of -48 to -60 m NAP and has a resistance of 1,000 to 2,500 days around Groenekan, with a maximum of 12,500 days under the Bethunepolder. This is a crucial ground layer, since it functions as a confining aquitard within the geohydrological system. The thickness of the clay decreases from approximately 20 m in the Bethunepolder to 12 m at Groenekan, and 0 m at Bilthoven (Figure 3.2). Furthermore, the Waalre clay is intersected by the north-south oriented gully (NL: *geul*) from Hilversum to De Bilt. As a result, the base of the complex soil composition of the Utrechtse Heuvelrug layer does not connect directly to the Waalre clay. Due to the gully, the phreatic aquifer is connected to the deeper aquifers, and groundwater exchange between those aquifers is possibly occurring.

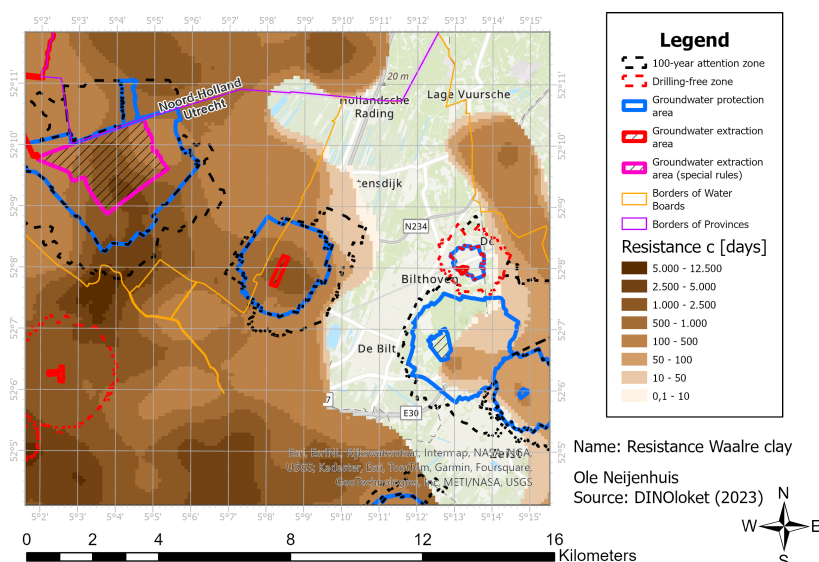


FIGURE 3.4: Resistance [days] of Waalre clay aquitard (WAK1) around Groenekan extraction (TNO, 2023a).

The Sterksel clay lies at a depth of -30 to -48 m NAP and has a resistance of up to 500 days (Figure A.8). The layer is broken up into smaller sections at varying depths. Providing the fragmentation and

relatively low resistance, the Sterksel clay will most likely have a minimal confining effect on vertical groundwater flow between the aquifers. Therefore, its effects are not considered in this study.

To support the claim of the confining effect of the Waalre aquitard, two groundwater streamline analyses (NL: *stroombaananalyses*) for 0.0 and 5.0 Mm³/yr are presented in Figure 3.5. These analyses show how groundwater flows in both the phreatic and deep aquifers and where the extracted water of Groenekan finds its origin for different extraction scenarios. Differences between both scenarios are highlighted with cyan circles. The superficial and deep groundwater flows described in Figure 3.2 (blue dashed lines) can be seen here as well. The water for Groenekan mainly comes laterally from all directions in the second aquifer. On the contrary, only east of Groenekan phreatic groundwater is seeping toward the deeper wells, since no confining Waalre and Sterksel aquitards are present there.

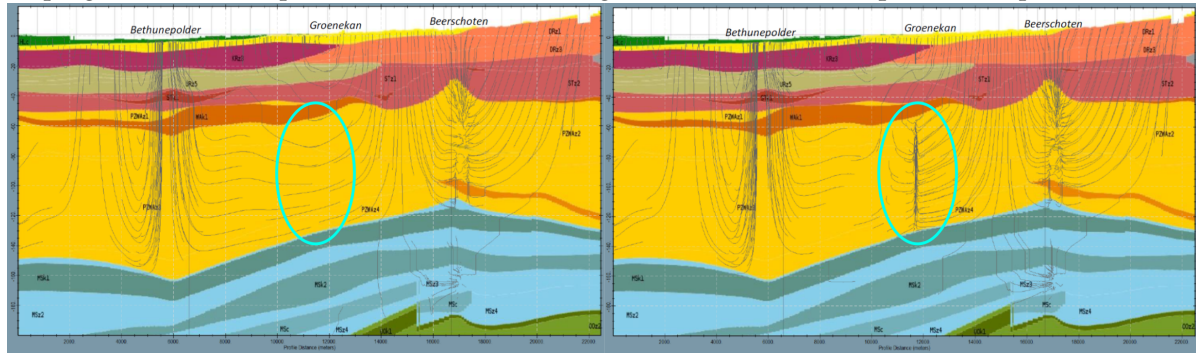


FIGURE 3.5: Groundwater streamline analysis of two different extraction scenarios for Groenekan (Arcadis, 2023). Left: 0.0 Mm³/yr. Right: 5.0 Mm³/yr. Differences highlighted in cyan circles.

Given the figures above, a high level of spatial heterogeneity for the thickness, soil type, and percentage of organic material of layers vulnerable to subsidence (Holocene peat/clay top layer and deeper Waalre clay aquitard) is shown. Toward the west, the Holocene and Waalre layers seem to increase in thickness and more peat is present, thus more organic content which is vulnerable to BDOM and shrinkage. However, from ~1 km east of Groenekan onward the Holocene and Waalre layers are not present anymore, and the soil only consists of sand. Therefore, subsidence calculations based on the geohydrological system around Groenekan should be handled with care.

3.3. Historical Groundwater Extraction Discharge

Figure 3.6 illustrates the annual groundwater extraction discharge of Groenekan from the opening in 1961 to 2023. The permitted discharge is included as well, which was 10.0 Mm³/yr until 2001, but due to prolonged drought effects on the Utrechtse Heuvelrug, the permit was reduced to 7.5 Mm³/yr from 2001 onwards (CLO, 2001).

Agricultural & Industrial Extractions

Other parties with extraction permits besides Vitens may play a role in the influence on the groundwater level and increasing the effective stresses in the deeper aquifers.

First, small extractions (< 100,000 m³/yr) for agricultural irrigation, greenhouse farming, cattle drinking water, and gardening are present around Groenekan and have the legal duty to register their extraction discharge (Unie van Waterschappen, 2021). However, in practice it is unknown how many farmers and inhabitants registered their wells. Therefore, little is known about how much groundwater is extracted in total from these extra private wells (CBS, 2023; Provincie Utrecht, 2022a; RIVM, 2023). However, Unie van Waterschappen (2021) has made an estimation of 50,000 m³ (1% of Groenekan extraction) for small extractions

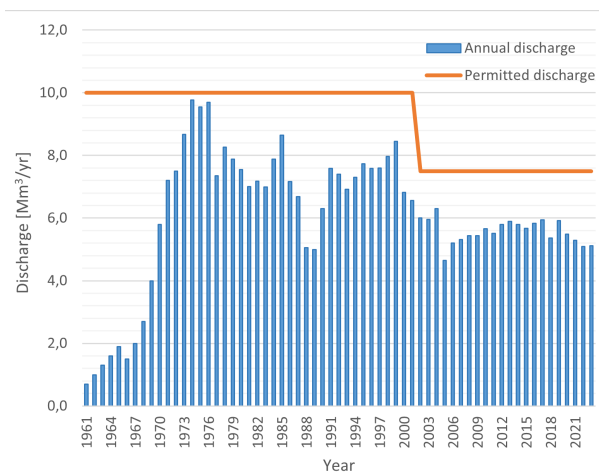


FIGURE 3.6: Annual extraction and permitted discharges of location Groenekan (Vitens, 2023).

within the service area of [HDSR](#), where Groenekan is located. Thus, the impact of these small extractions on the overall water balance is minimal and negligible compared to the 5.0 Mm³/yr that Vitens extracts in Groenekan. During conversations with employees of [HDSR](#) and [V&V](#), this statement was discussed and confirmed.

Second, large-scale industrial extractions (>150,000 m³/yr) need to have a permit for groundwater extraction (Provincie Utrecht, [2022a](#)). These extractions are mainly used for production of food/drinks or as cooling water within an industrial process. The closest industrial extraction to Groenekan is soda producer Vrumona in Bunnik with 200,000 m³/yr from the second and third aquifer (-60 to -140 m [NAP](#)). Unie van Waterschappen ([2021](#)) states that in reference year 2019, a total of ~88 Mm³ was extracted in the Province of Utrecht, from which ~85 Mm³ was pumped as drinking water and ~3 Mm³ as industrial extraction. This results in a share of 3.5% of industrial water use from the total extraction, which is negligible for the effects on the groundwater level. In summary, agricultural and industrial extractions play a minor role in the total groundwater extraction around Groenekan.

3.4. Surface Water System Polder Maartensdijk

Waterboard “Hoogheemraadschap De Stichtse Rijnlanden” ([HDSR](#)) is a Dutch water board and are obliged to publish and assess the [TLDs](#) of the low-lying polders, characterised by a dense pattern of ditches, in their entire service area. The [TLD](#) (NL: *peilvak*) of Maartensdijk, specifically subsection *MTD011*, includes Groenekan and dictates a summer level of -0.20 m [NAP](#) and a winter level of -0.40 m [NAP](#) ([HDSR, 2023](#)). Due to drought and high evaporation in summer, seepage and precipitation around Groenekan are retained as much as possible and additional water is brought from the Amsterdam Rhine Canal to maintain the [TLD](#) ([Arcadis, 2022](#); [KNMI, 2023c](#)). However, in winter, the [TLD](#) is lower and the precipitation surplus is drained into the Amsterdam Rhine Canal.

Older Dutch “Waterstaatskaarten” in [Table 3.1](#) show that the [TLD](#) of [TLD](#) Maartensdijk has slowly decreased in the past decades. Although the data are not complete, it shows that over the course of 112 years (1869-1981) the summer level of the [TLD](#) has dropped 70 cm, which may be translated to an average subsidence rate of ~6 cm/10yrs if one assumes the [TLD](#) follows the cycle of [Figure 2.7](#).

TABLE 3.1: Five historical “Waterstaatskaarten” and their corresponding target level decisions in summer (SL) and winter (WL), plus the incremental and total summer level [TLD](#) decrease ([Rijkswaterstaat, 2023a](#)).

No.	Year	SL [m NAP]	WL [m NAP]	Incremental / total SL TLD decrease [m]
#1	1869	+0.50	Unknown	-
#2	1920	+0.32	Unknown	0.18 / 0.18
#3	1952	0.00	-0.10	0.32 / 0.50
#4	1972	Unknown	Unknown	Unknown
#5	1981	-0.20	-0.40	0.20 / 0.70

Thus, the current 2008 [TLD](#) for Groenekan is similar to the fifth “Waterstaatskaart” of 1981, meaning that no [TLD](#) changes were made in the last 40 years. However, compared to the third “Waterstaatskaart” of 1952, the current [TLD](#) is 0.20 and 0.30 metres lower for summer and winter level respectively, which is not a large difference over 70 years.

In [Section 2.1](#), these two equations are applied to the case of Groenekan to understand the system and to analytically estimate what hydraulic head lowerings can be expected. Also, the analytical results are compared with the [AZURE](#) groundwater model.

3.5. Hypotheses

Six hypotheses were established from the Groenekan analysis of previous paragraphs. These are individually assessed and discussed in Chapters 5 and 6 to see whether the expectations comply with the results.

1. Hydraulic heads in the phreatic and second aquifer are similar where there no confining aquitard is present, and thus the extraction influences the phreatic groundwater level. However, the heads in the first and second aquifer differ where an aquitard is present in between;
2. Factors as the TLD, groundwater recharge, vegetation root uptake and drainage have significantly more influence on the phreatic groundwater level than deeper groundwater extraction;
3. Groenekan extraction causes the Holocene top layer and the Waalre clay aquitard to compress over time, due to an increase in effective stress in the soft soil particles. This compression manifests in the form of consolidation and creep;
4. Shrinkage and BDOM are expected to play a minor role around Groenekan, since there is a thin Holocene peat/clay layer present;
5. Expansion of Groenekan extraction will further decrease the phreatic groundwater level and hydraulic heads, which in turn results in higher effective stresses in the Holocene and Waalre layers and compress them even more;
6. Extreme climate scenarios with prolonged droughts and extreme precipitation events results in less groundwater recharge, more dry spells, and a lower groundwater level, thereby influencing the BDOM and shrinkage drivers.

Data & Models

The main objective of this research is to quantify the historical and future effects of groundwater extraction on subsidence around Groenekan. In this chapter, various datasets and models are explained which are used to calculate groundwater levels, heads, and [SGE](#) around Groenekan. First, Section [4.1](#) shows how the Bodemdalingskaart method can be adopted for historical subsidence data analysis. Furthermore, in Section [4.2](#) is explained how [AZURE](#) quantifies the differences in groundwater levels and heads. Next, Section [4.3](#) briefly describes the calculation method of [BDOM](#) and shrinkage in the Holocene top layer. Subsequently, the [AZURE](#) output from Section [4.2](#) is used as input for [D-Settlement](#) in Section [4.4](#), which computes the amount of settlement in the Holocene and Waalre layers through consolidation and creep. Lastly, Section [4.5](#) presents the formulation and approach for the modelling of eight future scenarios for Groenekan in [D-Settlement](#).

4.1. Bodemdalingskaart Measured Subsidence Data

Subsidence data are measured and collected through three methods: field measurements, remote sensing ([InSAR](#)), and photogrammetry data. Appendix [B.3](#) further elaborates on these three measurement methods. On top of that, four different methods are available to analyse historical subsidence data specifically for Groenekan:

1. Comparison of historical [TLDs](#) (1869-2008, field measurements);
2. Comparison of "Meetkundige Dienst" ([MD](#)) (1954-1970, field measurements) and [AHN4](#) data (2023, photogrammetry);
3. Historical peat oxidation maps (field measurements) (Provincie Utrecht, [2008](#), [2022b](#));
4. Bodemdalingskaart data (2017-2022, [InSAR](#)) (SkyGeo, [2023](#)).

The analysis of Bodemdalingskaart data is considered to be the most valuable and reliable method for determining historical subsidence. Although the data are only available for a short period, it has millimetre-scale accuracy and a dense point population. The methodologies and results of the other three historical subsidence analyses can be found in Appendix [E](#).

Subsidence and uplift data from Bodemdalingskaart are available in metres from the period of 4 October 2017 to 26 October 2022, approximately five years. Three filtering steps are done to create a reliable dataset:

1. Only descending orbit data;
2. Only persistent scattering data;
3. Only surface level data, no infrastructure and buildings;

First, Schouler and SkyGeo ([2023](#)) states that Bodemdalingskaart data points from an [InSAR](#) descending orbit satellite signal are more stable and reliable than from an ascending orbit. This is because there is more from atmospheric pollution and reflection in the afternoon and ascending orbits take place in the afternoon compared to the morning for the descending orbits. As a result, the signal-to-noise ratio is generally better for the descending orbit. Second, data points from persistent scattering are preferred over distributed scattering. Although points from distributed scattering tend to reflect more from the ground level and persistent scattering from objects or buildings, persistent scattering has a more accurate positioning. This is because the reflection back to the satellite is coming from a single point on the Earth's surface (Schouler & SkyGeo, [2023](#)), and often has a better signal-to-noise ratio as well. Third, the data points measured from the surface level are filtered from the buildings/infrastructure by subtracting the point's Digital Elevation Model (DEM) height from the actual point height. If the

difference between the actual and DEM height is greater than 2 metres, then the data point is assumed to be either a building or higher infrastructure and is excluded from the analysis. Buildings and infrastructure are founded on piles, which do not properly represent the subsidence of the surface level. The remaining data have vertical displacement values in the range of -13.32 to +6.20 cm/10yrs, which are reliable data values (Verberne et al., 2023). Also, the NAP revision in 2005 was taken into account for Groenekan (map sheet 31H), which was reduced by 8 mm compared to the previous NAP level (Rijkswaterstaat, 2005, 2023b).

4.2. AZURE Groundwater Model

The AZURE groundwater model is used to model the lowerings in phreatic groundwater level and head due to Groenekan extraction. Appendix C.2 elaborates on the steps taken in selecting the AZURE groundwater model.

4

4.2.1. Structure AZURE

The calibrated AZURE v1.03 is used as a base model. The model period is from 1 January 2004 to 31 March 2017. Both a "Gemiddeld Laagste Grondwaterstand" (GLG) and "Gemiddeld Hoogste Grondwaterstand" (GHG) are calculated, but the GLG is assumed to represent the groundwater level, because that is most extreme situation for subsidence calculations (Van Asselen et al., 2019). The initial inaccuracies in the geohydrological profile of Groenekan have been calibrated and tested, which makes the model ready to use (Arcadis, 2019). Appendix F, explains essential assumptions and conditions for using AZURE. In addition, Table F.1 lists essential packages for AZURE. In Table F.2, the REGIS.II soil formations are linked to AZURE layers.

4.2.2. Validation AZURE

The validation of AZURE's model performance is crucial to ensure the accuracy and reliability of the output. Arcadis (2019) calibrated and validated the model in a hydrological study. Moreover, to investigate whether Groenekan has a significant influence on measured head values, a Time Series Model (TSM) was made per piezometer in the Python package Pastas (Collenteur et al., 2019) by Artesia (2023). Analysis of TSMs in Pastas supports in the quantification of the effect of different stresses (rainfall, evaporation, river stages, groundwater extraction, etc.) and the detection of trends and outliers (Collenteur et al., 2019). These models were tested against evaluation criteria and compared with each other to finally select the best model. The final objective is to compare the head lowerings in Pastas with the results of the AZURE groundwater model. Hereby, it is validated whether the predicted AZURE effects are in line with the historical changes in the head due to the variation in the extraction discharges of Groenekan. Appendix D presents an additional explanation on understanding the Pastas tool and the methodology used for the case of Groenekan. Section 5.2.2 discusses the results of the study. It was determined that the model performs adequately to capture the hydrological effects of expanding the Groenekan extraction with the scenario simulations. Figure 5.4 shows that the measured hydraulic heads match versus the simulated ones, where the differences between a piezometer TSM and the AZURE results are within an acceptable range of ± 10 cm.

4.3. Analytical BDOM & Shrinkage Calculations

As explained in Section 2.2.2, two essential compaction processes are BDOM and shrinkage. In the case of Groenekan, both processes need to be considered, because the Holocene top layer could both consist of peat and clay. Thus, the groundwater level lowerings induced by Groenekan extraction may have an effect on both BDOM and shrinkage. For the BDOM and shrinkage calculations, two analytical approaches are used, whereas the consolidation and creep of the Holocene and Waalre layers are quantified with D-Settlement.

Based on a qualitative statement from Schothorst (1982) and a comparable study area and soil composition in Flevoland by Fokker et al. (2019), it was concluded that the modelling approaches (Equations 2.7 and 2.8) are reasonable to use for the quantification of BDOM and shrinkage. Values for V_{BDOM} , $\lambda_{r,BDOM}$, V_{sh} and $\lambda_{r,sh}$ for peat, organic clay, and clean clay, were found based on project data from Flevoland through ensemble smoothing with multiple data assimilation (Fokker et al., 2019). Table 4.1 shows the values found for these six parameters which are suitable for a NEN-Bjerrum calculation.

Taking **AZURE**'s **GLG** lowerings as a basis, **BDOM** and shrinkage plots are shown in Section 5.3.

TABLE 4.1: Estimated values for the parameters of the BDOM and shrinkage equations for peat, organic clay, and clean clay (Fokker et al., 2019). Number in the brackets is the standard deviation in units of the last digit.

Parameter - soil type	NEN-Bjerrum Estimate	Unit
V_{BDOM} – Peat	0.0123 (17)	m/m/year
$\lambda_{r,\text{BDOM}}$ – Peat	0.090 (30)	-
V_{sh} – Organic Clay	0.138 (6)	m/m/year
V_{sh} – Clean Clay	0.27 (2)	m/m/year
$\lambda_{r,sh}$ – Organic Clay	0.469 (12)	-
$\lambda_{r,sh}$ – Clean Clay	0.67 (2)	-

4.4. D-Settlement Subsidence Model

Deltares Settlement (**D-Settlement**) is used to model the consolidation and creep of the Holocene top layer and deeper Waalre aquitard in a 2D frame. Calculations within **D-Settlement** are done with the aid of the NEN-Bjerrum isotach model (**NEN-Bjerrum**) (Section 2.5.2). Furthermore, **AZURE**'s groundwater level and head lowerings over a distance to Groenekan are essential inputs for the **D-Settlement** model, since they play an important role in determining the total amount of settlement over time. Appendix C.3 summarises the steps taken in selecting the **D-Settlement** subsidence model.

4.4.1. Structure D-Settlement Groenekan Base Scenario

Table 4.2 presents the overall **D-Settlement** model structure for the Groenekan base scenario, which consists of fifteen layers. With L1 as the phreatic Holocene aquifer, L2 is the first aquifer, L3-14 for the Waalre clay aquitard, and L15 as the second aquifer under the Waalre clay where extraction takes place. Furthermore, it is deemed favourable to discretise of the aquitard in multiple layers to enhance the accuracy of the subsidence output (Visschedijk et al., 2009), therefore the aquitard is divided into twelve layers of 1 m thickness.

TABLE 4.2: Fifteen layer D-Settlement model structure for base scenario Groenekan extraction. Including soil type, depth in NAP and geohydrology.

Layer	REGIS.II formation	Soil type	Depth [m NAP]	Geohydrology
1	Holocene	Sandy clay	0 to -1	Phreatic aquifer
2	Drente, Urk	Medium dense sand	-1 to -48	First aquifer
3-14	Waalre	Sandy clay	-48 to -60	Aquitard
15	Peize & Waalre	Dense sand	-60 to -140	Second aquifer

Two **D-Settlement** models are built: one over western distance to Groenekan and one over eastern distance. Hereby, spatial effects of the extraction on settlement are clarified in two directions. In Appendix H, both model structures are visualised in Figures H.1 and H.2. Also, Table H.1 lists the **D-Settlement** model parameter values for the four main soil layers in the base scenario.

DINOlaket shows that weakly sandy clay is the most common soil type around Groenekan for the Holocene and Waalre layers. Therefore, both the Holocene top layer and the Waalre clay are assumed to be "weakly sandy clay". Other considered soil types and their corresponding **NEN-Bjerrum** parameters are listed in Tables H.2 and H.3. Other assumptions within **D-Settlement** are found in Appendix H.2.

4.4.2. Sensitivity Analyses D-Settlement

Three sensitivity analyses for the **D-Settlement** base scenario model of Groenekan are performed to measure how susceptible the output of **D-Settlement** is to alterations in the value of the inputs:

- Groundwater level and head lowerings;
- Thickness of Holocene and Waalre layers;
- Soil type of Holocene top layer (from Table H.2).

For each sensitivity analysis, one parameter is altered in the model runs to isolate its effect on the final subsidence. Ideally, a 3D transient model visually maps and models the subsurface layers and the subsidence over space and depth. However, the **D-Settlement** model is a 2D simplification of reality, and sensitivity analyses help to put the output into perspective if conditions are slightly different from the assumed base scenario. The results of the three sensitivity analyses are presented in Section 5.4.2.

4.4.3. Validation D-Settlement

As mentioned in Section 4.1, the **D-Settlement** results can be validated by comparing it to Bodemdalingskaart subsidence data of the period 2017 to 2022. However, it should be noted that the Bodemdalingskaart method includes subsidence through **BDOM**, shrinkage, and other influences, since the total subsidence is derived from **InSAR** data. However, **D-Settlement** focuses solely on consolidation of the Holocene top layer and deeper Waalre clay, plus the long-term creep of the whole system. Therefore, **BDOM** and shrinkage calculations are performed in Section 5.3 in addition to the **D-Settlement** calculations to obtain a complete picture of **SGE** around Groenekan.

4.5. Future Scenarios Groenekan

To measure how the **SGE** around Groenekan develops from the base scenario onward, eight future scenarios until the year 2100 are designed in **D-Settlement**. The scenarios consist of two variable components: two **KNMI** climate scenarios and four extraction discharges for Groenekan. The **KNMI** (2023b) climate scenarios show what the Netherlands will face in the year 2100 if greenhouse gas emissions continue to increase at the current rate until 2080 (high emissions). They also show that the rate of climate change will be lower if the world abides by the Paris Climate Agreement of 2015 (low emissions).

The High emissions & Desiccation (**HD**) and Low emissions & Wetter (**LW**) climate scenarios are chosen to have a comparison between two extremities. On the one hand, a scenario that becomes drier and hotter through high emissions. On the other hand, a scenario which maintains a relatively similar temperature, with a slightly wetter climate. Table 4.3 shows the temperature, precipitation, and evaporation data expected for the year 2100 for the two scenarios (**KNMI**, 2023a).

TABLE 4.3: **KNMI** (2023a) HD and LW data for the Netherlands in the year 2100 compared to the climatology of 1991 to 2020.

Period	Variable	Indicator	Climatology 1991-2020	2100 LW	2100 HD
Dutch temperature rise relative to 1991-2020			10.5 °C	+0.9 °C	+4.4 °C
Year	Precipitation	Average amount	851 mm	+3%	-3%
		10-day precipitation sum for T = 10 years	127 mm	+3%	+8%
	Evaporation	Potential evaporation	603 mm	+6%	+17%

Although previous studies have explored the effects of temperature, precipitation and evaporation on groundwater recharge, the long-term effect of climate change on the groundwater level remains unclear. This long-term effect on changes in groundwater level until the year 2100 has not been studied by anyone in the Netherlands thus far and is therefore beyond the scope of this research. However, it is essential to translate the **KNMI** (2023a) data into a change in groundwater level, so that **D-Settlement** can calculate different final settlements of the Holocene and Waalre layers and compare the effect of groundwater level change to a higher extraction discharge. Therefore, it is assumed that a change in groundwater recharge equals a change in groundwater level according to a simple equation:

$$R = P - E \quad (= \Delta GWL) \quad (4.1)$$

Where R is the recharge, P is precipitation, and E is evaporation, all in percentage changes. Assuming each percentile change in recharge is equal to a centimetre of groundwater level change, the groundwater level lowering due to climate change can be quantified. Equations 4.2 and 4.3 give approximations of ΔGWL_{HD} and ΔGWL_{LW} , two future groundwater levels for the **HD** and **LW** scenarios relative to the current groundwater level of -0.50 m **NAP**. The calculations are based on the data from Table 4.3:

$$\Delta GWL_{HD} = (P_{2100} - P_c) - (E_{2100} - E_c) = -3\% - 17\% = -20\% = \mathbf{-20 \text{ cm}} \quad (4.2)$$

$$\Delta GWL_{LW} = (P_{2100} - P_c) - (E_{2100} - E_c) = +3\% - 6\% = -3\% = -3 \text{ cm} \quad (4.3)$$

Where P_{2100} is the percentile change in precipitation in 2100 compared to the current precipitation P_c . E_{2100} is the percentile change in evaporation in 2100 compared to the current evaporation E_c . Compared to the equilibrium groundwater level of -0.50 m [NAP](#), the projected groundwater levels are -0.70 and -0.53 m [NAP](#) for the [HD](#) and [LW](#) scenarios respectively.

Combining the [HD](#) and [LW](#) climate scenarios with four extraction discharges for Groenekan (0.0, 5.0, 7.5, and 10.0 Mm^3/yr), give eight future scenarios. Subsequently, these eight future scenarios are implemented in [D-Settlement](#) to generate results and see how the subsidence develops until the year 2100. By considering 0.0, 5.0, 7.5, and 10.0 Mm^3/yr extraction discharges and two extreme climate scenarios, a bandwidth is created between which the future subsidence will lie. Assumptions and conditions for the [D-Settlement](#) future scenario experiments are listed in Appendix [H.2](#). The results of the experiments are presented in Section [5.6](#).

Section 5.1 illustrates the historical Bodemdalingskaart subsidence results around Groenekan in GIS. Next, Section 5.2 visualises the groundwater level and head lowerings around Groenekan from AZURE. Subsequently, these data were used in Sections 5.3 and 5.4, displaying the output of BDOM, shrinkage, consolidation and creep in the Holocene and Waalre layers. Lastly, subsidence predictions for the future scenarios in Groenekan are shown in Section 5.6.

5.1. Bodemdalingskaart

After the filtering of persistent scattering, descending orbit, and surface level data, 14,861 InSAR points were investigated. Figure 5.1 presents a histogram, including 19 bins and their count, on the distribution of subsidence or uplift around Groenekan. The mean μ of all points is -0.99 cm/10yrs and the standard deviation σ is 1.28.

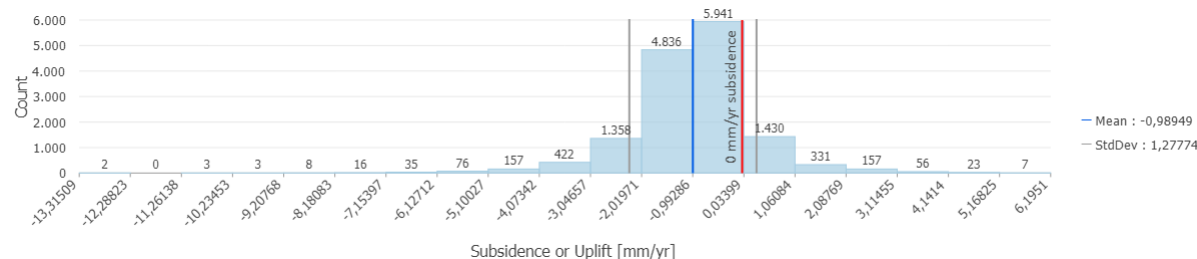


FIGURE 5.1: Distribution histogram of subsidence or uplift rates around Groenekan, divided over 19 bins. 0-subsidence line is plotted in red, mean μ in blue and the standard deviation σ in grey.

In Figure 5.2, all data points that fall within a radius 5 km of Groenekan are plotted.

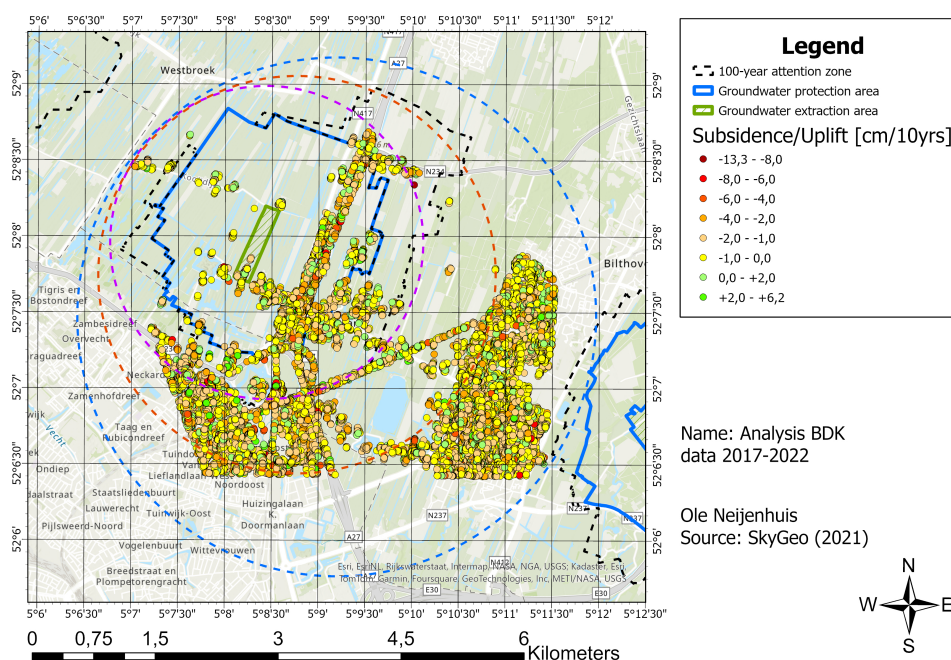


FIGURE 5.2: Subsidence and uplift data points [cm/10yrs] within three circles with 1, 2, and 3 km radii (SkyGeo, 2023).

It is attempted to isolate the effects of Groenekan, so that conclusions can be drawn from this data. The groundwater protection area and three circles with 1, 2, and 3 km radii (purple, orange, and blue dashed circles respectively) have been plotted within the map and the data within the four circles are analysed. Data points are categorised in eight legend classes, from dark red for high subsidence rates to bright green for high uplift rates. The points seem to be evenly scattered throughout the area. Unfortunately, hardly any data were available in the peatland meadow areas to the west and north of Groenekan, since vegetation poorly reflects satellite signals (Section B.3). Table 5.1 compares the data points within each area, so it can be investigated if subsidence decreases over a distance further from Groenekan. The similar mean subsidence rates, irrespective the distance to Groenekan, seem to prove that the groundwater extraction has little effect on subsidence during the period 2017 to 2022.

TABLE 5.1: Bodemdalingskaart data analysis around Groenekan (GK) in four areas increasing in size.

Area	No. of points	Mean subsidence rate [cm/10yrs]	Standard deviation σ
Protection area GK	2,517	-0.95	1.46
1 km radius	4,437	-1.00	1.49
2 km radius	8,676	-1.03	1.39
3 km radius	14,861	-0.99	1.28

5

5.2. Groundwater Level & Hydraulic Head

5.2.1. AZURE

Four extraction discharge scenarios (0.0, 5.0, 7.5, and 10.0 Mm³/yr) gave simulated groundwater level and head lowerings around Groenekan extraction location spatially (in a 25x25 metre grid) and temporally (from 2004 to 2016). The comparison of 5.0 vs. 0.0 Mm³/yr extraction is shown in Figure 5.3. It shows the differences in head for the GLG in AZURE model layers 1, 6, and 11. Where L1 represents the phreatic Holocene top layer, L6 is the layer above the Waalre clay in the first aquifer (-40 m NAP), and L11 is located below the Waalre clay in the second aquifer (-65 m NAP), where Groenekan extraction takes place. In addition, scenarios 7.5 and 10.0 Mm³/yr are compared to 5.0 Mm³/yr to investigate how much more the groundwater level and heads will be lowered if Groenekan is expanded. Both overviews are presented in Figures F.1 and F.2.

The following points are observed in Figure 5.3:

- Phreatic groundwater lowerings up to ~30 cm and head lowerings of ~1.5 m;
- Lowerings of the phreatic groundwater level (L1) and heads in the first aquifer (L6) occur mainly to the east of Groenekan;
- Head differences are more symmetrical and severe in the second aquifer, with ~1.5 m of head difference around the wells and a maximum influence circle of ~8.5 km;
- Heads from the analytical calculations in Figure 2.1 are slightly higher than the results from AZURE. This is because the analytical approach assumes a fully confining Waalre aquitard, which is not the reality.

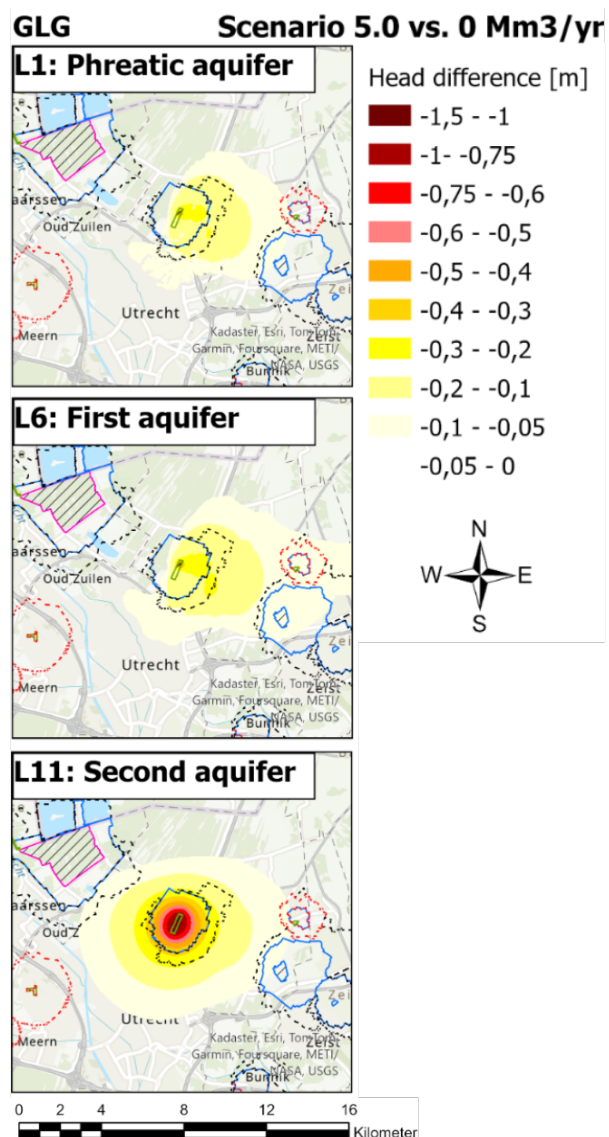


FIGURE 5.3: 5.0 vs. 0.0 Mm³/yr extraction: Differences in head for the GLG in AZURE model layers 1, 6, and 11.

5.2.2. Pastas Time Series Models

Piezometer TSMs from Python tool Pastas are essential in understanding the impact of different stresses (groundwater extraction, precipitation, evaporation, et cetera) on hydraulic heads (Artesia, 2023). An essential requirement in the study was that only filter depths of piezometers below -10 m NAP were taken to exclude phreatic measurement data. Due to the complex interaction with surface water and meteorological influences in the heterogeneous Holocene aquifer, phreatic measurements are expected to be less useful to estimate the influence of Groenekan on phreatic groundwater levels (Artesia, 2023). Appendix D presents the methodology and other results regarding TSM analysis around Groenekan.

Comparison Pastas vs. AZURE

TSMs head lowerings were compared with the results of AZURE to see if there is any agreement between the two models. Figure 5.4 shows the results of the comparison, with on the x-axis the head lowering in the TSMs and on the y-axis the lowering in AZURE. In the analysis, only reliable models were considered. There seems to be a good match between the TSM and AZURE results, since most dots are located close to the dashed "zero-line", where TSM = AZURE. The differences are mainly between 5 and 10 cm. The rejected models have been included to analyse whether the models perhaps still provide a plausible estimate of the head lowering due to extraction. The colour of the dots indicates in which geohydrological layer the piezometer filter is located. The filled dots indicate that the TSM was considered reliable, whereas the unfilled dots represent rejected TSMs.

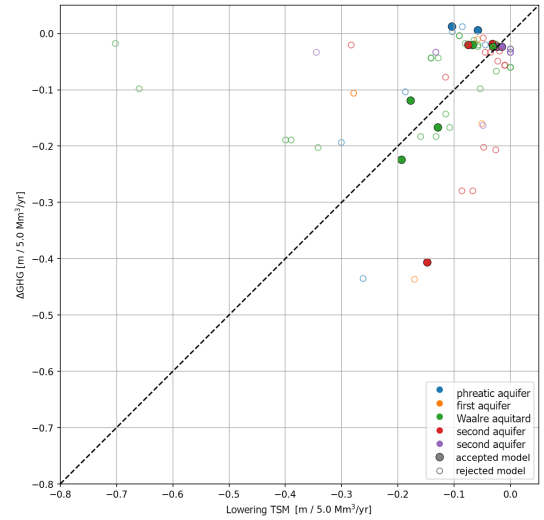


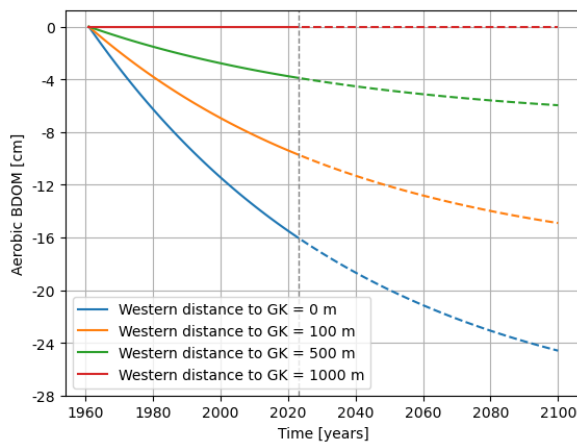
FIGURE 5.4: Head lowerings in four geohydrological layers. Piezometer TSMs (x-axis) plotted against AZURE results (y-axis) for scenario 5.0 Mm³/yr (Artesia, 2023).

5.3. Analytical BDOM & Shrinkage

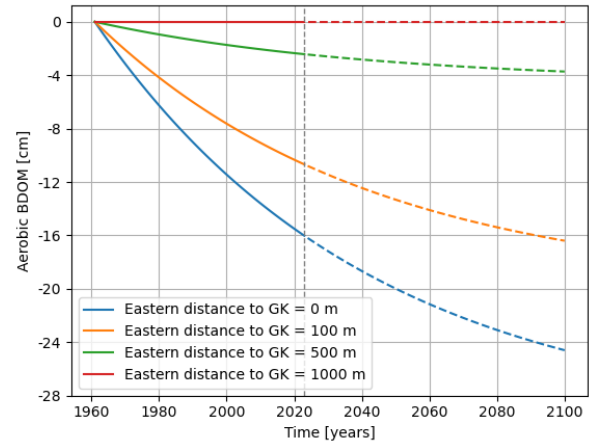
Equations 2.7 and 2.8 are used to calculate the potential BDOM and shrinkage to the west and east of Groenekan over time. Tables G.1 and G.2 list the total BDOM and shrinkage results for each distance to Groenekan. Underlying Python scripts for the calculations are found in Appendices I.2 and I.3.

5.3.1. BDOM

Figure 5.5 illustrates the potential subsidence due to aerobic BDOM in centimetres for the period 1961–2023 (solid lines) and 2023–2100 (dashed lines), assuming a clean peat top layer. Sub-figure 5.5a gives the BDOM west of Groenekan, whereas Sub-figure 5.5b to the east of Groenekan. Table G.1 lists the total aerobic BDOM and the BDOM rate [cm/10yrs] results for four distances to Groenekan.



(A) Aerobic BDOM west of Groenekan.



(B) Aerobic BDOM east of Groenekan.

FIGURE 5.5: Aerobic BDOM graphs of Holocene peat top layer with four distances to Groenekan for period 1961 to 2100. The year 2023 is shown with a grey dotted vertical line and future BDOM is plotted in dashes from 2023 onwards.

The western and eastern results 100 and 500 m from Groenekan slightly differ. **BDOM** has a small degradation velocity V_{BDOM} and residual thickness $\lambda_{r,\text{BDOM}}$. Therefore, the **BDOM** process still continues after 2100 if groundwater level lowerings are maintained.

5.3.2. Shrinkage

Figure 5.6 shows the potential subsidence caused by shrinkage in centimetres from 1961 to 2023. Both clean clay (Sub-figures 5.6a and 5.6b) and organic clay, a mixture of peat and clay (Sub-figures 5.6c and 5.6d), are assumed as a top layer.

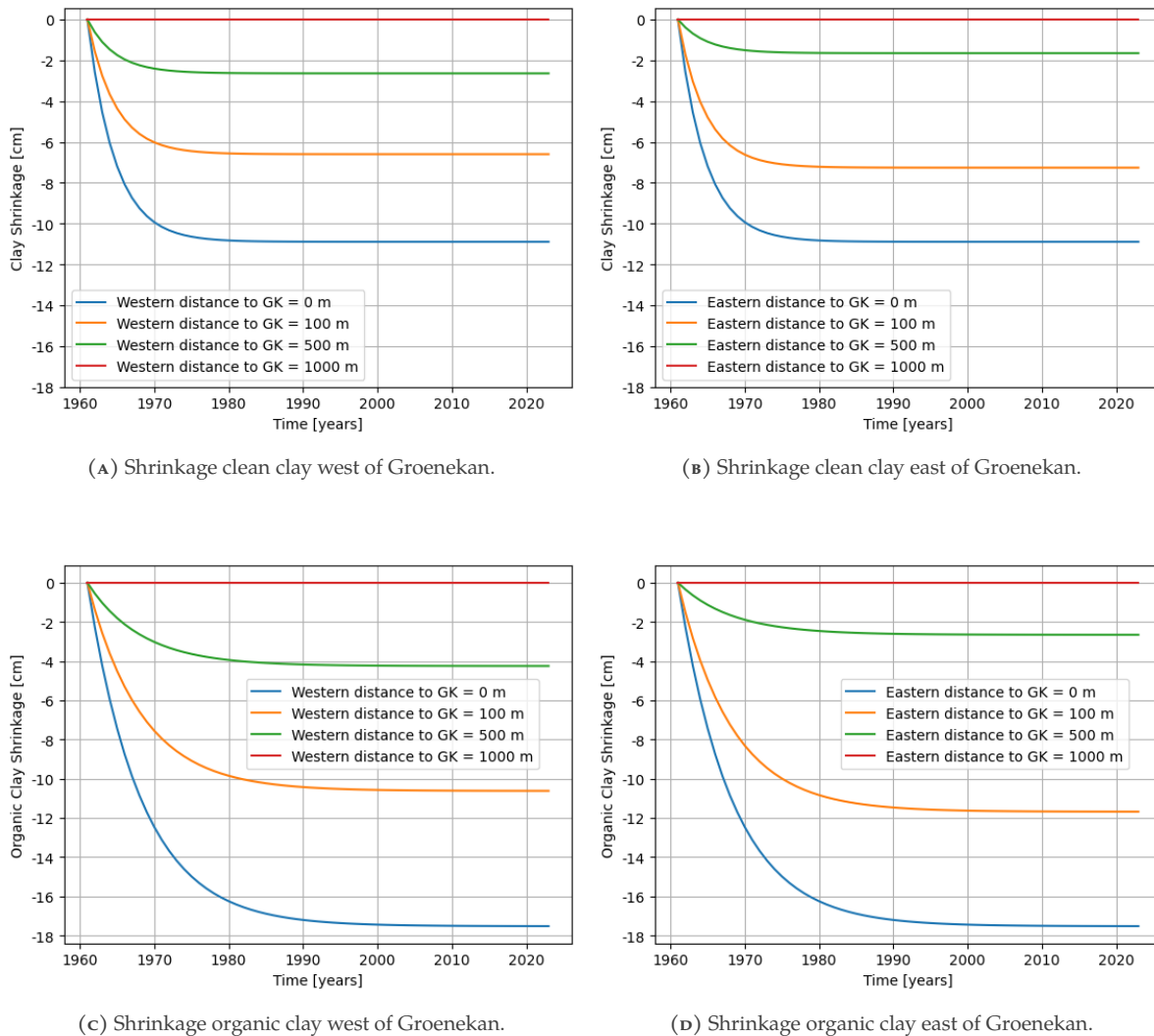


FIGURE 5.6: Shrinkage graphs of the Holocene top layer with four distances to Groenekan for period 1961 to 2023.

It is evident that more than half of the exposed Holocene eventually shrinks and compacts at Groenekan. The most striking result to emerge from Figure 5.6 is that the final settlements are reached in 1975 and 1990 for clean and organic clay respectively. Therefore, no additional analysis of year 2100 needs to be made, since all shrinkage occurs well before then.

5.4. Consolidation & Creep in Holocene and Waalre Layers

In this section, the compression of the Holocene and Waalre layers due to consolidation and creep are computed with **AZURE** and **D-Settlement** and is illustrated in settlement-time graphs. This is done for the base scenario (Section 4.4.1), west and east of Groenekan over the period 1961 to 2023. Furthermore, the results of three sensitivity analyses are discussed.

5.4.1. Settlement Groenekan Base Scenario

Figures 5.7 and 5.8 show linear settlement-time graphs to the west and east of Groenekan respectively. With the aid of the AZURE GLG data in Figure 5.3 and Tables F.3 and F.4, settlements were calculated and plotted at distances of 0, 100, 500, 1,000, 2,500, and 5,000 m from Groenekan.

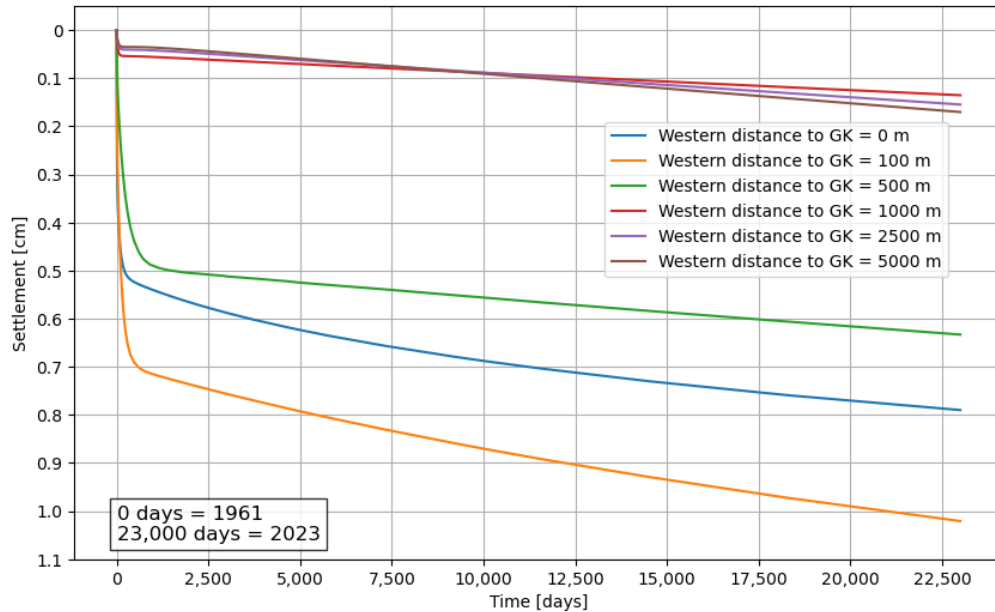


FIGURE 5.7: Settlement-Time linear graphs: Base scenario west of Groenekan over the period 1961 to 2023. The six coloured graphs represent a different distance to Groenekan.

The following key insights to the west of Groenekan are found:

- Maximum final settlement is ~1.0 cm at 100 m west of Groenekan;
- From 500 m western distance onwards, the settlements become negligible;
- At ~12,000 days, the settlement for the 5,000 m distance graph exceeds the 1,000 m graph;
- Consolidation contributes ~75% to the final settlement, creep ~25%;
- Consolidation of the Holocene layer occurs within first ~250 days;
- Slow creep rates (in the order of 0.01 to 0.05 cm/10yrs) from 250 to 23,000 days.

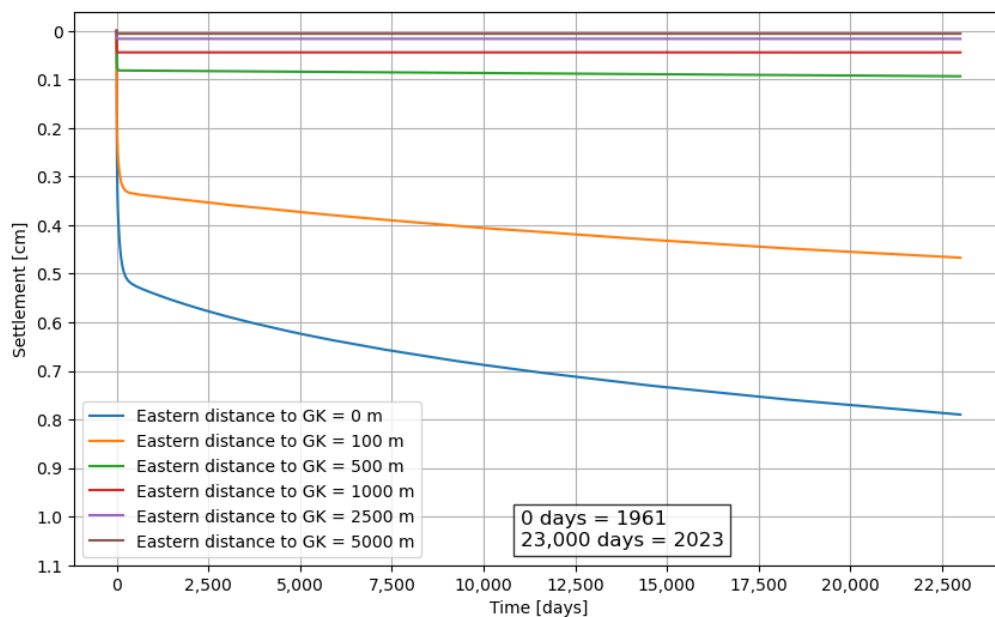


FIGURE 5.8: Settlement-Time linear graphs: Base scenario east of Groenekan over the period 1961 to 2023. The six coloured graphs represent a different distance to Groenekan.

The following key insights to the east of Groenekan are found:

- Maximum settlement is ~ 0.8 cm at Groenekan;
- From 100 m eastern distance onwards, the settlements become negligible;
- Similarly to the west of Groenekan, equal consolidation and creep behaviour is observed.

5.4.2. Sensitivity Analyses Groenekan Base Scenario

Three sensitivity analyses for the Groenekan base scenario model from 1961 to 2023 computed in **D-Settlement** are presented in this section. The groundwater level and head, soil thickness and soil types are varied to measure how susceptible the output of **D-Settlement** is to alterations in the value of the inputs.

Groundwater Level and Head Lowerings

Figure 5.10 shows the sensitivity analysis for ten variations in groundwater level and head lowerings at Groenekan base scenario over the period 1961 to 2023. All results are presented in Table H.6.

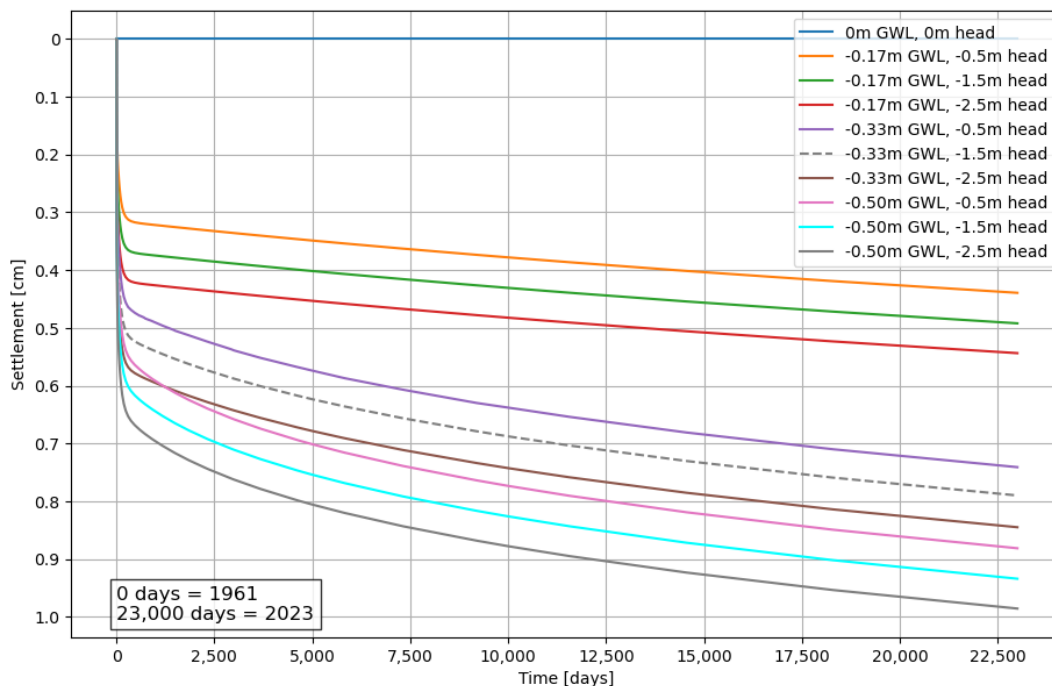


FIGURE 5.9: Settlement-Time linear graphs: Sensitivity analysis groundwater level and head lowerings for Groenekan base scenario (grey dashed). The ten coloured graphs represent different lowering variations.

Figure 5.9 illustrates considerable differences between each different groundwater level and head scenario. The final settlement is more sensitive to changes in groundwater level than in head. Compared to the base scenario (dotted grey graph), a 0.17 m groundwater level increase (green graph) has a relatively larger settlement reduction than an additional 0.17 m groundwater level lowering (cyan graph) which causes extra settlement.

Thickness of Holocene and Waalre Layers

Figure 5.10 presents the sensitivity analysis for eight variations in Holocene and Waalre layer thicknesses at Groenekan base scenario over the period 1961 to 2023. The eight scenarios are based on the most-probable **DINOloket** data (Figure 3.2). All results are presented in Table H.7.

Figure 5.10 shows a trend in line with expectations: the thicker the Holocene and Waalre layers become, the more settlement occurs. However, a change in the Holocene thickness has a significantly greater impact than a change in the Waalre thickness. Also, doubling the thicknesses has relatively more effect than halving the thicknesses.

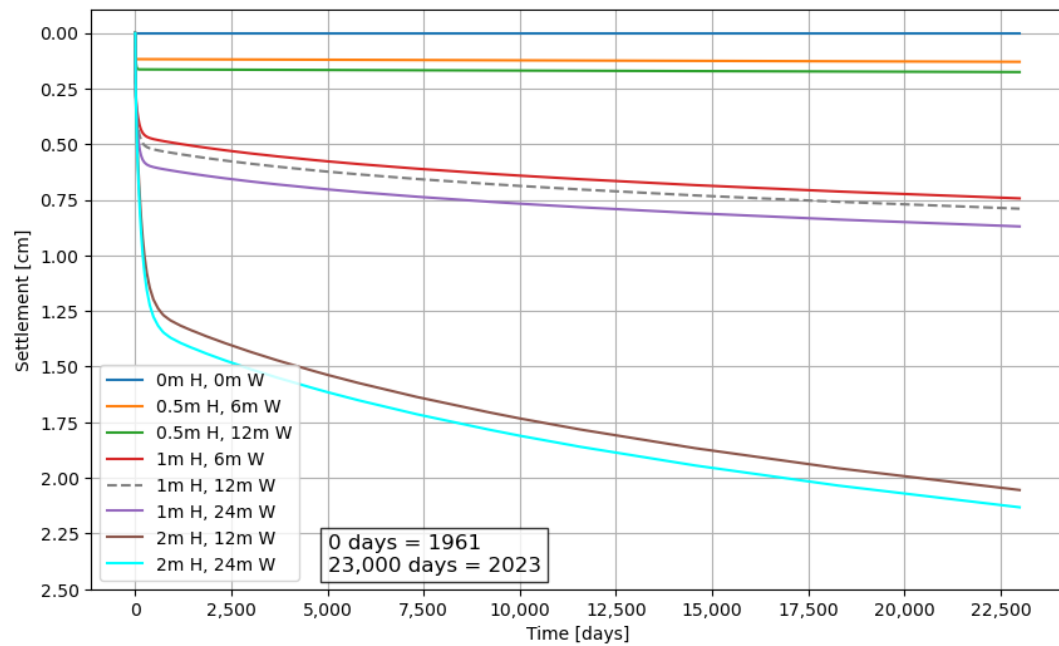


FIGURE 5.10: Settlement-Time linear graphs: Sensitivity analysis layer thickness for Groenekan base scenario (grey dashed). The eight coloured graphs represent different thickness variations for the Holocene (H) and Waalre (W) layers.

Soil Type of Holocene Top Layer

Figure 5.11 shows the sensitivity analysis for five Holocene soil types at Groenekan base scenario over the period 1961 to 2023. All results are presented in Table H.8.

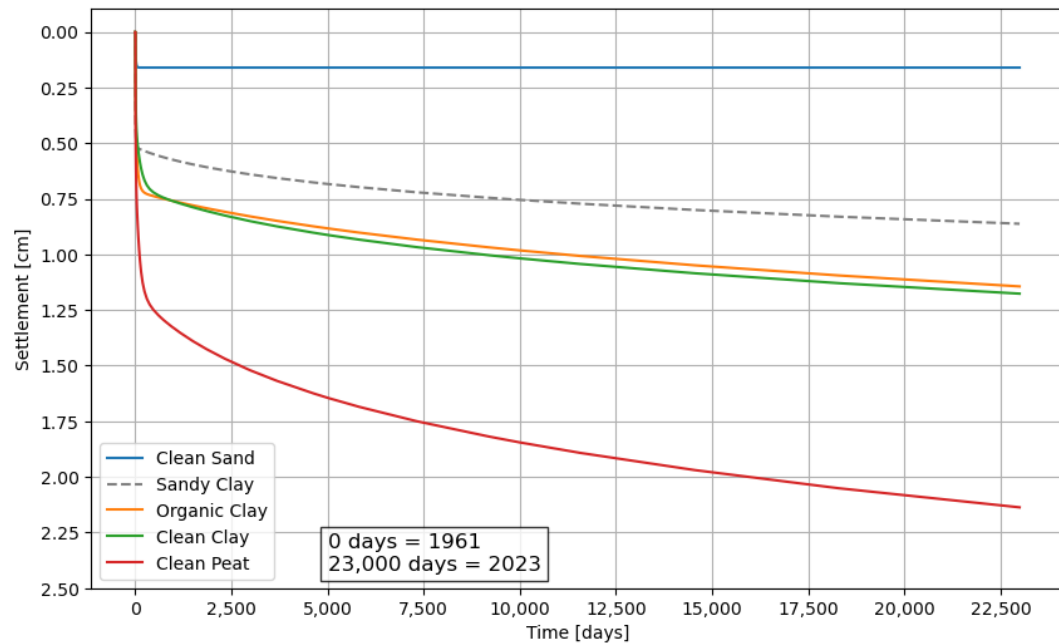


FIGURE 5.11: Settlement-Time linear graphs: Sensitivity analysis Holocene soil type for Groenekan base scenario (grey dashed), including 0.16 cm Waalre settlement. The five coloured graphs represent a different soil type for the Holocene top layer.

In Figure 5.11, the soil type medium clean sand gives a negligible settlement of 0.001 cm and proves that sand is not sensitive to consolidation and creep. The residual 0.16 cm settlement visible in the blue graph, is due to compression of the Waalre clay. Compared to the base scenario with sandy clay, both organic and clean clay give larger, similar settlements of ~ 1.1 and 1.2 cm respectively. Clean peat settles significantly the most with ~ 2.1 cm and has the longest consolidation phase of ~ 500 days.

5.5. Modelled SGE & Bodemdalingskaart Validation

In this section, the modelled **SGE** results from the base scenario are validated with the measured Bodemdalingskaart data. Furthermore, this section is used as a bridge to the discussion and conclusion chapters. Figure E.4 shows an additional comparison of the **MD** vs. **AHN4** data (1961 to 2023) with the modelled **SGE**. The raw settlement results are presented in Appendix H.4.

In Figure 5.12 and Table 5.2, an overview of all results obtained 5 km west and 5 km east of Groenekan is shown, which are re-scaled to the period 2017 to 2022 such that comparison with Bodemdalingskaart is possible. Sub-figure A) illustrates the geohydrological profile together with the modelled **AZURE** groundwater level and head lowerings. Note that the y-axis of this plot is not scaled to improve visualisation. Also, Sub-figure B) shows the cumulative subsidence rate in cm/10yrs of all relevant subsidence processes (compression of Waalre and Holocene, geological processes, and **BDOM**), which is then validated with the measured Bodemdalingskaart data. Note the geological processes occur irrespective of groundwater extraction, therefore they are not categorised as **SGE**. The graph which includes **BDOM** is shown in dotted red, since a clean peat Holocene top layer cannot be confirmed around Groenekan.

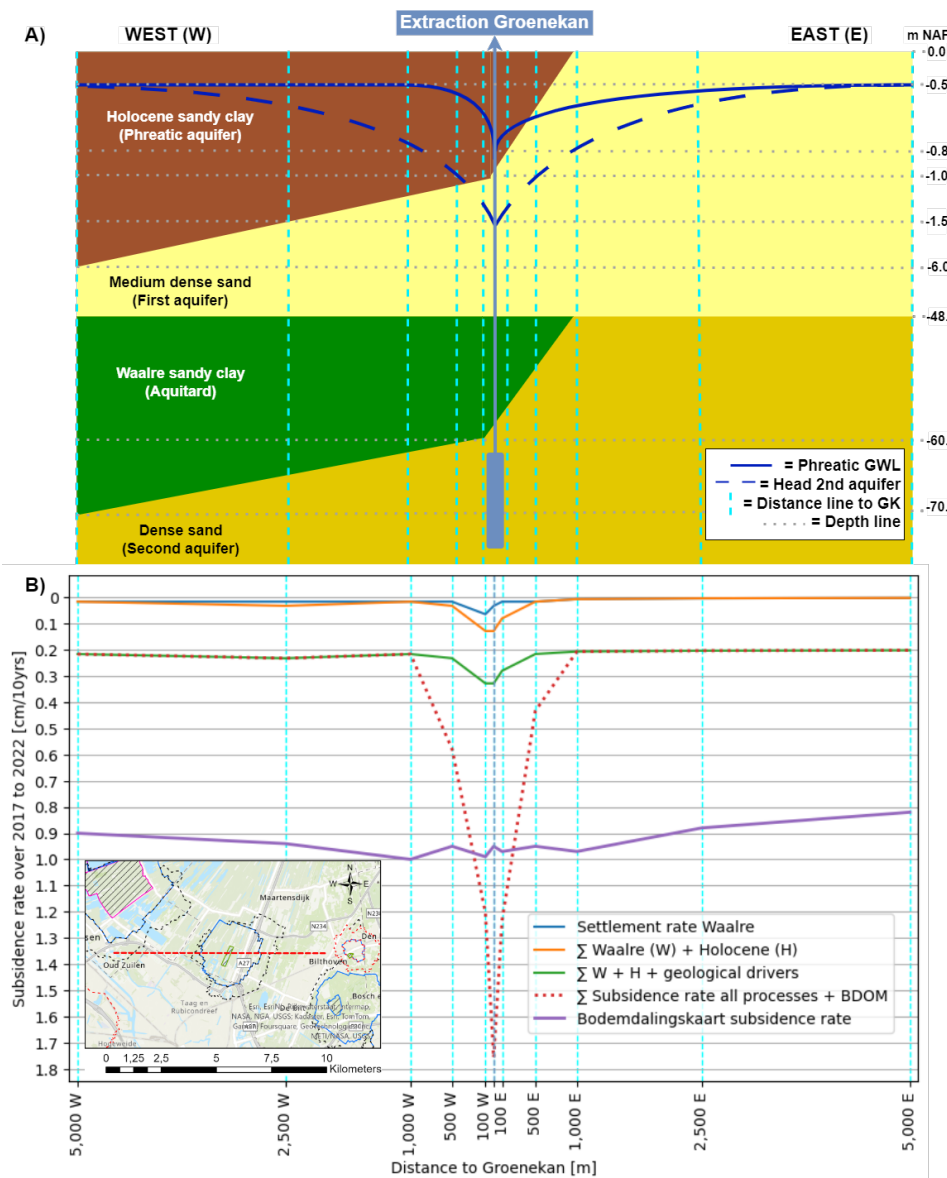


FIGURE 5.12: Results overview for base scenario of Groenekan over the period 2017 to 2022 on a 10 km west to east cross-section (bottom left). A) Schematic geohydrological profile of Groenekan including groundwater level and head lowerings. Note: the y-axis (m NAP) is not to scale. B) Subsidence rate [cm/10yrs] around Groenekan. All modelled subsidence processes are presented as cumulative plots and the measured Bodemdalingskaart data is given.

TABLE 5.2: Measured Bodemdalingsskaart (BDK) subsidence rate vs. SGE results west (W) and (E) of Groenekan (GK) for period 2017 to 2022 in [cm/10yrs]. One column excluding and one including BDOM.

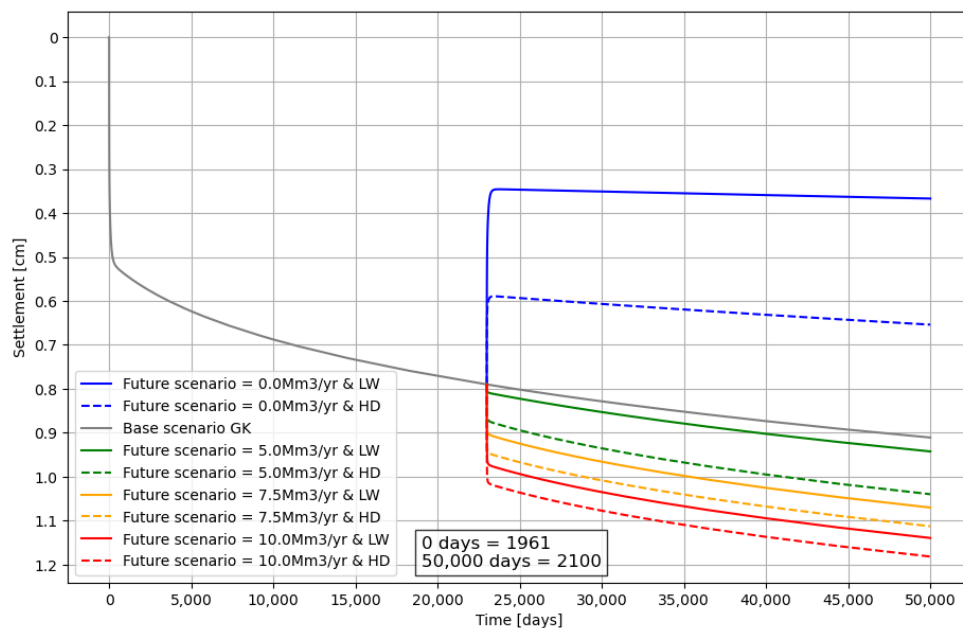
Period	Distance to GK [m]	BDK rate [cm/10yrs]		SGE rate excl. BDOM		SGE rate incl. BDOM	
2017-2022	0	~0.9		~0.1		~1.7	
2017-2022	100	~1.0 (W)	~1.0 (E)	~0.1 (W)	~0.1 (E)	~1.2 (W)	~1.2 (E)
2017-2022	500	~0.9 (W)	~0.9 (E)	~0.0 (W)	~0.0 (E)	~0.6 (W)	~0.4 (E)
2017-2022	>1,000	~1.0 (W)	~0.8 (E)	~0 (W)	0 (E)	~0 (W)	0 (E)

Key insights:

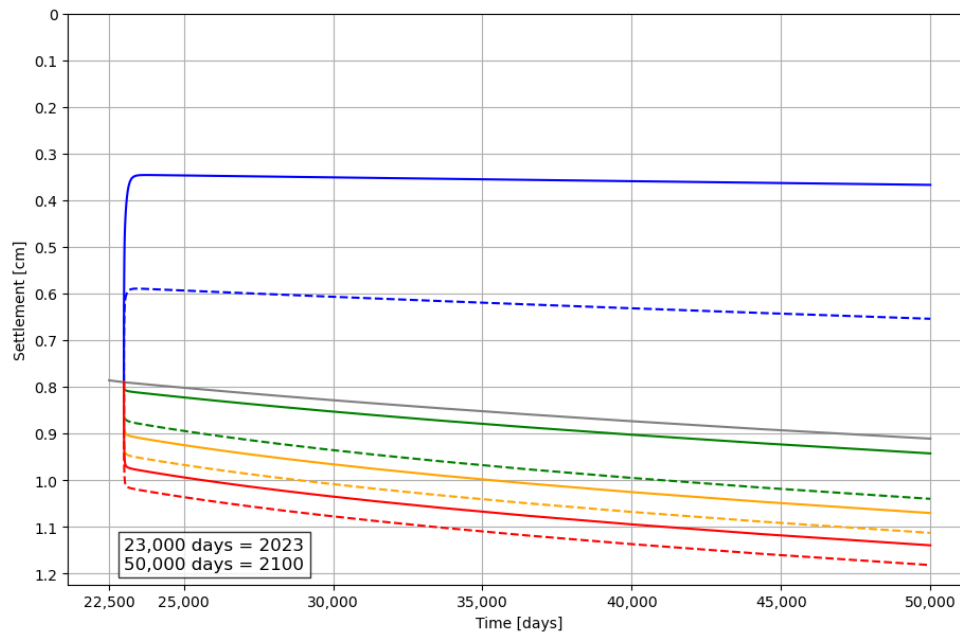
- Total measured Bodemdalingsskaart subsidence rate is ~1.0 cm/10yrs over 2017-2022;
- Subsidence rate at Groenekan is ~0.03 and 0.1 cm/10yrs for the Waalre clay and Holocene top layer respectively. This is an even lower value than their overall subsidence rates, since the most settlement has already occurred in both layers during the consolidation phase in the first years. During the creep phase, the soil subsides significantly slower than in the consolidation phase;
- Geological processes auto-compaction, isostasy, and tectonics are assumed to contribute 0.2 centimetres per 10 years (Figure 2.5);
- BDOM with 33 cm exposed Holocene is potentially ~1.4 cm/10yrs until it dissipates quickly toward the west and east. However, this assumes that the top layer is clean peat, which is not consistently the case around Groenekan;
- The gap between measured Bodemdalingsskaart data and the modelled SGE varies between +0.7 cm/10yrs (including BDOM, red dotted graph) and -0.9 cm/10yrs (orange graph);
- Shrinkage with 33 cm exposed Holocene is potentially ~1.8 cm/10yrs, assuming a clean clay top layer. However, as proven in Figure 5.6, this shrinkage has probably already occurred in 1975 and is fully completed. Thus, for the period 2017-2022 no shrinkage contribution is expected and therefore no shrinkage graph is plotted.

5.6. Future Scenarios

Figure 5.13 shows the settlement-time graphs at Groenekan for the eight future scenarios, where Sub-figure 5.13a displays the entire period of 1961 to 2100 and Sub-figure 5.13b zooms into the future period of 2023 to 2100. The base scenario has been plotted in grey until 2100 as a reference to the future scenarios. Table H.9 presents the total consolidation and creep in the phreatic Holocene and the Waalre aquitard in centimetres over the period 1961 to 2100 (139 years or ~50,000 days).



(A) Entire period 1961 to 2100.



(B) Zoomed in to future scenario period 2023 to 2100.

FIGURE 5.13: Settlement-Time linear graphs: Future scenarios at Groenekan over the period 1961 to 2100 (139 years or 50,000 days). The eight coloured graphs each represent a different future scenario from 2023 (day 23,000) onwards. The grey graph is the base scenario which is plotted until 2100 as a reference scenario.

Key insights:

- A different extraction discharge seems to have a larger impact on the final settlement than the climate scenarios, looking at the differences between the solid lines and dotted graphs;
- Changes in settlement at 23,000 days (year 2023) seem sudden due to the large timescale on the x-axis. However, the change in settlement is happening over the course of ~100 to 250 days;
- Creep rate (gradient of the graphs) increases for each scenario with a larger final settlement;
- Uplift or a "jump in settlement" on day 23,000 for the 0.0 Mm³/yr scenarios is clearly visible. The Holocene swells ~0.20 (HD) to 0.45 (LW) cm and Waalre swells back to its original state;
- The difference between the coupled 0.0 and 5.0 Mm³/yr LW and HD scenarios is larger than the differences between the coupled 7.5 and 10.0 Mm³/yr scenarios.

Discussion

In general, the objective of quantifying the effects of (increased) groundwater extraction on subsidence at Groenekan groundwater extraction has been achieved. However, the methods and results are worth discussing. In Section 6.1, the limitations of all methodologies are explained. Due to the theoretical nature of this research, the results rely on assumptions and specific conditions which might lead to uncertainty and errors. In Section 6.2, the results of Chapter 5 are discussed and compared with the hypotheses set up in Section 3.5.

6.1. Limitations of Methodologies

DINoloket & Geological Processes

DINoloket data of the sub-surface soil layers are subject to inaccuracies. REGIS.II presents approximations of the characteristics of soil layers based on national geotechnical research and fieldwork. Characteristics like thickness and soil type have proven to be crucial in determining the final settlement; however, these may vary locally. Therefore, DINoloket data need to be interpreted with care, and additional fieldwork and geotechnical research is required to draw more definitive conclusions.

In Figure 2.5, Groenekan was estimated to lie on the border of the green and orange class, which stands for -0.4 to 0.0 cm/10yrs of subsidence due to geological processes. Hence, auto-compaction, isostasy, and tectonics were assumed to have a combined subsidence rate of -0.2 cm/10yrs. Though, this assumption needs to be interpreted with caution, since it has a maximum standard deviation of 0.3 and does not take into account the arbitrary nature of tectonic movements (Kooi et al., 1998).

Isotach Model Selection

Houkes (2016) compared multiple settlement prediction methods and their limitations for soft soils in the Netherlands. Practical case studies yielded the best results for NEN-Bjerrum isotach model (NEN-Bjerrum), though it was mentioned that: "theoretically, a,b,c isotach model (a,b,c) provides the most sound and versatile description of soil behaviour upon compression as well as unloading, as a function of time and stress, in a natural strain formulation" (Houkes, 2016, p105). Parameter determination is crucial for the use of all IMs. Compression coefficients for the Koppejan and the NEN-Bjerrum models can be easily converted to each other. For converting these parameters to a,b,c compression parameters, more caution is needed because these are natural strain parameters and the others are linear strain parameters. In the case of the little subsidence around Groenekan, NEN-Bjerrum is suitable to use. However, locations with a large subsidence rate should consider using a,b,c, since the natural strain describes the subsidence rate better than linear strain (Figure 2.10).

NEN-Bjerrum Parameterisation

Subsidence results from IMs are extremely sensitive to the parameterisation of recompression coefficient RR , compression coefficient CR , creep coefficient C_α , but mainly to the pre-consolidation stress σ'_p and Over-Consolidation Ratio (OCR) of the Holocene and Waalre layers. The effect of varying these parameters for the final subsidence was significant. This was proven by the sensitivity analysis for five different Holocene soil types. In the base scenario of Groenekan for the period 1961 to 2023, medium dense sand resulted in hardly any settlement, sandy clay gave ~ 0.6 cm settlement and clean peat caused ~ 2.0 cm (214% more settlement), which is still negligible. Thus, if the groundwater level and head lowerings are well known, subsidence modelling can go 'all ways' as long as you do not carefully choose the parameters.

Bodemdalingskaart Measured Subsidence Data

Hardly any Bodemdalingskaart data was available to the west and north of Groenekan. This was a limiting factor in conducting a complete [InSAR](#) analysis around the extraction. The assumption of a 2 metre difference in Digital Elevation Model (DEM) and point height is perhaps not precise enough to filter all the buildings/infrastructure from the surface level. On the other hand, Bodemdalingskaart gives accurate results on the millimetre scale combined with a large dataset. Therefore, it is a reliable method to measure subsidence, which may potentially be even more helpful in the future when the time scale of measurements becomes larger.

AZURE Groundwater Model

First of all, the modelling period for [AZURE](#) is from 2004 to 2016. Hence, changes in land use, [TLD](#), climate, and extraction before 2004 are not included in the model, which may influence the outcome of the groundwater level and head lowerings. In addition, [AZURE](#) model results of groundwater level or head lowerings less than 5 cm have not been taken into account at all, because these are too insignificant and fall within the uncertainty of the model (Arcadis, 2019). Also, there is a larger uncertainty in modelling the groundwater level lowering in the phreatic aquifer than the head in the deeper aquifers. Since more processes affect the first few metres of the sub-surface, it is harder to predict whether the [AZURE](#) model results are correct. Namely, besides extraction the groundwater level is subject to the [TLD](#), vegetation root uptake, soil storativity, and precipitation/evaporation as well. Especially the [TLD](#) is expected to play a significant role in maintaining the groundwater level. The local interaction between the groundwater level lowering due to the extraction and the [TLD](#) is complex and signals the need for additional studies. Therefore, modelled groundwater level lowerings between 5 and 10 cm from [AZURE](#) should be interpreted with caution.

Analytical BDOM & Shrinkage Calculations

Given the generalised geohydrological profile, it was necessary to make assumptions on calculating [BDOM](#) and shrinkage. First, [BDOM](#) is only possible if the top layer consists of clean peat that can be oxidised and shrinkage is only triggered if (organic) clay is present. Additionally, the assumption that the phreatic groundwater level is located in the soft soil top layer implies that any groundwater level lowering may cause additional [BDOM](#) or shrinkage. However, if the groundwater level is located under that top layer, then a lowering would not have any effect on either process, since the soil needs to contain organic material. Detailed geotechnical fieldwork measurements can provide conclusive information in determining the thickness and soil type of the top layer.

Multiple equations and methods for calculating [BDOM](#) and shrinkage are available in literature. Most of these equations are based on the organic content of peat or clay. Unfortunately, this information was not known for the area of Groenekan. However, Equations 2.7 and 2.8 of Fokker et al. (2019) were based on the parameters of residual thickness λ_r and degradation velocity V . The parameterisation was based on test locations in Flevoland, which showed similar geohydrological profiles as Groenekan. Since only the groundwater level lowering around Groenekan was known and thus the residual thickness of the Holocene, the choice for this calculation method was strengthened.

D-Settlement Subsidence Model

[D-Settlement](#) has proven to be a reliable method for quantifying [SGE](#). Although the software is originally meant for calculating settlements through embankments or external loading, it is very user-friendly and has a quick model run time. The feature of allocating a groundwater level and head to certain soil layers indirectly implemented a groundwater extraction, as long as the groundwater level and head lowerings are known. However, there are several limitations to [D-Settlement](#). First, effective stress changes are assumed to be instant. This is clearly visible in the settlement-time graphs, where sudden “jumps” occur. In reality, a groundwater level or head change happens in the order of months when an extraction is expanded or if a precipitation surplus recharges the groundwater. Furthermore, seasonality is not taken into account in the [D-Settlement](#) calculations. As shown in Figure 2.1, groundwater and head fluctuations may already have a noticeable effect over distance to an extraction within 60 days. During summers and droughts, the groundwater level lowerings may temporarily be even higher and thus cause additional subsidence.

The research methodology of quantifying [SGE](#) in [D-Settlement](#) can be applied to other groundwater extractions in the Netherlands. Results of [BDOM](#), shrinkage, and sensitivity analyses (Sections 5.3

and 5.4.2) already showed the bandwidths of *SGE* at Groenekan. However, other extraction locations should be individually assessed to draw firm conclusions, since potential subsidence is extremely dependent on heterogeneous parameters such as soil composition, extraction discharge, and groundwater recharge. Therefore, the assessment of another extraction location should consist minimally of a geohydrological system analysis like Chapter 3, measured or modelled time series of groundwater level and head lowerings due to the extraction (like in Pastas or *AZURE*, and a *D-Settlement* model which incorporates a detailed geohydrological profile and groundwater level and head lowerings).

Future Scenarios Groenekan

Climate change is an extremely complex phenomenon, and quantifying its long-term effects on groundwater level dynamics is even harder. The simplified Equation 4.1 for the decrease in recharge in the year 2100 for two *KNMI* climate scenarios might not be representative. Furthermore, extreme caution must be exercised in translating this reduction in groundwater recharge to a lowering of groundwater level for the year 2100, as this effect has not been studied for Groenekan specifically. This methodological decision may have led to an overestimation of settlement for the *HD* climate scenarios, which assumed a groundwater level lowering of 20 cm. On the other hand, it might be possible that the 3 cm lowering for *LW* is also not appropriate and it underestimates the groundwater level lowering. The reality probably lies somewhere in between the two extreme groundwater level changes and can therefore be seen as a future bandwidth. Nevertheless, it is expected that future national policy decisions in water politics and local *TLDs* are likely to have a greater impact on the groundwater level than the assumed lowerings due to the *KNMI* climate scenarios. *BDOM* and shrinkage proved to be dominant in possible future *SGE* (if peat and/or clay is present in the top layer) and both processes are extremely sensitive to thickness of the Holocene layer and the phreatic groundwater level.

6

6.2. Interpretation of Results

Analytical Groundwater Flow

The analytical groundwater flow results must be interpreted with caution, since it is a simple equation to quickly determine a head lowering around a well due to an extraction. Nevertheless, the outcome was closely matched with *AZURE* further away from the extraction, but the head was slightly higher at the extraction. This different result can be partly explained by the assumption that groundwater is extracted from a homogeneous confined aquifer beneath an aquitard (Waalre clay) and a Holocene phreatic top layer with ditches. However, in reality, this Waalre clay does not have a fully confining effect since it is absent in the east. Also, parameter assumptions are taken as a constant, whereas in *AZURE* these parameters are spatially variable. One must take into account that both are just approaches to calculate a groundwater level lowering and that *AZURE* may also not be fully representative for reality.

Pastas Time Series Models

The differences between *TSM* and *AZURE* can be explained by the uncertainties present in both types of models. Also, the comparison between the determined head lowerings with *TSMs* and modelled *AZURE* lowering remains complex, since the piezometer time series analysis is based on measured head values and the heads in *AZURE* are modelled. This causes the error margin to be approximately 10 cm between *AZURE* and the Pastas *TSMs*. Hence, it is not possible to draw firm conclusions about either or both types of models based on this comparison, but Figure 5.4 gives some confidence that there is reasonable agreement between the models. Therefore, *AZURE* is considered to be a reliable tool to model the groundwater level and heads lowerings due to Groenekan extraction.

Bodemdalingskaart

Measured Bodemdalingskaart subsidence rates were expected to linearly decline over a larger distance to Groenekan, however this behaviour was not visible in the data. Mean subsidence rate results are all within 10% of each other and the circle with a radius of 2 km gave the highest mean subsidence rate μ . This is not in line with expectations, since the highest amount of subsidence was expected at the extraction. Additionally, the scattering of subsidence and uplift data points seem to be arbitrary and no conclusive statement could be made on e.g. clustering of subsidence or uplift points. The Bodemdalingskaart results are considered reliable, since the standard deviation is ~ 1.4 for all areas. Thus, no decisive conclusion can be drawn on the basis of the Bodemdalingskaart results if Groenekan

extraction has influenced subsidence during the period 2017 to 2022. This outcome suggests other drivers besides SGE are causing the subsidence.

Groundwater Level & Hydraulic Head

Observed lowerings of the phreatic groundwater levels and hydraulic heads in the second aquifer primarily to the east of Groenekan highlight the critical role of geological formations in regulating groundwater dynamics. The absence of the Waalre clay aquitard to the east allows for unrestricted groundwater flow between the phreatic zone and the second aquifer, leading to more pronounced lowerings in response to extraction (Figure 5.3). This finding aligns with the hypothesis from Section 3.5, which suggested that areas lacking a confining layer would experience a larger influence to groundwater extraction. Compared to the groundwater level, head lowerings were more severe in the second aquifer, since Vitens extracts their drinking water there and no confining effect of an aquitard is present.

Analytical BDOM & Shrinkage

BDOM and shrinkage calculations resulted in similar subsidence values in the order of 10 to 20 centimetres over 62 years. However, subsidence due to BDOM could potentially be higher than shrinkage in the long-term, since final settlement of BDOM has not been established after 62 years (1961-2023) and continues even until after 2100. Proofing BDOM is a slow process compared to shrinkage follows from the 10 times smaller degradation velocity V and the 5 to 7 times smaller residual thickness of peat $\lambda_{r,BDOM}$. Moreover, the spatial heterogeneity around Groenekan makes it extremely hard to distinguish where potentially BDOM or shrinkage may occur. Plus, TLDs of the local water boards possibly have an even larger influence on the phreatic groundwater level than the lowering due to Groenekan extraction. Therefore, it directly influences the BDOM and shrinkage rates as well.

In Figure 5.5b, the BDOM first seems to accelerate until 2023 and then flattens until the year 2100. However, BDOM still continues to accumulate after 2100 due to its low residual thickness $\lambda_{r,BDOM}$ and slow velocity V_{BDOM} . However, shrinkage is a faster subsidence process, since final settlements are reached in 1975 and 1990 for clean and organic clay respectively.

Consolidation & Creep in Holocene and Waalre Layers

The total subsidence of ~ 0.8 cm in the Holocene (~ 0.6 cm) and Waalre (~ 0.2 cm) layers over the period 1961 to 2023 does not fully support the hypothesis from Section 3.5, since more SGE was expected in specifically the deeper Waalre aquitard. Considering the theory and the AZURE results, the little settlement can be explained by the fact that its equivalent age of minimally 1,000,000 years, high OCR and relatively small NEN-Bjerrum isotach parameters. During those one million years, the layer has already settled significantly. Thus, a relatively small reduction in head in the clay layer does not cause large extra settlements. Also, the thin 1 metre Holocene layer and relatively small groundwater level lowerings limited the amount of Holocene settlement significantly.

Specific remarks for the results west of Groenekan were that from 1,000 m distance, the influence of Groenekan on the phreatic groundwater level disappeared (Figure 5.12) and therefore caused no more additional settlement in the Holocene. Also, Figure 5.7 illustrated that the final settlement at 5,000 m west of Groenekan is higher than at 2,500 or 1,000 m due to the thicker Holocene and Waalre layers at that 5,000 m. Since groundwater level and head lowerings are negligible here, creep is dominant over a large time-scale and thus the 5,000 m graph surpasses the 2,500 and 1,000 m graphs at 12,000 days. East of Groenekan, the settlements were negligible (< 0.1 cm) from 500 m distance. This is due to the disappearing Holocene top layer to the east of Groenekan (Figure H.2). Hence, only the creep in the Waalre clay dictates.

Modelled SGE & Bodemdalingskaart Validation

Section 5.1 showed that between 2017 and 2022 the total subsidence rate around Groenekan is ~ 1.0 cm/10yrs. In Figure 5.12, the modelled SGE rate was ~ 0.1 cm/10yrs for consolidation and creep of the Holocene and Waalre alone. However, if BDOM is included in the analysis, it overestimates the Bodemdalingskaart measurements locally with ~ 1.7 vs. 1.0 cm/10yrs. The gap between the measured subsidence and modelled SGE is worth highlighting, as it puts the results into perspective and future research suggestions may be identified to clarify this gap. The difference in measured and modelled subsidence (Figure 5.12) is most likely caused by the many assumptions made in this research. The

Holocene layer at Groenekan in the base scenario was assumed to be sandy clay soil type and have a thickness of 1 metre. In reality, the Holocene might be thicker and peat and clay may be more prominently present in the Holocene, causing the subsidence to be closer to the Bodemdalingskaart. Also, the groundwater level was assumed to be at -0.5 m **NAP**, which is spatially heterogeneous as well. Besides, the **NEN-Bjerrum** parameterisation of the Holocene and Waalre layers are based on approximations from **NEN (2017)** Table 2b, whereas Figure 3.3 illustrated these values vary over space. Furthermore, **BDOM** is only included in the results if the top layer is clean peat, however in reality the top layer is a mix of sand, clay and peat, where the last two likely contributed to subsidence during the period 2017 to 2022. Lastly, results are generated by **AZURE** and **D-Settlement**, which are naturally prone to errors and uncertainty. Validation over longer time scales is necessary to confirm the reliability of both models.

Additionally, the gap between the measured and modelled subsidence rates can be explained by five reasons which have not been studied. First, other Vitens groundwater extractions in the area (i.e. Beerschoten, Bilthoven, Zeist, Bunnik) potentially have an influence area that overlaps with the influence circle of Groenekan. This may intensify **SGE** in the study area, which is not necessarily caused by Groenekan extraction. Second, the **TLD** of Groenekan has not changed since 2008, however the **TLDs** of surrounding polders may have changed, causing gradual subsidence in the adjacent polders in the period 2017 to 2022. The surrounding polders overlap with the influence area of Groenekan, thus a recent **TLD** lowering could have affected the subsidence around Groenekan. Third, periods of extended drought with little groundwater recharge and summer/winter seasonality both may have an enforcing effect on Holocene consolidation, **BDOM**, and shrinkage. This potentially lower groundwater level during dry spells has not been considered in this study, and thus the additional effects of the subsidence drivers are also not known. Fourth, **InSAR** data of Bodemdalingskaart still have inaccuracies on a millimetre scale, which may play a vital role since the final subsidence is also not large. Also, the current filtering of persistent scattering, descending orbit, and surface level points might not result in the most optimal dataset. Fifth, loading of buildings and infrastructure in the urban areas of Utrecht and Bilthoven might have affected the subsidence during 2017 to 2022, though this is supposed to be negligible.

Overall, comparing measured Bodemdalingskaart subsidence rates with modelled **SGE** predictions showed a gap of ~ 0.8 cm/10yrs. This proves that unravelling an overall subsidence signal into separate contributing drivers remains a challenge. In theory, an infinite number of combinations of sub-models and calculations could lead to a similar agreeable result. Therefore, in the assumptions made in this study, differences in outcome are imposed. In general, the used modelling techniques in this thesis can reliably approximate subsidence measurements, but the nature of the models themselves is sometimes questioned, as these often do not include or distinguish all relevant influences and couplings between different groundwater and subsidence processes.

Future Scenarios Analysis

The investigated future scenarios for Groenekan give a good impression of the possible prospective effects around the extraction. The additional groundwater level and head lowering by expanding the extraction to 7.5 of even 10.0 Mm^3/yr has resulted in realistic outputs by **D-Settlement**. The extraction discharge seems to have a larger impact on the final settlement than the climate scenarios, since the differences between the extraction discharges are larger. This is caused by the fact that the extraction discharge has an impact on both the groundwater level and heads, and it lowers both more than the climate scenarios. Also, uplift or a “jump in settlement” on day 23,000 for the 0.0 Mm^3/yr scenarios is clearly visible. This is caused by the return of the phreatic groundwater level and deeper hydraulic heads to their original state, because the extraction is stopped. This causes the Holocene top layer to swell ~ 0.20 (**HD**) to 0.45 (**LW**) cm and the Waalre aquitard to swell back to its original state. The difference between the coupled 0.0 and 5.0 Mm^3/yr **LW** and **HD** scenarios is larger than the differences between the coupled 7.5 and 10.0 Mm^3/yr scenarios. This is caused by the 1 metre thick Holocene layer, where groundwater level lowerings larger than -0.5 m in groundwater level have relatively less effect on the final settlement, since they only affect the medium dense sand layer underneath. Medium dense sand is not vulnerable to subsidence, since sand isotach parameters (Table H.2) are so small that subsidence is negligible for this soil type, as illustrated by the sensitivity analysis in Figure 5.11.

Conclusions & Recommendations

7.1. Conclusions

The objective of this research was to quantify the historical and future effects of groundwater extraction on subsidence at location Groenekan in the Province of Utrecht. This section answers the main question:

"From a subsidence perspective, can Vitens responsibly expand Groenekan groundwater extraction from 5.0 to 10.0 million m^3/yr ?"

Expansion of Groenekan from 5.0 to 10.0 Mm^3/yr is considered to be responsible from a subsidence perspective, as long as the compaction processes **BDOM** and shrinkage are exercised with extreme caution within a radius of 500 m to Groenekan. The research showed that the groundwater level and heads are lowered by Groenekan extraction, but the subsidence-sensitive Holocene and Waalre layers are relatively thin and both contain sand in addition to clay and peat. Sand was proven to not be vulnerable to subsidence. Practically, this results in negligible subsidence over a period of 139 years compared to other locations in the Netherlands with dozens of centimetres of subsidence in the same period. The highest absolute subsidence value was found for the extreme future scenario of 10.0 Mm^3/yr + **HD** climate, which showed ~ 1.2 cm of compression, in the form of consolidation and creep, in the Holocene and Waalre layers, which is 30% additional subsidence compared to the base scenario of 0.9 cm over the period 1961 to 2100. Though, **BDOM** and shrinkage can locally cause few centimetres of subsidence on the long-term if the groundwater level is further lowered by extraction in a soft soil Holocene top layer. Compared to this potential **BDOM** and shrinkage, compression of the Holocene and Waalre layers play a minor role.

Geohydrological system analysis and measured subsidence around Groenekan

In the Holocene top layer and in deeper soil layers, there is a high level of spatial heterogeneity for the thickness and soil type of particular layers. The Holocene and Waalre absence to the east of Groenekan enables groundwater to flow between shallow and deep aquifers. Subsequently, the phreatic groundwater level is influenced by the extraction, since there is no confining aquitard present. In the west however, the Waalre clay is minimally 12 metres thick and works as an aquitard between the phreatic aquifer and the second aquifer where Groenekan extracts. Considering the geohydrological profile, **SGE** around Groenekan consists of four major subsidence processes: compression of the Holocene top layer and Waalre aquitard in the form of 1) consolidation and 2) creep, and compaction due to 3) **BDOM** and 4) shrinkage. Subsidence due to geological processes as auto-compaction, isostasy, and tectonics will happen nevertheless. Compression by loading is negligible in the rural area of Groenekan. Furthermore, agricultural and industrial extractions play a minor role in the total groundwater extraction around Groenekan compared to Vitens. Lastly, the measured Bodemdalingskaart results indicated a subsidence rate of ~ 1 cm/10yrs during the period 2017 to 2022. Distance-to-extraction analyses could not prove a substantial contribution of Groenekan to the subsidence for this period, since subsidence rates did not linearly decline over a larger distance to Groenekan.

Quantification of **SGE** around Groenekan from 1961 to 2023

In **AZURE**, groundwater level and head lowerings for three extraction discharges (5.0, 7.5, and 10.0 Mm^3/yr) have been simulated around Groenekan. Phreatic groundwater level lowerings at Groenekan were approximately 30 cm for 5.0 Mm^3/yr and 60 cm for 10.0 Mm^3/yr . It was found that the groundwater lowerings toward the west of Groenekan quickly faded. At more than 500 m western distance from Groenekan, no significant lowering was found due to the confining effect of the Waalre clay. On the contrary, 5,000 m east of Groenekan still small groundwater level lowerings were observed. Additionally, the **AZURE** results confirm the hypothesis that the Waalre clay functions as a confining aquitard. Compared to the groundwater level lowering, head lowerings of 1.5 to 2.9 m were observed for for

5.0 and 10.0 Mm³/yr in the second aquifer, gradually declining over distance. To the west and east of Groenekan, the influence areas were symmetrical and spanned approximately 8.5 and 12.5 km for 5.0 and 10.0 Mm³/yr respectively.

In a radius of 500 m around Groenekan, the groundwater level lowerings exposed more Holocene, which is susceptible to **BDOM** and shrinkage. For the period 1961 to 2023, a 1 m thick clean peat Holocene top layer could reveal ~16 cm of **BDOM**, which is ~2.6 cm/10yrs. Conversely, ~11 or ~18 cm of shrinkage could occur assuming a clean clay or organic clay Holocene soil type respectively. Shrinkage rates for both clays are ~1.8 or ~2.9 cm/10yrs. Literature showed that **BDOM** is a 10 times slower process than shrinkage. Moreover, peat's residual thickness is 5 to 7 times smaller than organic clay and clean clay respectively. Both characteristics confirmed that **BDOM** is a long-term process, since the Holocene might oxidise ~25 cm for the period 1961 to 2100 if the groundwater level lowering is not reverted. However, the shrinkage processes of clean clay and organic clay were already completed in 1975 and 1990 respectively. Despite the assumptions of the Holocene thickness and soil type around Groenekan, these calculations give valuable insights in the potential compaction of soft soils.

The past 62 years, consolidation and creep in the Holocene and Waalre layers have contributed relatively little to **SGE** around Groenekan. Within a 500 m radius of Groenekan, settlements due to the extraction are noticeable, beyond that the settlements are negligible. **D-Settlement** simulated a maximum total settlement of ~1.0 cm at 100 m west of Groenekan, since the Holocene and Waalre layers there are relatively thicker than at Groenekan. On the location of the extraction, the Holocene settled ~0.6 cm and Waalre ~0.2 cm, resulting in a total settlement rate of ~0.1 cm/10yrs. In the Holocene, settlement by consolidation occurred within the first 250 days after the extraction started and from there the slower creep process became dominant. Generally, consolidation contributed 75% to the total settlement, whereas creep was responsible for 25%. Thus, the majority of the settlement in the Holocene and Waalre layers occurred before the year 1970. Furthermore, although the groundwater level lowerings are relatively smaller than the head lowerings, the Holocene compresses more than the Waalre clay due to two reasons: 1) The relatively young equivalent age t_{age} of the Holocene results in a lower **OCR**, which guarantees the soil to 'collapse' easier and more long-term settlement is realised and 2) Holocene **NEN-Bjerrum** isotach parameters (Table **H.2**) are larger than those of the Waalre clay (Table **H.3**) and thus potentially cause more final settlement, including a faster creep rate.

Sensitivity analyses over the period 1961 to 2023 revealed that the Holocene soil type is the most sensitive parameter in calculating the final settlement. Clean peat gave ~2.0 cm of settlement in the Holocene compared to ~0.6 cm for sandy clay in the base scenario, which equals 213% more settlement. On the contrary, medium dense sand resulted in no settlement. Thickness of soft soil layers is a crucial parameter as well. Double the thickness for both Holocene and Waalre showed a total settlement of ~2.1 cm, which is an increase of 170% compared to the base scenario. Assuming half the thickness of both layers presented only ~0.1 cm settlement, a 84% decrease. Variations in groundwater level and head lowerings were less sensitive. A 50% increase of groundwater level and head lowering compared to the base scenario resulted in 25% more settlement, while a 50% decrease gave 44% less settlement. Within the Groenekan system, the 1 metre Holocene thickness is dominant over the groundwater level lowering, because no additional effects are found if the groundwater level drops below the Holocene.

Future scenarios: Quantification of future **SGE** from 2023 to 2100

For the period 1961 to 2100, future scenario results confirmed that consolidation and creep in the Holocene and Waalre layers at Groenekan will increase to ~0.9 cm (an increase of 15% in 77 years, compared to 2023) if groundwater extraction is continued in the base scenario. However, the extreme scenario of 10.0 Mm³/yr + High emissions & Desiccation (**HD**) climate scenario resulted in ~1.2 cm, which is 30% more than the base scenario of ~0.9 cm. Furthermore, both 0.0 Mm³/yr scenarios caused uplift in the Holocene and Waalre layers, since groundwater levels and heads were restored. For 0.0 Mm³/yr + Low emissions & Wetter (**LW**) climate scenario, a final settlement of ~0.4 cm was expected, which is 60% less settlement than the base scenario. The extraction discharge appears to affect the final settlement more than the climate scenarios, since more subsidence is found for a higher extraction scenario than a more extreme climate scenario. Lastly, it is expected a lower **TLD** is highly likely to have a greater impact on the groundwater level than the assumed lowerings due to the **KNMI** climate scenarios, since a **TLD** has a permanent and direct effect on the groundwater level, whereas the recharge is dependent on multiple uncertain factors as precipitation, evapotranspiration, and soil parameters.

7.2. Recommendations

Future Research

This study provides a springboard for more research related to [SGE](#). Future studies should be concentrated on the following five points:

1. **Study the effects of extended drought periods (dry spells) on the groundwater level.** Geertzen (2021) calculated a drought-induced subsidence of 1 to 1.5 mm during the extreme drought in 2018 in two soft-soil areas of Diemen and Kampen in the Netherlands. Although this research concludes droughts may cause permanent subsidence, it needs to be separately investigated for Groenekan, since the soil composition is decisive in the sensitivity to subsidence;
2. **Investigate the effects of TLDs of Groenekan and surrounding polders on the groundwater level.** The exact influence of a TLD on the groundwater level is not known. Hence, the study can research if a TLD has more influence on the groundwater level than the extraction of groundwater. In addition, historical TLD lowerings can be studied to check whether a correlation can be found between a TLD lowering and the subsidence it may have caused in the past.
3. **Examine the effects on subsidence of other Vitens groundwater extractions in the vicinity of Groenekan.** Hereby, the couplings between various extractions can be studied and overlapping influence areas can be found. This may partly explain the gap between the measured Bodemdalingskaart data and modelled [SGE](#);
4. **Research the effects of various KNMI climate scenarios on the change in groundwater level.** This could be done locally with a case study, monitoring the groundwater level on a detailed grid over an extended period of time. Also, general piezometer groundwater level and head data throughout the Netherlands can be investigated to see if long-term trends arise and if any correlation can be made with climate change and the coupling with groundwater extraction. Subsequently, examine if the future precipitation and evaporation cause a permanent groundwater level lowering and what its magnitude is. Include seasonality as well to account for winter and summer groundwater levels;
5. **Validate the isotach parameterisation of soft soil layers by performing a Cone Penetration Test (CPT) and other laboratory tests.** Isotach parameters for the Holocene and Waalre clay would be more accurate if a CPT was available instead of assuming a value from the NEN (2017) Table 2b. Besides, laboratory results on the organic content of the Holocene layer could validate the Equations 2.7 and 2.8 used for [BDOM](#) and shrinkage.

Recommendations for Vitens

Based on the distinct results for Groenekan, eight recommendations are made specifically for Vitens:

1. **Extract groundwater from deep, confined aquifers with a sandy top layer for maximal [SGE](#) mitigation.** Preferably under a confining aquitard to minimise the impact of the extraction on the groundwater level and thus subsidence processes as Holocene consolidation, [BDOM](#), and shrinkage;
2. **Create a 3D transient subsidence model over time and space, which includes seasonality, specifically around Groenekan.** In this study, sensitivity analyses gave a perspective on the sensitivity of the subsidence parameters. However, it would be favourable to model the 3D geohydrology around an extraction to spatially map the subsidence instead of the 2D calculation in [D-Settlement](#). Also, the differences in climate and seasons can then be identified and further researched;
3. **Evaluate other extraction locations to validate the results and conclusions from this study.** Investigating other extraction locations could help understand [SGE](#). Because the subsidence components are location specific and depend on the geohydrology, it is recommended to evaluate locations with different characteristics;
4. **Conduct frequent in-situ fieldwork measurements around extraction locations.** For example, with extensometers it is possible to monitor subsidence on a regular basis. Simultaneously, the accuracy of subsidence modelling is improved and the outcome of this study can be validated. Also, availability of CPTs data could determine [NEN-Bjerrum](#) subsidence parameters for the Holocene and Waalre layers more accurately;

5. **Measure the degradation sensitivity of peat and clay top layers around Groenekan.** Hereby, other [BDOM](#) and shrinkage calculations may be done which include the organic matter density of peat and clay. Uncertainty on this organic content contributes significantly to the uncertainty of the [BDOM](#) and shrinkage forecasts;
6. **Consider surface water extraction from lakes and rivers (e.g. Amsterdam-Rijnkanaal, Eemmeer, IJssel) as a long-term alternative to groundwater extraction.** Although the costs of purifying surface water to drinking water are significantly higher, it may be a sustainable alternative or addition to the existing groundwater extraction system. A combination of surface and groundwater extraction may mitigate the negative effects on [SGE](#), ecology, and the groundwater system;
7. **Apply a consistent and universal subsidence policy around Vitens' groundwater extractions.** For example, Gilles Erkens from Deltares gave a promising presentation on the MAALS (Maximum Allowable Amount of Land Subsidence) policy during the National Subsidence Conference on 14 November 2023 in Amsterdam. He stated that the metropolitan area of Shanghai allows for a maximum subsidence rate of 3 cm/10yrs by actively combating subsidence drivers, which seems to avoid serious damage and unforeseen costs in the long-term;
8. **Vitens could use the results of this study to justify their expansion plans from a subsidence perspective.** Relevant stakeholders (local residents, water boards, municipalities etc.) around an extraction site like Groenekan may be more likely to support an expansion if [SGE](#) can be proven to be a manageable/negligible factor. Also, the research might serve as legal support for potential claims regarding (infra)structural and/or ecological damage.

References

- Abidin, H. Z., Andreas, H., Gumilar, I., Fukuda, Y., Pohan, Y. E., & Deguchi, T. (2011). Land subsidence of Jakarta (Indonesia) and its relation with urban development. *Natural Hazards*, 59(3), 1753–1771. <https://doi.org/10.1007/s11069-011-9866-9>
- AHN. (2023, March 27). *Kwaliteitsbeschrijving AHN metingen*. Retrieved January 9, 2024, from <https://www.ahn.nl/kwaliteitsbeschrijving>
- Allan Freeze, R., & Cherry, J. A. (1979). *Groundwater*. <https://gw-project.org/books/groundwater/>
- Antea Group. (2023). *Bodemdaling in nederland: Oorzaken, gevolgen en duurzame oplossingen*. Retrieved April 22, 2024, from <https://anteagroup.nl/nieuws-media/blogs/bodemdaling-in-nederland>
- Aqua Assistance. (2018). *Kaart drinkwaterbedrijven Nederland*. Retrieved September 18, 2023, from <https://www.aquaassistance.nl/wet-en-regelgeving/overheid-en-instanties/>
- Arcadis. (2019). *Uitgangspuntennotitie Grondwatermodellering Drinkwaterwinning Groenekan* (tech. rep.).
- Arcadis. (2022). *Drinkwaterwinning Groenekan: Geohydrologische effectenstudie* (tech. rep.).
- Arcadis. (2023). *Visualisatie stroombanen rondom Groenekan* (tech. rep.).
- Artesia. (2023). *Tijdreeksanalyse winning Groenekan* (tech. rep.).
- Bishop, A. W., & Lovenbury, H. T. (1969). Creep characteristics of two undisturbed clays. *International Conference on Soil Mechanics and Foundation Engineering*, 7. <https://www.issmge.org/publications/publication/creep-characteristics-of-two-undisturbed-clays>
- Bjerrum, L. (1967). Engineering Geology of Norwegian Normally-Consolidated Marine Clays as Related to Settlements of Buildings. *Géotechnique*, 17(2), 81–118. <https://doi.org.tudelft.idm.oclc.org/10.1680/geot.1967.17.2.83>
- Bootsma, H., Kooi, H., & Erkens, G. (2020). Atlantis, a tool for producing national predictive land subsidence maps of the Netherlands. *Proceedings of the International Association of Hydrological Sciences*, 382, 415–420. <https://doi.org/10.5194/piahs-382-415-2020>
- Brakenhoff, D. A., Vonk, M. A., Collenteur, R. A., Van Baar, M., & Bakker, M. (2022). Application of Time Series Analysis to Estimate Drawdown From Multiple Well Fields. *Frontiers in Earth Science*, 10. <https://doi.org/10.3389/feart.2022.907609>
- BRO. (2023a). *GeoTOP (GTM)* [Basisregistratie Ondergrond]. Retrieved December 4, 2023, from <https://basisregistratieondergrond.nl/inhoud-bro/registratieobjecten/modellen/geotop-gtm/>
- BRO. (2023b). *REGIS II (HGM)* [Basisregistratie Ondergrond]. Retrieved December 4, 2023, from <https://basisregistratieondergrond.nl/inhoud-bro/registratieobjecten/modellen/regis-ii-hydrogeologisch-model-hgm/>
- Bronswijk, J., & Evers-Vermeer, J. (1987). *Krimpkaracteristieken van kleigronden in Nederland*. ICW. Retrieved February 6, 2024, from <https://edepot.wur.nl/333030>
- Bronswijk, J., & Evers-Vermeer, J. (1990). Shrinkage of Dutch clay soil aggregates. *Netherlands Journal of Agricultural Science*, 38(2), 175–194. <https://doi.org/10.18174/njas.v38i2.16603>
- CBS. (2017). *Bestand Bodemgebruik*. Retrieved October 30, 2023, from <https://www.cbs.nl/nl-nl/dossier/nederland-regionaal/geografische-data/bestand-bodemgebruik>
- CBS. (2023). *Watergebruik bedrijven en particuliere huishoudens; nationale rekeningen*. Retrieved October 16, 2023, from <https://opendata.cbs.nl/#/CBS/nl/dataset/82883NED/table>
- CLO. (2001). *Herstel van verdroogde gebieden, 2001 | Evaluatie Verdrogingsbestrijding Utrechtse Heuvelrug (EVUH)* [Compendium voor de Leefomgeving]. Retrieved January 11, 2024, from <https://www.clo.nl/indicatoren/nl028403-herstel-van-verdroogde-gebieden>
- Collenteur, R. A., Bakker, M., Caljé, R., Klop, S. A., & Schaars, F. (2019). Pastas: Open Source Software for the Analysis of Groundwater Time Series. *Groundwater*, 57(6), 877–885. <https://doi.org/10.1111/gwat.12925>
- Crombaghs, M., de Min, E., Strang van Hees, G., & NCG. (2002). *The first absolute gravity measurements in The Netherlands : period 1991-1999* (50th ed., tech. rep.). NCG Netherlands Geodetic Commission.
- De Glee, G. J. (1930). *Over grondwaterstromingen bij wateronttrekking door middel van putten* [Doctoral dissertation]. <http://resolver.tudelft.nl/uuid:c3e13209-4626-41b9-9038-c223d61e35c4>

- Deltares. (2023). *About iMOD 5.5*. Retrieved December 8, 2023, from <https://oss.deltares.nl/web/imod/about-imod5>
- Den Haan, E. (1994). *Vertical compression of soils* [Doctoral dissertation]. <https://doi.org/10.4233/uuid:b8dc88e0-f400-4d86-9a2e-4e00b68d0472>
- Den Haan, E. (2007). A History of the Development of Isotache Models. <https://doi.org/10.13140/RG.2.2.32972.13441>
- Dieudonné, A.-C. (2023). *Infographic cycle surface level lowering, peat oxidation and subsidence*.
- Dinar, A., Esteban, E., Calvo, E., Herrera, G., Teatini, P., Tomás, R., Li, Y., & Albiac, J. (2019). *Land Subsidence: The Forgotten Enigma of Groundwater (Over)Extraction* (tech. rep.). <https://www-semantic scholar-org.tudelft.idm.oclc.org/paper/Land-Subsidence%3A-The-Forgotten-Enigma-of-Dinar-Esteban/80f893e033e062afbd1f188405217b1ac3602993#cited-papers>
- Edil, T. B., & Dhowian, A. W. (1979). Analysis of long-term compression of peats. *Geotechnical Engineering*, 10. <https://www.researchgate.net/publication/283945849>
- Erkens, G., Kooi, H., & Melman, R. (2021). *Actualisatie bodemdalingsvoorspellingskaarten: Hoog scenario 2100* (tech. rep.). Deltares. <https://storymaps.arcgis.com/stories/89c12cdd9f54453ead3b9d85e71f8bdc>
- Ernst, L., & Feddes, R. (1979). *Involed van grondwateronttrekking voor berekening en drinkwater op de grondwaterstand*. ICW. <https://edepot.wur.nl/212093>
- Feng, R., Peng, B., Wu, L., Cai, X., & Shen, Y. (2021). Three-stage consolidation characteristics of highly organic peaty soil. *Engineering Geology*, 294, 106349. <https://doi.org/10.1016/j.enggeo.2021.106349>
- Fokker, P. A., Gunnink, J. L., Koster, K., & de Lange, G. (2019). Disentangling and parameterizing shallow sources of subsidence: Application to a reclaimed coastal area, flevoland, the netherlands. *Journal of Geophysical Research: Earth Surface*, 124(5), 1099–1117. <https://doi.org/10.1029/2018jf004975>
- Fokker, P. A., Van Leijen, F. J., Orlic, B., Van Der Marel, H., & Hanssen, R. F. (2018). Subsidence in the Dutch Wadden Sea. *Geologie en Mijnbouw/Netherlands Journal of Geosciences*, 97(3), 129–181. <https://doi.org/10.1017/njg.2018.9>
- Geertzen, A. J. J. (2021). *Determining drought-induced subsidence in urban areas: An in-practice analysis of drought impacts on subsidence in two Dutch soft-soil cities* [Doctoral dissertation, TU Delft]. <http://repository.tudelft.nl/>
- Geologische Dienst Nederland. (2023). *Grondwaterstanden in beeld - Isohypsen*. Retrieved October 16, 2023, from <https://www.grondwatertools.nl/gwsinbeeld/>
- Guzy, A. (2020). *Groundwater Withdrawal-Induced Land Subsidence* (tech. rep.). <https://www-semantic scholar-org.tudelft.idm.oclc.org/paper/Groundwater-Withdrawal-Induced-Land-Subsidence-%7C-Guzy/91141a3964d95c2866ddd3efa41d2d23b8c22d81>
- H2O Waternetwerk. (2014, January 21). *AZURE: Innoveren in de 'gouden driehoek'*. Retrieved November 7, 2023, from <https://www.h2owaternetwerk.nl/vakartikelen/azure-innoveren-in-de-gouden-driehoek>
- Hantush, M., & Jacob, C. (1955). Non-steady radial flow in an infinite leaky aquifer. *Eos, Transactions American Geophysical Union*, 36(1), 95–100. <https://doi.org/10.1029/TR036i001p00095>
- Harbaugh, A. W. (2005). *MODFLOW-2005, The U.S. Geological Survey Modular Ground-Water Model-the Ground-Water Flow Process* (tech. rep.). <https://pubs.usgs.gov/tm/2005/tm6A16/>
- HDSR. (2023). *Peilbesluit met oppervlaktewaterpeilen Groenekan in peilvak Maartensdijk* [Hoogheemraadschap de Stichtse Rijnlanden]. Retrieved December 27, 2023, from <https://hdsr.maps.arcgis.com/apps/webappviewer/index.html?id=82aa7241868b47a9a7d87af35ecacdc5>
- Holzer, T. L., & Galloway, D. L. (2005, November). Impacts of land subsidence caused by withdrawal of underground fluids in the United States. In *Humans as geologic agents*. Geological Society of America. [https://doi.org/10.1130/2005.4016\(08\)](https://doi.org/10.1130/2005.4016(08))
- Hommes, S., Philippen, S., Ypma, F., Schreuder, C., & Van Reeken-Van Wee, J. (2023). *Gemelde funderingsschade leidt tot forse prijskorting bij woningverkoop* (tech. rep.). https://esb-nu.tudelft.idm.oclc.org/wp-content/uploads/2023/03/136-139_Hommes.pdf
- Houkes, C. B. (2016). *Review and validation of settlement prediction methods for organic soft soils, on the basis of three case studies from the Netherlands* [Doctoral dissertation]. <http://repository.tudelft.nl/>
- Ireland, R. (2018, October 19). *Land subsidence* | U.S. Geological Survey. Retrieved December 21, 2023, from <https://www.usgs.gov/mission-areas/water-resources/science/land-subsidence>

- ISO. (2004). *Geotechnical investigation and testing – laboratory testing of soil – part 5: Incremental loading oedometer test* (tech. rep.). ISO 17892-5.
- ISO. (2019). *NEN-EN-ISO 14688-1&2: Geotechnical investigation and testing - Identification and classification of soil* (tech. rep.).
- Keverling Buisman, S. (1936). Results of long duration settlement tests. *International Society for Soil Mechanics and Geotechnical Engineering*. <https://www.issmge.org/publications/publication/results-of-long-duration-settlement-tests>
- KNMI. (2023a). *Kerncijfers klimaatscenario's*. Retrieved September 30, 2023, from <https://klimaatscenario-data.knmi.nl/kerncijfers>
- KNMI. (2023b). *KNMI 2023 klimaat scenario's voor Nederland*. Retrieved September 30, 2023, from https://cdn.knmi.nl/system/data_center_publications/files/000/071/901/original/KNMI23_klimaatscenario's_gebruikersrapport_23-03.pdf
- KNMI. (2023c). *Waarnemingen weer- en regenstations*. Retrieved December 4, 2023, from <https://daggegevens.knmi.nl/klimatologie/daggegevens>
- Kooi, H., Bakr, M., de Lange, G., den Haan, E., & Erkens, G. (2018). *User guide to SUB-CR: a MODFLOW package for land subsidence and aquifer system compaction that includes creep* (tech. rep.). Deltares. <https://www.deltares.nl/en/expertise/publicaties/user-guide-to-sub-cr-a-modflow-package-for-land-subsidence-and-aquifer-system-compaction-that-includes-creep>
- Kooi, H., & Yuherdha, A. (2018). *Updated subsidence scenarios Jakarta: MODFLOW SUB-CR calculations for Sunter, Daan Mogot and Marunda* (tech. rep.). Deltares. <https://www.deltares.nl/en/expertise/publicaties/updated-subsidence-scenarios-jakarta-modflow-sub-cr-calculations-for-sunter-daan-mogot-and-marunda>
- Kooi, H., Johnston, P., Lambeck, K., Smither, C., & Molendijk, R. (1998). Geological causes of recent (app. 100 yr) vertical land movement in the Netherlands. *Tectonophysics*, 299, 297–316. [https://doi.org/10.1016/S0040-1951\(98\)00209-1](https://doi.org/10.1016/S0040-1951(98)00209-1)
- Koppejan, A. (1948). A formula combining the Terzaghi load-compression relationship and the Buisman secular effect. *2nd International Conference on Soil Mechanics and Foundation Engineering* (Rotterdam). <https://www.issmge.org/publications/publication/a-formula-combining-the-terzaghi-load-compression-relationship-and-the-buisman-secular-time-effect>
- Leake, S. A., & Galloway, D. L. (2007). MODFLOW Ground-Water Model - User Guide to the Subsidence and Aquifer-System Compaction Package (SUB-WT) for Water-Table Aquifers. In *Techniques and methods*. USGS. <https://doi.org/10.3133/tm6A23>
- Maas, K. (2018). *De invloed van de winning Delft-Noord op de wegzijging en de grondwaterstand op basis van waarnemingen* (tech. rep.). Middelburg.
- Mankor, H. (2023). *Data points and GIS maps of Meetkundige Dienst & AHN viewers* (tech. rep.).
- Mesri, G. (1973). Coefficient of secondary compression. *ASCE J Soil Mech Found Div-v 99*, (SM1), 123–137. <https://api.semanticscholar.org/CorpusID:126671498>
- Minderhoud, P. S., Erkens, G., Pham, V. H., Bui, V. T., Erban, L., Kooi, H., & Stouthamer, E. (2017). Impacts of 25 years of groundwater extraction on subsidence in the Mekong delta, Vietnam. *Environmental Research Letters*, 12(6). <https://doi.org/10.1088/1748-9326/aa7146>
- Minderhoud, P. S., Erkens, G., Pham, V. H., Vuong, B. T., & Stouthamer, E. (2015). Assessing the potential of the multi-Aquifer subsurface of the Mekong Delta (Vietnam) for land subsidence due to groundwater extraction. *Proceedings of the International Association of Hydrological Sciences*, 372, 73–76. <https://doi.org/10.5194/piahs-372-73-2015>
- NEN. (2017). *Tabel 2b: Karakteristieke waarden van grondeigenschappen* (tech. rep.). NEN 9997-1+C2:2017.
- NHI. (2023a). *Data input voor hydrologische modellen*. Retrieved November 20, 2023, from <https://nhi.nu/data/>
- NHI. (2023b). *Hydrologische modellen*. Retrieved November 20, 2023, from <https://nhi.nu/modellen/>
- Provincie Utrecht. (2008, February 15). *GIS kaart van kwetsbaarheid voor oxidatie van organische stof*. Retrieved February 15, 2024, from <https://metadata.geodata-utrecht.nl/metadata/dataset/a0421e2d-2689-4a6e-9c1a-beb11cd029e0.xml>
- Provincie Utrecht. (2022a). *Bodem- en Waterprogramma provincie Utrecht 2022-2027* (tech. rep.). [Bodem-20en-20waterprogramma-20provincie-20utrecht-202022-2027](https://www.bodem-20en-20waterprogramma-20provincie-20utrecht-202022-2027)
- Provincie Utrecht. (2022b, March 29). *GIS kaart van historische bodemdaling door veenoxidatie*. Retrieved February 15, 2024, from <https://metadata.geodata-utrecht.nl/metadata/dataset/5c2b2f74-fa75-4a88-b325-ba611bcfdb13.xml>

- Provincie Utrecht. (2023). *Gebiedsdossiers grondwaterwinningen Provincie Utrecht*. Retrieved February 15, 2024, from <https://www.provincie-utrecht.nl/zoeken?search=gebiedsdossier>
- Rijkswaterstaat. (2005). *NAP herziening 01-01-2005*. Retrieved March 4, 2024, from https://open.rijkswaterstaat.nl/publish/pages/129139/nap_herziening_2005-verschillen.pdf
- Rijkswaterstaat. (2023a). *Dataregister Waterstaatskaarten*. Retrieved December 28, 2023, from <https://maps.rijkswaterstaat.nl/dataregister/srv/eng/catalog.search#/metadata/822ff575-eef7-4ca9-b399-8c2edd55117e>
- Rijkswaterstaat. (2023b). *NAP info GIS kaart*. Retrieved March 4, 2024, from <https://maps.rijkswaterstaat.nl/geoweb55/index.html?viewer=NAPinfo>
- RIVM. (2023). *Waterbeschikbaarheid voor de bereiding van drinkwater tot 2030 - knelpunten en oplossingsrichtingen* (tech. rep.). <https://doi.org/10.21945/RIVM-2023-0005>
- Roelofsen, F., Goorden, N., Buma, J., Van Gessel, S., Goes, B., De Lange, G., Van Meerten, H., Van Oostrom, N., Oude Essink, G., Sperna Weiland, F., Veldkamp, H., Vergroesen, T., Verkaik, J., & Gehrels, H. (2008). *Grondwatereffecten aan de oppervlakte: Onderzoek naar effecten van stopzettingen grondwateronttrekking dsm delft - hoofdrapport*. <http://resolver.tudelft.nl/uuid:f72e7825-709e-4e56-806a-bd9e3ece4825>
- Schothorst, C. (1982). *Drainage and behaviour of peat soils*. ICW.
- Schoular, J., & SkyGeo. (2023). *InSAR Technical Guide*. <https://skygeo.com/the-ultimate-guide-to-using-insar/>
- SkyGeo. (2023). *Bodemdalingskaart 2.0 Expert Viewer* [Initiative of Nederlands Centrum voor Geodesie en Geo-Informatica (NCG)]. Retrieved November 21, 2023, from <https://bodemdalingenkaart.portal.skygeo.com/portal/bodemdalingskaart/u2/viewers/basic/>
- Syvitski, J. P., Kettner, A. J., Overeem, I., Hutton, E. W., Hannon, M. T., Brakenridge, G. R., Day, J., Vörösmarty, C., Saito, Y., Giosan, L., & Nicholls, R. J. (2009). Sinking deltas due to human activities. *Nature Geoscience*, 2(10), 681–686. <https://doi.org/10.1038/ngeo629>
- Temmink, R. J., Robroek, B. J., van Dijk, G., Koks, A. H., Käärmelahti, S. A., Barthelmes, A., Wassen, M. J., Ziegler, R., Steele, M. N., Giesen, W., Joosten, H., Fritz, C., Lamers, L. P., & Smolders, A. J. (2023). Wescapes: Restoring and maintaining peatland landscapes for sustainable futures. *Ambio*, 52(9), 1519–1528. <https://doi.org/10.1007/S13280-023-01875-8>
- Ten Bosch, S. (2020). *Modelling subsidence in the Dutch Holocene coastal-plain Investigating subsidence components and their relevance for different situations* [Doctoral dissertation]. <http://resolver.tudelft.nl/uuid:2c308062-e0fa-4704-9b10-c745505a8cdd>
- Terzaghi, K. (1925). *Erdbaumechanik auf bodenphysikalischer grundlage*. Deuticke. <http://lib.ugent.be/catalog/rug01:000197953>
- TNO. (2023a). *Ondergrondgegevens | DINOloket* [Piezometer and subsurface data]. Retrieved October 7, 2023, from <https://www.dinoloket.nl/ondergrondgegevens>
- TNO. (2023b). *Ondergrondmodellen | BROloket* [REGIS II v2.2.1 subsurface models]. Retrieved October 7, 2023, from <https://www.broloket.nl/ondergrondmodellen/kaart>
- Unie van Waterschappen. (2021). *Overzicht grondwateronttrekkingen - Provincies en Waterschappen* (tech. rep.). <https://open.overheid.nl/documenten/ronl-50bd0112-74f0-4a63-855a-cec5a39efcaf/pdf>
- Unie van Waterschappen. (2023). *Overgang van winterpeil naar zomerpeil*. Retrieved December 28, 2023, from <https://www.waterschappen.nl/overgang-winterpeil-naar-zomerpeil/>
- USGS. (2018a, October 18). *Aquifer Compression due to Groundwater Pumping*. Retrieved February 14, 2024, from <https://www.usgs.gov/centers/land-subsidence-in-california/science/aquifer-compaction-due-groundwater-pumping>
- USGS. (2018b, November 30). *Extensometers and Compression*. Retrieved February 14, 2024, from <https://www.usgs.gov/centers/land-subsidence-in-california/science/extensometers-and-compaction#overview>
- Van Asselen, S., Erkens, G., & De Graaf, F. (2020). Monitoring shallow subsidence in cultivated peatlands. *Proceedings of the International Association of Hydrological Sciences*, 382, 189–194. <https://doi.org/10.5194/piahs-382-189-2020>
- Van Asselen, S., Kooi, H., & Van den Akker, J. (2019). *Deltafact Bodemdaling* (tech. rep.). STOWA. <https://www.stowa.nl/%20deltafacts/ruimtelijke-adaptatie/adaptief-deltamanagement/bodemdaling>

- Van de Plassche, O., & Roep, T. B. (1989). Sea-Level Changes in the Netherlands During the Last 6500 Years: Basal Peat vs. Coastal Barrier Data. In D. Scott, P. Pirazzoli, & C. Honig (Eds.), *Late quaternary sea-level correlation and applications: Walter s. newman memorial volume* (pp. 41–56). Springer Netherlands. https://doi.org/10.1007/978-94-009-0873-4{_}3
- Van den Akker, J., Kuikman, P., De Vries, F., Hoving, I., Pleijter, M., Hendriks, R., Wolleswinkel, R., Simões, R., & Kwakernaak, C. (2010). Emission of CO₂ from agricultural peat soils in the Netherlands and ways to limit this emission. *Proceedings of the 13th International Peat Congress After Wise Use – The Future of Peatlands, Vol. 1 Oral Presentations, Tullamore, Ireland, 8 – 13 June 2008*, 645–648. <https://research.wur.nl/en/publications/emission-of-co2-from-agricultural-peat-soils-in-the-netherlands-a>
- Van der Meulen, M. J., Van der Spek, A. J. F., De Lange, G., Gruijters, S. H. L. L., Van Gessel, S. F., Nguyen, B.-L., Maljers, D., Schokker, J., Mulder, J. P. M., & Van der Krogt, R. A. A. (2006). Regional sediment deficits in the dutch lowlands: Implications for long-term land-use options. *Journal of Soils and Sediments*, 7(1), 9–16. <https://doi.org/10.1065/jss2006.12.199>
- Verberne, M., Koster, K., Lourens, A., Gunnink, J., Candela, T., & Fokker, P. A. (2023). Disentangling Shallow Subsidence Sources by Data Assimilation in a Reclaimed Urbanized Coastal Plain, South Flevoland Polder, the Netherlands. *Journal of Geophysical Research: Earth Surface*, 128(7). <https://doi.org/10.1029/2022JF007031>
- Verruijt, A. (2010). *Grondmechanica* (Vol. 3). Delft University of Technology. <https://doi.org/10.1007/978-1-349-00175-0>
- Visschedijk, M., Trompille, V., Best, H., Den Haan, E. J., Sellmeijer, J. B., & Van Zantvoort, E. (2009). *MSettle Version 8.2: Embankment Design and Soil Settlement Prediction* (tech. rep.). Deltares. <http://resolver.tudelft.nl/uuid:88aa11df-55a9-4266-89f1-ae5568dca2>
- Vitens. (2023). *Data of extraction discharges of Vitens locations & hydraulic heads at piezometers* (tech. rep.).
- Wald, A., & Wolfowitz, J. (1943). An Exact Test for Randomness in the Non-Parametric Case Based on Serial Correlation. *The Annals of Mathematical Statistics*, 14(4), 378–388. <https://doi.org/10.1214/aoms/1177731358>
- WUR. (2023). *Parameters grondwaterdynamiek - Wageningen University of Research*. Retrieved December 8, 2023, from <https://www.wur.nl/nl/onderzoek-resultaten/onderzoeksinstituten/onderzoeksinstituut-research/faciliteiten-tools/software-en-modellen/grondwaterdynamiek/parameters.htm>
- Ye, S., Xue, Y., Wu, J., Yan, X., & Yu, J. (2016). Progression and mitigation of land subsidence in China. *Hydrogeology Journal*, 24(3), 685–693. <https://doi.org/10.1007/s10040-015-1356-9>
- Yilmaz, E., & Saglam, A. (2001). Secondary and tertiary compression behavior of Samsun soft blue clay. <https://www.issmge.org/publications/publication/secondary-and-tertiary-compression-behavior-of-samsun-soft-blue-clay>
- Zuur, A. (1958). Bodemkunde der Nederlandse bedijkingen en droogmakerijen, deel C: Het watergehalte, de indroging en enkele daarmee samenhangende processen. *Landbouw Hogeschool, Wageningen, Nederland*. <https://edepot.wur.nl/109962>

Appendices

List of Appendices

A	Background Figures & Maps	54
A.1	Explainer Maps	54
A.2	Groenekan Figures	56
B	Additional Theory	61
B.1	Stationary vs. Transient Groundwater Flow & Models	61
B.2	Tertiary Compression	62
B.3	Measuring Subsidence	62
C	Selection Procedures	64
C.1	Location Selection	64
C.2	Groundwater Model Selection	64
C.3	Subsidence Model Selection	65
D	Pastas Time Series Model Analysis	68
D.1	Piezometer Hydraulic Head Data	68
D.2	Methodology Piezometer Time Series Models	69
D.3	Results Piezometer Time Series Models	70
E	Other Historical Subsidence Data Analyses	73
E.1	Meetkundige Dienst vs. Actueel Hoogtebestand Nederland	73
E.2	Historical Peat Oxidation in Province of Utrecht	76
F	AZURE	78
F.1	AZURE Packages & Layers	78
F.2	AZURE Assumptions & Conditions	79
F.3	AZURE Result Tables	79
F.4	AZURE Maps	80
G	BDOM & Shrinkage	82
G.1	BDOM & Shrinkage Parameterisation & Assumptions	82
G.2	BDOM & Shrinkage Result Tables	82
H	D-Settlement	83
H.1	D-Settlement Structure of Western and Eastern Models	83
H.2	D-Settlement Layer Parameterisation	84
H.3	D-Settlement Base Scenario Assumptions & Conditions	85
H.4	Consolidation & Creep in Holocene and Waalre Result Tables	86
I	Python Scripts	88
I.1	Analytical Groundwater Flow Calculations: Glee & Hantush	88
I.2	Aerobic BDOM Calculation	90
I.3	Shrinkage Calculation	92

Background Figures & Maps

A.1. Explainer Maps

Figure A.1 shows the service area of Vitens and other drinking water companies in the Netherlands. Vitens clearly has the largest service area, delivering drinking water to 5.6 million clients spanning from Utrecht to the German border in the east to the Waddeneilanden in the north.



FIGURE A.1: Drinking water companies and their service area in the Netherlands (Aqua Assistance, 2018).

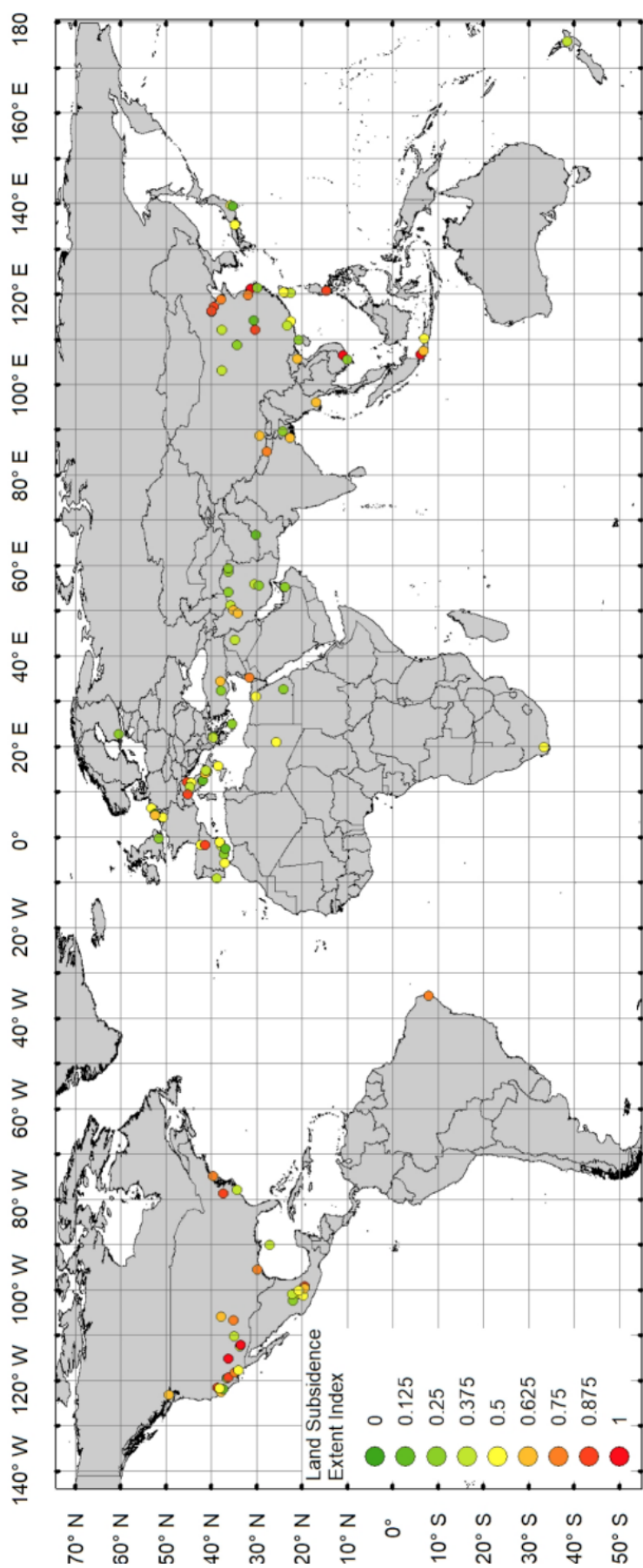


FIGURE A.2: Global extent of subsidence due to groundwater extraction (Dinar et al., 2019, p5).

A

A.2. Groenekan Figures

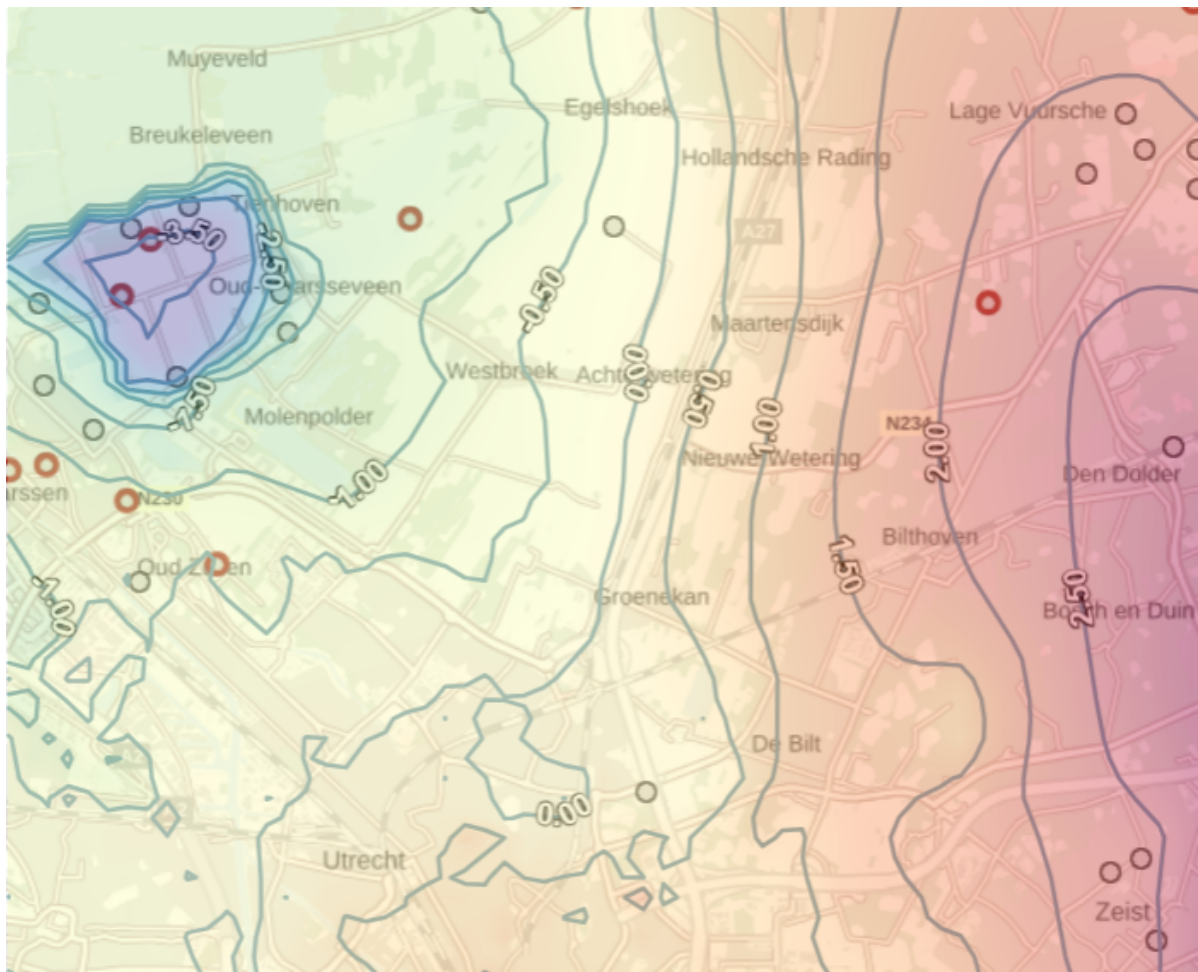


FIGURE A.3: Isohypse map around extraction Groenekan (Geologische Dienst Nederland, 2023). Groenekan groundwater level is between -0.5 and 0.0 m NAP.

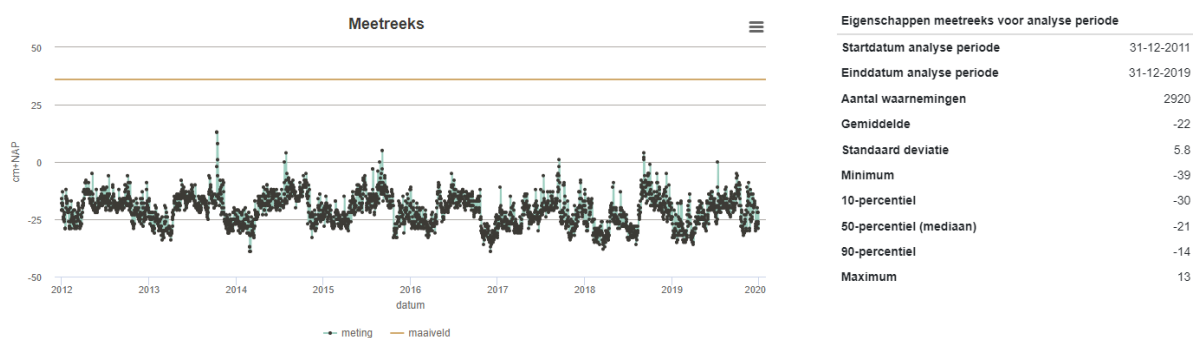


FIGURE A.4: Measured groundwater level at Groenekan in piezometer B31H0794-001 (Geologische Dienst Nederland, 2023). GXG is -0.22 m NAP and GLG is -0.30 m NAP from 2012 to 2019.

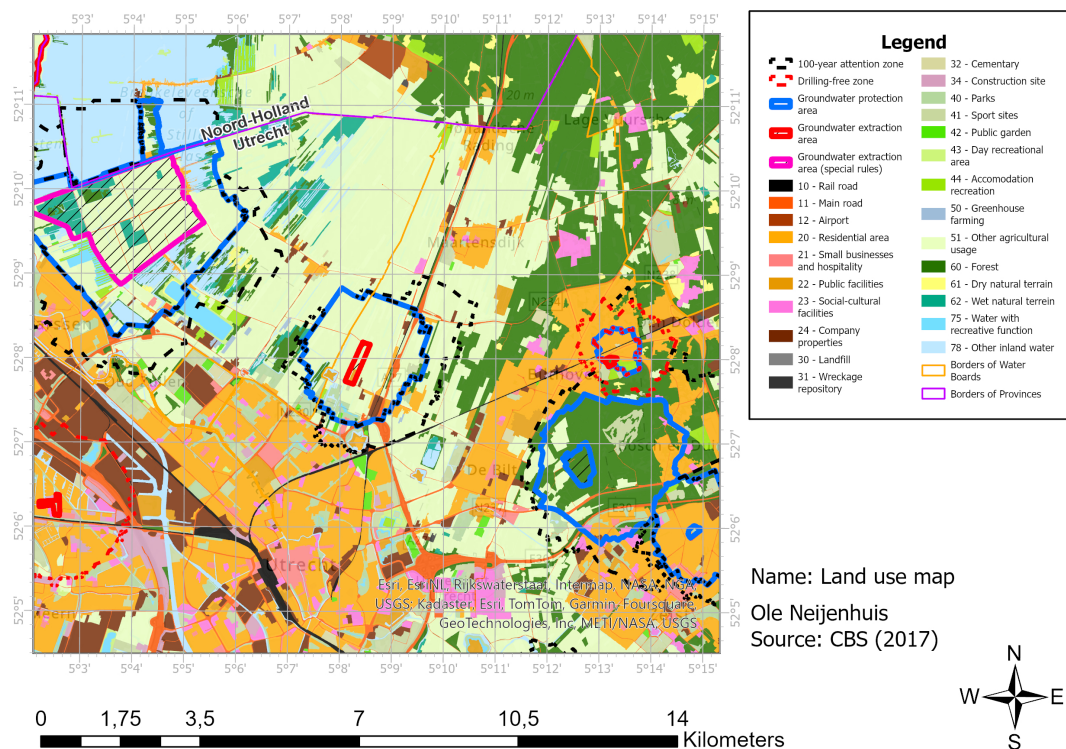


FIGURE A.5: Land use (BBG) around extraction Groenekan (CBS, 2017).

In Figure A.6, two ground drill (NL: *grondboring*) tests until -120 m NAP are shown. Sub-figure A.6a, 1 kilometre to the west of Groenekan, clearly indicates a 15 m thick Waalre clay layer. On the contrary, Sub-figure A.6b, 1 kilometre to the east of Groenekan, shows a complete sand composition without any aquitard.

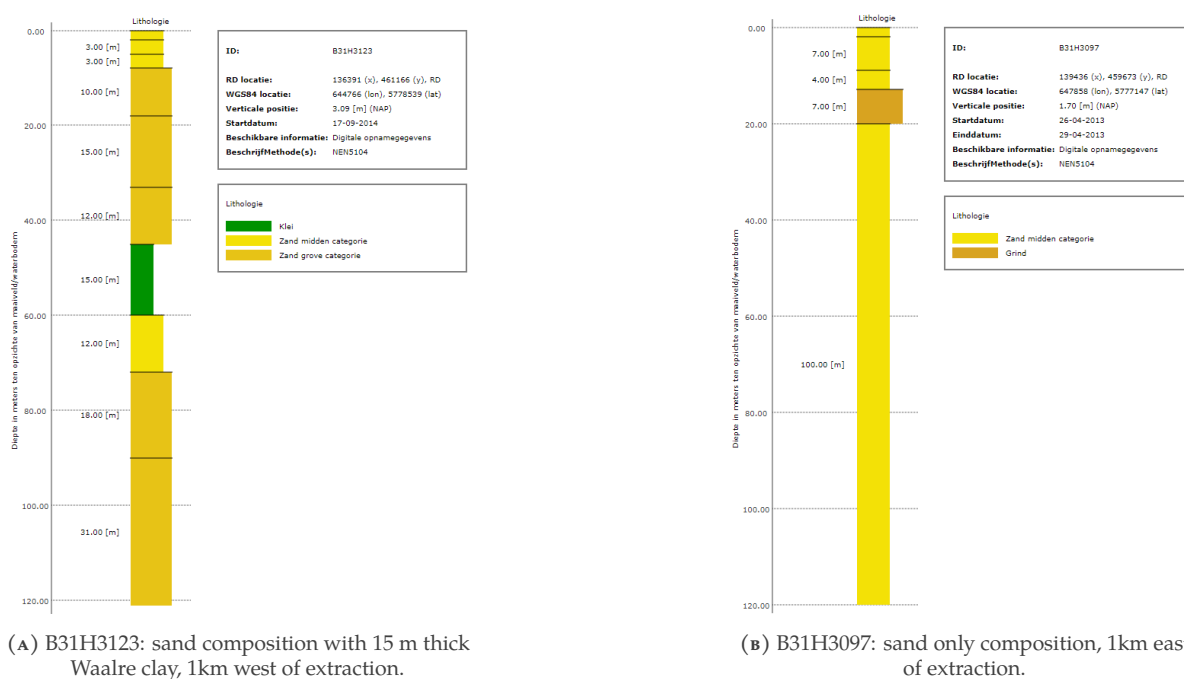
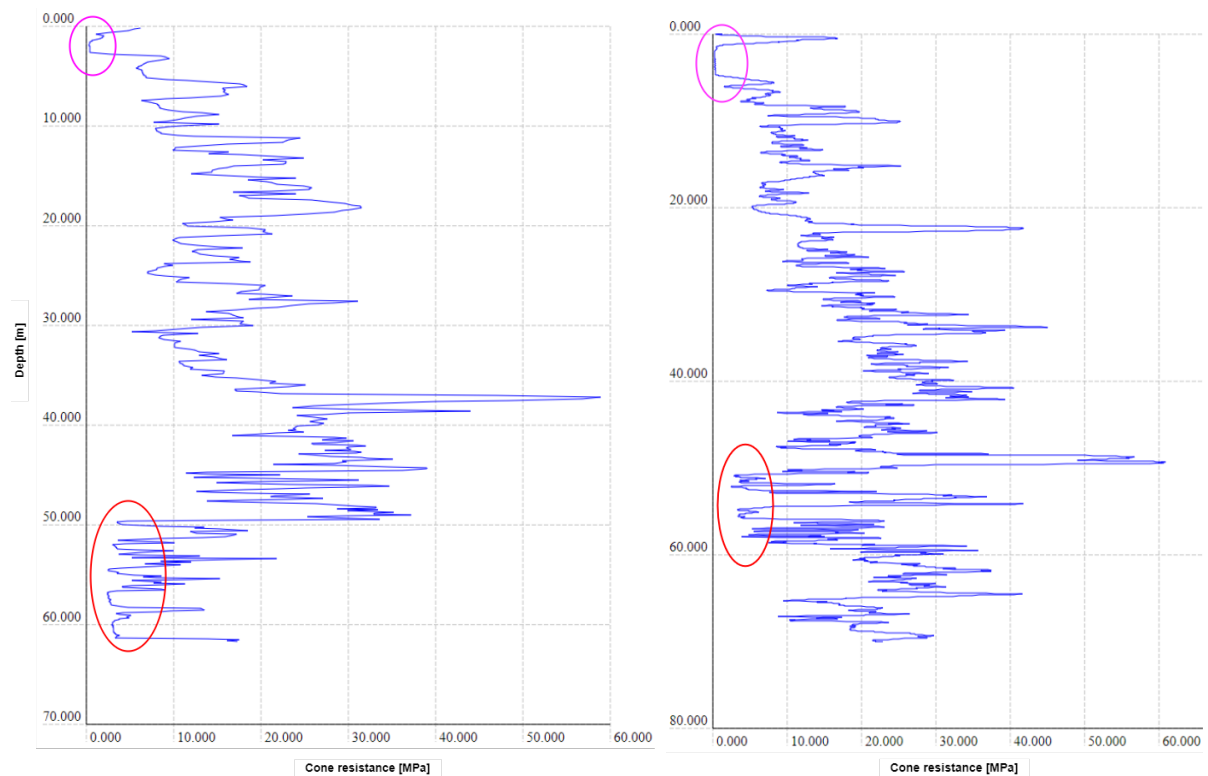


FIGURE A.6: Ground drill tests until -120m NAP in a 1km radius around Groenekan extraction (TNO, 2023a).

Table A.1 presents the REGIS.II soil profile at Groenekan, which mainly consists of sandy aquifers ranging from very fine to very coarse sand and two aquitards (Waalre and Sterksel clay).

TABLE A.1: REGIS.II soil formation and geohydrology at Groenekan extraction (TNO, 2023a).

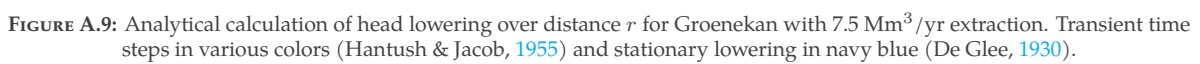
Code	Formation	Soil	Depth [m NAP]	Geohydrology
DTc	Propagated deposits	Complex	+45 to -30	-
HLc	Holocene	Clay/Peat	0 to -1	Phreatic aquifer
BXz	Boxtel	Sand	-1 to -8	First aquifer
KRz/Drz	Kreftenheye/Drente	Sand	-8 to -20	First aquifer
URz	Urk	Sand	-20 to -30	First aquifer
STz	Sterksel	Sand/Clay	-30 to -48	First aquifer
Wak	Waalre	Clay	-48 to -60	Aquitard
PZWaz	Peize & Waalre	Sand	-60 to -140	Second aquifer
MSk	Maassluis	Clay	-140 to -160	Aquitard



(A) CPT17432 at Wittevrouwen, 3.0 km from Groenekan.

(B) CPT11707 at Haarrijnseplas, 8.5 km from Groenekan.

FIGURE A.7: Cone resistances from two independent CPT tests in Utrecht (TNO, 2023b). Holocene top layer is located from 0 to -1 m NAP. Waalre clay is located from -48 to -60 m NAP. Both layers are highlighted with pink and red circles respectively.



A

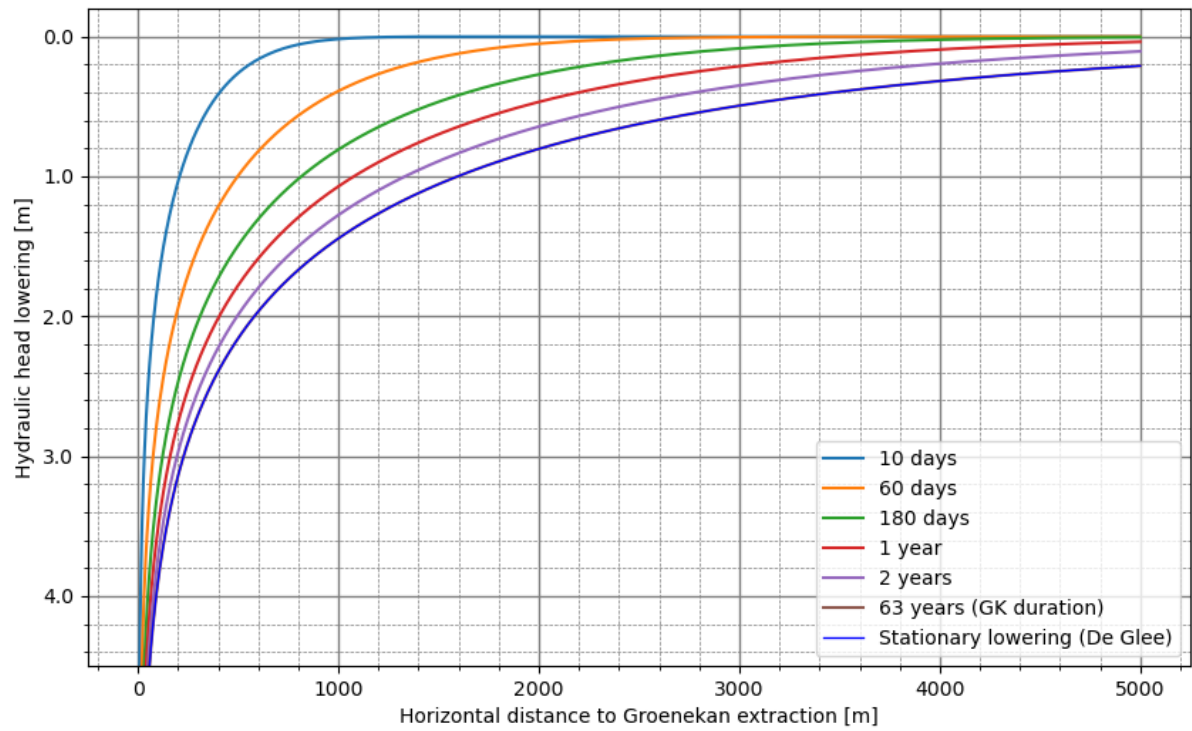


FIGURE A.10: Analytical calculation of head lowering over distance r for Groenekan with $10.0 \text{ Mm}^3/\text{yr}$ extraction. Transient time steps in various colors (Hantush & Jacob, 1955) and stationary lowering in navy blue (De Glee, 1930).

Additional Theory

B.1. Stationary vs. Transient Groundwater Flow & Models

When the heads do not change with time, the storage volume remains constant in time, which implies that the inflow and outflow of water are equal in the system, implying a stationary (NL: *statisch*) situation. In reality, groundwater flow is always transient (NL: *dynamisch*). Transient flow occurs because boundary conditions and system stresses change through time, for example changing aquifer recharge, river levels, or pumping rates of wells. A specific application of transient flow analysis is the evaluation of aquifer properties by induced stresses, such as pumping tests. The storage in an unconfined aquifer increases when the water table rises (Verruijt, 2010).

A MODFLOW2005 model can be computed both stationary and transient over time and space. The purpose of a stationary analysis is to predict average groundwater levels and heads. This is done by calculating average levels in rivers and drainage systems. It also uses a stationary, time-independent groundwater recharge rate, which can be imposed using the RCH package. However, the imposed stationary groundwater recharge can vary spatially (NHI, 2023b). The advantage of stationary models is that they run significantly faster than transient models.

A transient model aims to calculate changes in groundwater levels and flows over time and space. This is done on the basis of initial boundary conditions and time-dependent hydrological and meteorological model inputs. For a time-dependent calculation, coupling with an unsaturated zone model may pay off, which includes the feedback between evaporation and drought stress. The same applies to coupling a surface water module to simulate the effects of fluctuating water levels. One should always balance calculation speed and model accuracy; Stationary models are quick, but only for one time step. Transient models, however, are more accurate over time and space, but need significantly more running time than stationary models.

Dutch Groundwater Levels

Four important Dutch groundwater level benchmarks are listed and explained below. The GHG, GLG, "Gemiddelde Voorjaars Grondwaterstand" (GVG), and "Gemiddelde Grondwaterstand" (GXG) are the most important and are used within AZURE and D-Settlement as well to indicate average high, low or spring groundwater levels. WUR (2023) defined the following definitions for different groundwater levels over a 30-year period under given climatic and hydrological conditions:

- **GHG** (NL: *Gemiddeld Hoogste Grondwaterstand*): Average of the three highest groundwater levels in a hydrological year (1 April to 31 March) at a measurement frequency of twice a month (around the 14th and 28th).
- **GLG** (NL: *Gemiddeld Laagste Grondwaterstand*): Average of the three lowest groundwater levels in a hydrological year (1 April to 31 March) at a measurement frequency of twice per month (around the 14th and 28th).
- **GVG** (NL: *Gemiddelde Voorjaars Grondwaterstand*): Average of groundwater levels on 14 March, 28 March and 14 April in a given calendar year.
- **GXG** (NL: *Gemiddelde Grondwaterstand*): Average of all groundwater level averages.

B.2. Tertiary Compression

Edil and Dhowian (1979) observed in peat soils that sometimes the rate of creep is not constant over logarithmic time. Bishop and Lovenbury (1969) concluded this also for clay soils. This led to the term "tertiary compression", which indicates a change in the strain rate during creep. The component is shown in Figure B.1, along with the primary and secondary compression. Tertiary compression is defined as the decreasing rate of settlement observed in the strain rate (ϵ) - $\log(t)$ curve during the secondary compression phase.

Feng et al. (2021) performed consolidation tests on Chinese peat and clay soil and showed that strain during primary and secondary consolidation stages was mainly caused by drainage, accounting for 99.67% of the total strain. Strain during the tertiary compression stage is usually due to drainage and organic matter decomposition (Feng et al., 2021; Yilmaz & Saglam, 2001). Through the analysis of the relationship between strain and the permeability coefficient, the influence of permeability on the consolidation process of organic clay or peat soil mainly occurs in the primary and secondary consolidation stage, and has little effect on the tertiary consolidation process. Since the Netherlands consists mainly of peat and clay top layers and tertiary compression is not added in Dutch subsidence models (Fokker et al., 2018; Kooi et al., 2018; Van Asselen et al., 2019), the tertiary compression effect will not be considered in the rest of this thesis.

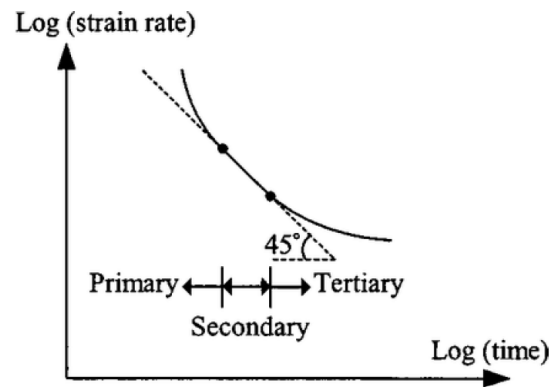


FIGURE B.1: Time vs. strain plots, including tertiary compression (Edil & Dhowian, 1979)

B.3. Measuring Subsidence

Subsidence usually is a very slow process of only a few millimetres per year. Therefore, effects of subsidence can only be noticed by inspecting surface levels with accurate equipment over a longer time span of years, or even decades. Moreover, the height of surface levels should be measured multiple times per year (Van Asselen et al., 2019) in order to observe seasonal trends such as droughts, TLDs for summer and winter, and varying extraction discharges. Subsidence can either be measured via field measurements or remote sensing. Their accuracy and limitations are discussed in the following two sub-sections.

Field Measurements

Various field measurement techniques exist to assess subsidence. The most proven method of measuring surface level movement uses spirit levels (NL: *waterpassen*). At point locations, the height of the ground level relative to NAP is measured with a spirit level instrument and staff. The measurements have a millimetre accuracy and are easy to execute.

Other field measurement techniques compute changes in elevation of various soil layers or depths by comparing variations in the height of plates or anchors. For example, an extensometer system is a well-founded measuring rod with multi-level anchors that allows the contribution of different soil layers to the total soil movement to be measured. It involves continuous point measurements with mm-scale accuracy. Extensometers, in various versions, are used worldwide for measuring soil subsidence, but have not yet been used much in the Netherlands, especially not in peatland areas. Figure B.2) shows an example used in Rouveen, Overijssel, with three anchor

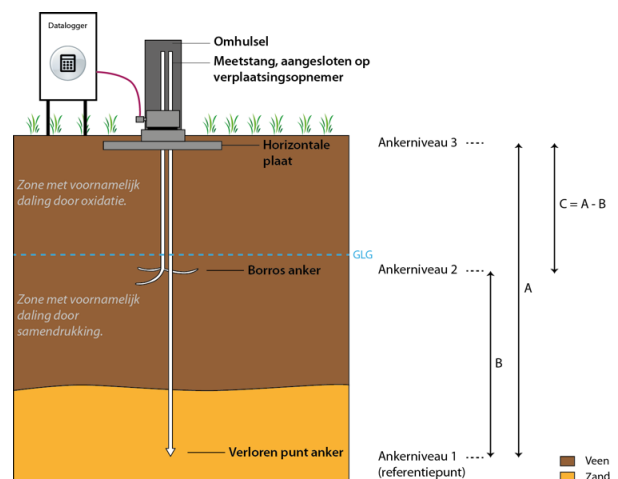


FIGURE B.2: Extensometer system with three anchor levels (Van Asselen et al., 2020).

levels (Van Asselen et al., 2019). Firstly, it consists of an anchor placed at a reference point in a stable sand layer (level 1). Secondly, level 2 is located under the GLG and mainly measures the subsidence caused by the consolidation and creep of peat. However, level 3 measures the total subsidence of the soil layer between roughly the surface level and the reference level. The difference between levels 2 and 3 is the decline caused by processes in the soil layer between the ground level the GLG level, which would be mainly oxidation, since the peat is exposed to oxygen. Lastly, the anchor rods exit into the displacement transducer, which measures the height changes of all anchors relative to anchor level 1. The displacement transducer (NL: *verplaatsingsopnemer*) is connected to a data logger which stores the subsidence rates over time.

Additionally, measuring plates or beacons (NL: *zakplaatjes of -bakens*) can also be used to measure subsidence at different depth levels. Measuring plates consist of a tube to which two fold-out stainless steel oval plates are attached. The plates are unfolded into the undisturbed profile at the bottom of a borehole with a defined depth. Another tube is slid over the tube attached to the plate so that it can be finished at the desired height. The plate and tubes are covered with a wooden tile. The top of the tubes can be measured to determine the vertical displacement of the different plate levels relative to NAP.

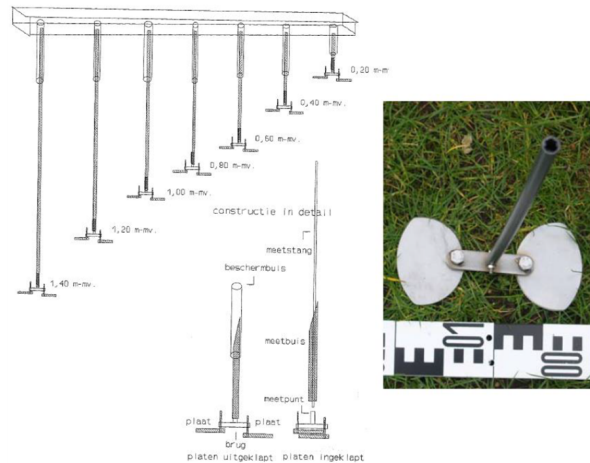


FIGURE B.3: Representation of a setup with seven measurement plates (Van Asselen et al., 2019).

Interferometric Synthetic Aperture Radar

InSAR is a remote sensing technique that generates radar images produced by a "scanner" attached to a satellite. Annually, dozens of images are made and processed to monitor deformations of the surface level, infrastructure, and buildings with a level of accuracy in the magnitude of millimetres. It is an active satellite system where the satellite sends a signal with a wave length, in the order of a couple of centimetres, to Earth and measures the reflected wave length of the signal. Subsequently, the difference between the sent and reflected wave length is compared and from there a height difference is derived. Figure B.4 shows a simplified visualisation of this principle.

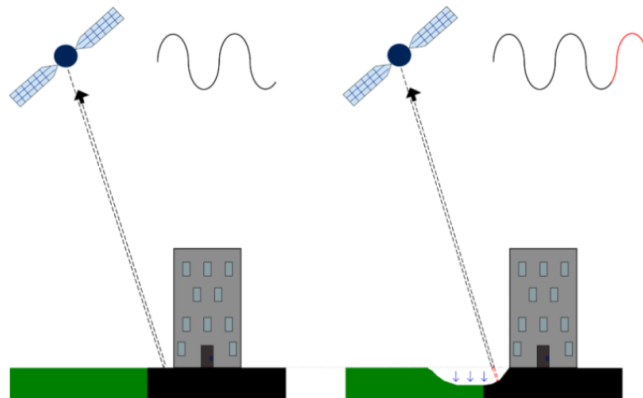


FIGURE B.4: InSAR measurements before and after subsidence, extra phase signal in red (SkyGeo, 2023).

After processing the **InSAR** images, there is thus no estimation of absolute surface level elevation, but rather relative displacements of the locations in time. The technique does not always work on smooth surfaces, such as water, due to a mirror bouncing effect of the signal. Nor does the signal reflect consistently with rapidly changing objects such as vegetation, unless the signal penetrates the vegetation and measures the surface level. Lastly, photogrammetry uses a drone or aircraft, which flies over and takes photos of the terrain. The photos are then overlaid to obtain a 3D image. For height measurements, more than five reference points are needed to create a reliable image. **AHN** is the Dutch example of photogrammetry maps.

Selection Procedures

C.1. Location Selection

Initially, eight potential Vitens groundwater extractions for drinking water production were considered. These extractions are located in the Provinces of Utrecht and Flevoland, which are Holocene and Pleistocene areas in the Netherlands (Van de Plassche & Roep, 1989).

For the argument of the available thesis time, one final location was selected by weighing the following three criteria:

1. Sensitivity to subsidence, based on geohydrological composition;
2. Expansion plans;
3. Model availability.

Table C.1 lists all considered extraction locations for this study, along with their sensitivity to subsidence, expansion plans of Vitens (RIVM, 2023), and existing model availability. The sensitivity to subsidence was mainly weighted on the geohydrological assessments done for each location. This translates to the presence of a peat and/or clay top layer which may oxidise due to low groundwater levels and deep thick clay layers which might compress through the higher effective stresses due to the groundwater extraction.

TABLE C.1: Sensitivity to subsidence, expansion plans, and model availability per considered extraction location in the Provinces of Utrecht and Flevoland in alphabetical order. Chosen location Groenekan in cyan.

Location	Sensitivity to subsidence	Expansion plans	Model availability
Benschop	Medium/High	3.0 Mm ³ /yr in 2024	No
Cothen	Low/Medium	None	No
Eempolder	Medium	3.0 Mm ³ /yr in 2029	No
Groenekan	Medium	2.5 Mm ³ /yr in 2025	Yes (AZURE)
Leersum	Low	None	No
Schalkwijk	High	7.0 Mm ³ /yr in 2026	No
Soestduinen	Low	None	No
South Flevoland	High	Expansion planned	No

In agreement with Vitens and Arcadis, Groenekan groundwater extraction was deliberately selected to investigate due to the calibrated AZURE model availability from Arcadis (2019), its medium sensitivity to subsidence, and its short term expansion plans. All in all, this location is the most feasible and interesting to assess within the given time frame, since it is potentially prone to subsidence and has a different future prospect for extraction discharge.

C.2. Groundwater Model Selection

To understand the groundwater flow and geohydrological processes at the extraction locations, it is necessary to select a suitable groundwater model. In this section, Dutch groundwater models "Actueel modelinstrumentarium voor de Zuiderzee Regio" (AZURE) and "Landelijk Hydrologisch Model" (LHM) are discussed and their advantages and disadvantages compared. Eventually, one is selected as the groundwater model for this research.

LHM

LHM is the integrated national groundwater and surface water model of the Netherlands in cells of 250x250 metres (NHI, 2023b). Using MODFLOW2005, **LHM** calculates the regional groundwater flow pattern of the Netherlands for the current climate and for climate scenarios. The instrument aims to simulate average and dry situations. Instruments can be used to calculate e.g. groundwater levels, heads in deeper aquifers, seepage and subsidence fluxes and the exchange between groundwater and surface water. In addition, the distribution of surface water is calculated over the national water distribution network and over the various regional surface waters in the Netherlands, so that surface water availability can be visualised at regional and national level.

AZURE

AZURE is a regional groundwater model derived from **LHM** for the central part of the Netherlands and works on the basis of MODFLOW2005 as well, combined with linkable modules in **iMOD**. The model covers the area of the Veluwe to the Utrechtse Heuvelrug, the Province of Flevoland and the IJsselmeer (NHI, 2023b). Figure C.1 shows the **AZURE** model boundaries.



FIGURE C.1: AZURE model boundaries (H2O Waternetwerk, 2014).

Advantages & Disadvantages of LHM & AZURE

In brief, **LHM** has one advantage and two disadvantages. Unlike **AZURE**, **LHM** has been fully calibrated, which decreases the probability of any outliers in the model output. On the other hand, the **LHM** model has a coarse cell grid of 250x250m, ten times bigger than **AZURE**'s 25x25m. This results in less accuracy over space on the sub-surface and surface water systems, which are both essential in determining hydraulic heads. Additionally, **AZURE** is specifically focused on the scope area of Groenekan and contains the latest versions of subsurface models REGIS and GeoTOP and up-to-date extraction discharge data of Vitens. On top of that, **LHM**'s model boundaries are significantly larger than **AZURE**, which may lead to other inaccuracies in ground composition and/or longer model calculation times. All in all, this may result in less accurate model output.

Conclusion Groundwater Model Selection

It is deemed essential to have the finest grid size possible to model hydraulic heads accurately. Moreover, a regional model usually has more detailed layers and input files than a national model because the scope area is smaller. Hence, it is decided that **AZURE** is chosen as the final geohydrological model to calculate groundwater levels and hydraulic heads at the scope locations.

C.3. Subsidence Model Selection

Multiple state-of-the-art subsidence models are considered for selection. Table C.2 displays all software packages which could model subsidence processes, including their scope and main limitations.

The NEN-Bjerrum and abc-isotach models discussed in Section 2.5.2 are used in almost all the packages in Table C.2, making them a crucial theoretical component when modelling subsidence. Furthermore, the effects of **BDOM** and shrinkage could be based on various empirical formulas. However, these formulas are not embedded in the packages, except for the Atlantis Python package (Bootsma et al., 2020).

The following section investigates and discusses the different models used in calculating subsidence. There are three important criteria for choosing a model:

1. Vitens extracts groundwater from a deeper aquifer for Groenekan, the second aquifer (NL: *tweede watervoerende pakket*) to be precise;
2. Aquitard compression and creep should be included, since these processes are dominant in **SGE**;
3. A transient model result is desired to map and analyse the influence of the groundwater extractions over time and space.

TABLE C.2: Overview of software packages used in the Netherlands to predict shallow subsidence through compression, oxidation, and/or shrinkage (Van Asselen et al., 2019).

Package	Processes	Scope application	Main limitation
Atlantis	Peat oxidation & Compression due to groundwater level change (isotach)	Regional/national maps; long time frames; focus on Holocene deposits	No Darcy (only Terzaghi); no shrinkage (or partially implicit in oxidation);
D-Settlement	Compression/creep due to loading and GWL/head lowering (isotach or Koppejan)	Local; settlement due to loading/structures; vertical drainage	Unsuitable for time-dependent phreatic level; no oxidation/shrinkage
FlexPDE	Compression due to surface loading and phreatic or hydraulic head change (isotach)	Local; settlement due to increment and subsidence due to variations in phreatic level and/or hydraulic head	Unsuitable for significant phreatic reductions; no oxidation/shrinkage
Plaxis	Compression/deformation due to general external/internal loads (2D soft soil creep)	Local; 2D geotechnical; situations involving multidimensional deformation and flow	No oxidation/shrinkage
MF SUB (SD)	Compression due to groundwater level change and hydraulic head change (isotach)	Regional, relatively deep (5.0 – 1,000 m) groundwater systems; impact of extractions	Unsuitable for significant phreatic level reduction; no oxidation/shrinkage
MF SUB-CR	Compression including creep due to groundwater level change and hydraulic head change (isotach)	Regional, relatively deep (5.0 – 1,000 m) groundwater systems; impact of extractions	Unsuitable for significant phreatic level reduction; no oxidation/shrinkage

Unfortunately, there was no license available to use either FlexPDE or Plaxis and these models are thus not taken into consideration for calculating subsidence.

Deltares - Atlantis

Atlantis allows the efficient and largely automated production of predictive subsidence maps on a national scale in the Netherlands. The tool, based on Python scripts, calculates the subsidence induced by phreatic groundwater level management in Holocene soft-soil areas through **BDOM**, shrinkage, and consolidation (Bootsma et al., 2020).

The modelling involves a grid of rectangular cells, which in reality is not the case but for simplicity this is assumed. Subsequently, the cells are grouped into **TLs** that each correspond to specific water board districts. The spatial variation of subsidence within these cells is influenced by factors such as the distribution, depth, and thickness of layers within Holocene deposits which are vulnerable to oxidation and consolidation. Atlantis interacts with external datasets, including surface elevation, phreatic groundwater level, and geology.

Figure C.2 shows the modelling process, which operates on individual columns, each consisting of 3-dimensional cells or “voxels”. These voxels are assigned lithology and parameter values necessary for oxidation and consolidation calculations. The voxel model is derived from GeoTOP (BRO, 2023a), which can be refined with regional datasets for higher resolution.

The time dimension in the model is categorised into several stress periods and time steps. Stress periods represent the time during which a constant stress is applied, such as surface water level or recharge, and are further discretised into individual time steps. Each time step involves consolidation and oxidation calculations, capturing the height loss of each voxel as a result of these processes. The total subsidence in a stress period informs the groundwater level lowering in the subsequent period.

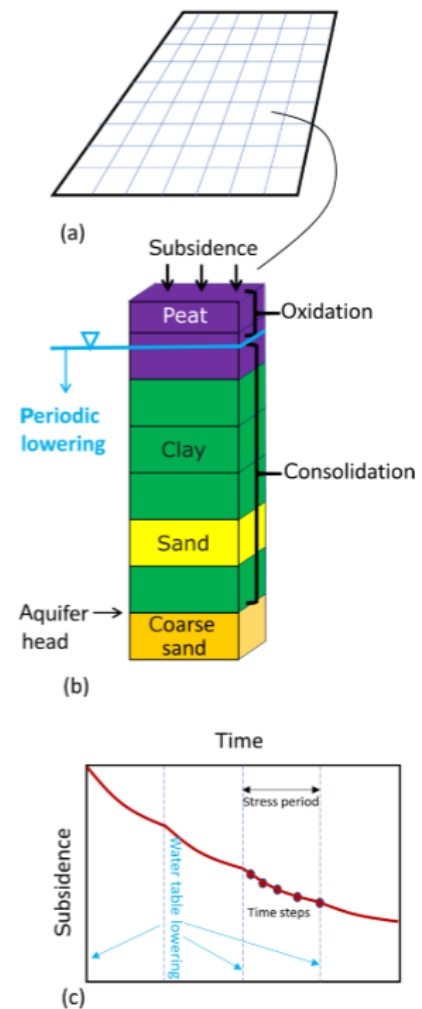


FIGURE C.2: (a) TLS. (b) Schematisation of a voxel stack for an individual cell. (c) Time discretisation through stress periods.

USGS - SUB & SUB-WT

This extension of MODFLOW2005 is designed specifically to simulate the subsidence caused by groundwater pumping. It considers the compression of aquifer sediments due to the removal of groundwater, which leads to a decrease in pore pressure and subsequent consolidation of the aquifer material. SUB includes capabilities to simulate both confined and unconfined aquifer systems. It models vertical deformation of the aquifer system based on stress-strain relationships and typically employs Terzaghi's theory of consolidation (Harbaugh, 2005).

SUB-WT, similar to SUB, is an extension used to model the subsidence and compression of the aquifer system resulting from groundwater extraction (Leake & Galloway, 2007). It considers not only vertical subsidence but also horizontal and areal deformations of the aquifer system. SUB-WT typically incorporates more advanced numerical techniques and may handle large scale, complex models.

Deltares - SUB-CR

SUB-CR is a MODFLOW2005-based subsidence package developed by Kooi et al. (2018) & Deltares that besides the primary elastic consolidation, also includes compression by creep. Many basic concepts and principles were borrowed from SUB-WT (Leake & Galloway, 2007). These concepts include 1-dimensional compression; total or geostatic stress calculated from local overburden; overburden and total stress depend on the water table; and the concept of interbeds. Some concepts and approaches have been modified in SUB-CR. Calculating effective stress, for example, is done based on cell-averaged stress and pore pressure, and soil above the water table is involved in compression.

In SUB-WT, effective stress is evaluated for the base of model cells, and unsaturated parts of cells do not contribute to subsidence. The most prominent difference, however, concerns the inclusion of creep and an isotach compression model, resulting in a more comprehensive and complete process representation of soft-sediment deformation. Creep is important in geotechnical applications involving soft-sediment (silt, clay, peat) consolidation. There is no obvious reason why creep would be irrelevant when these sediments consolidate and cause subsidence driven by groundwater pumping and management.

D-Settlement

Deltares Settlement ([D-Settlement](#)) is a finite element software programme specifically designed to model the settlement behaviour of soils under various loading conditions (Visschedijk et al., 2009). It plays a crucial role in geotechnical engineering, where understanding how soil compacts and settles is essential. Similarly to SUB-CR, [D-Settlement](#) analyses consolidation settlement due to excess dissipation of pore pressure in low-permeability soils such as clay and peat. Also, it models creep, which occurs over extended periods due to sustained loading or groundwater level and/or head lowering.

Conclusion Subsidence Model Selection

Although Atlantis is a suitable model to simulate subsidence through [BDOM](#) and shrinkage, it is not suitable for simulating subsidence due to increased effective stress, such as groundwater extraction. On top of that, Section 5.2 shows that the organic-rich top layers to the west of Groenekan are not affected by head lowering due to extraction. Additionally, SUB and SUB-WT are comparable to SUB-CR, since they all model vertical deformation. However, SUB and SUB-WT are older models and do not include creep, which is important to take into account when modelling in the Netherlands, since it is a soft soil-rich country. On the other hand, SUB-CR and [D-Settlement](#) practically model similarly, but [D-Settlement](#) is more user-friendly and gives quicker simulation results. Hence, it is decided that [D-Settlement](#) from Deltares is chosen as the final model to calculate subsidence rates at extraction location Groenekan. Detailed methodology on the [D-Settlement](#) model is given in Section 4.4.

Pastas Time Series Model Analysis

Section D.1 elaborates on the data input for the TSMs (KNMI, 2023c; TNO, 2023a; Vitens, 2023). Next, the methodology to make TSMs in Pastas, evaluating the set criteria and selecting the best TSMs, is presented in Section D.2. Lastly, Section D.3 includes the results of selecting the twelve best models, isolating Groenekan's influence on the heads specifically.

D.1. Piezometer Hydraulic Head Data

To investigate whether Groenekan has a significant influence on the measured head values per piezometer, several TSMs with different influences were prepared by Artesia (2023). These models are tested against evaluation criteria and compared with each other to finally select the best model. The final objective is to compare the head reductions in Pastas with the results of the AZURE groundwater model. Hereby, it is validated whether the predicted AZURE effects are in line with the historical changes in the head due to the variation in the extraction discharges of Groenekan.

The following criteria were used to select measurement sites for further analysis:

- Last measurement after 1990;
- Minimum of five consecutive years with 12 measurements;
- Filter depth is known and is below -10 m NAP.

The last criterion serves to exclude phreatic measurement data. Due to the complex interaction with surface water and meteorological influences in the heterogeneous Holocene aquifer, phreatic measurements are expected to be less useful to properly estimate the influence of Groenekan on phreatic groundwater levels. With those criteria, five piezometers from the monitoring network of Waternet and 136 piezometers from DINoloket remain.

For precipitation and evaporation, time series from 1957 of nearby stations were downloaded (KNMI, 2023c). Any gaps in the series were filled with the data from the closest measuring station. Furthermore, data on extraction discharges for Groenekan, Bilthoven, Beerschoten, Soestduinen, and Leidsche Rijn are shown in Figure D.1 (Vitens, 2023). Extracted volumes were partly recorded on a monthly basis. This is converted to a daily basis by spreading the monthly flow evenly over all days in the month. Note: the peaks in the series before 1970 are because in this period the extracted volumes per month are equal in the dates, resulting in a higher discharge rate in February.

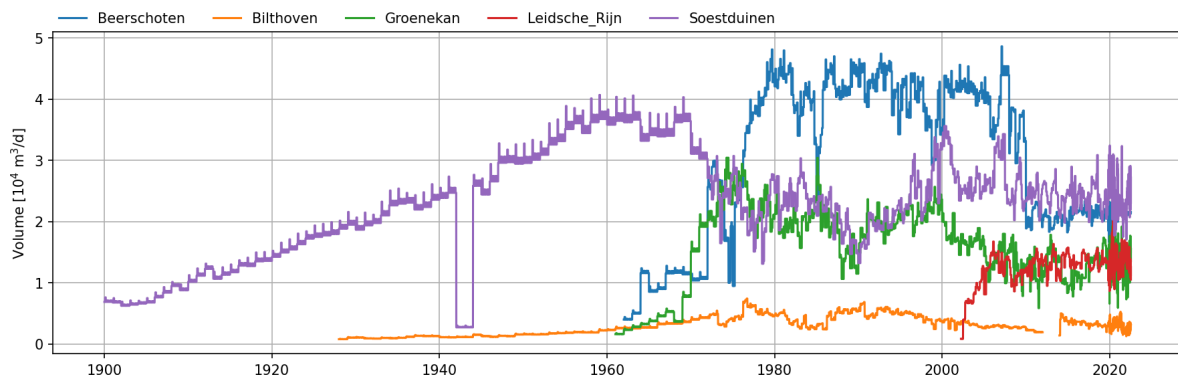
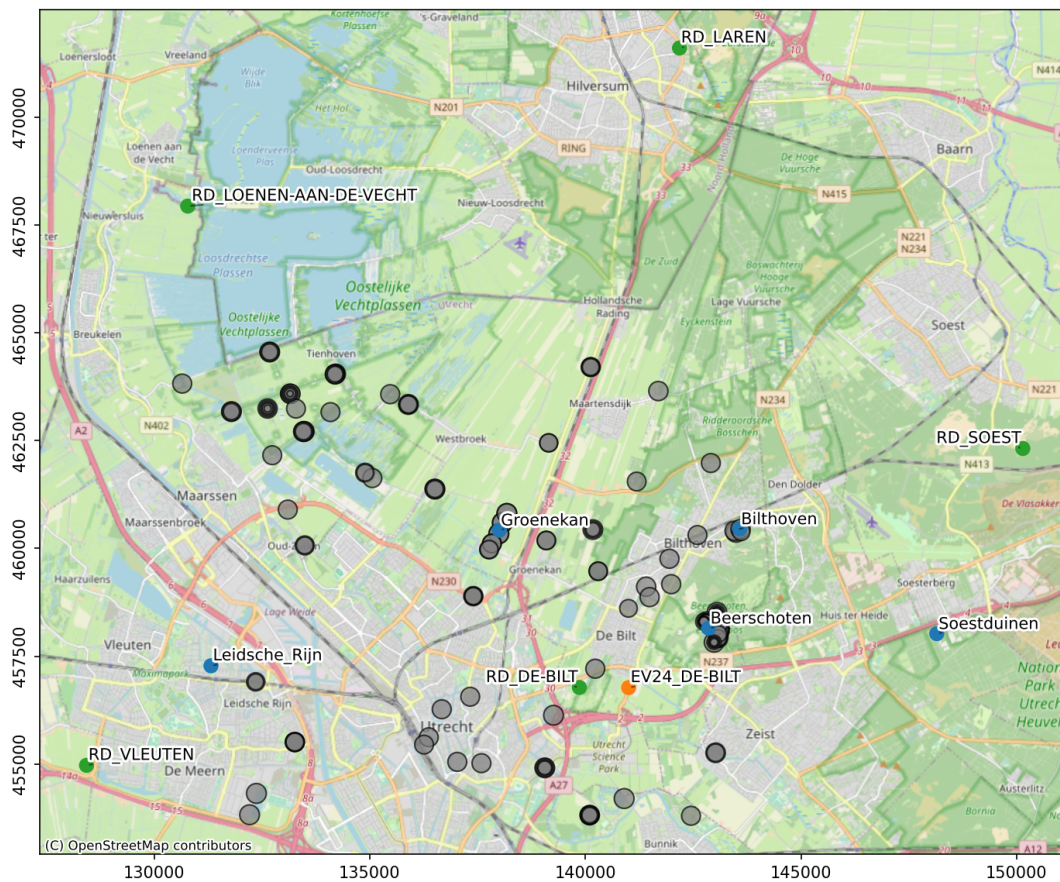


FIGURE D.1: Daily extraction discharge per location (Vitens, 2023).

Figure D.2 shows the locations of the used piezometers, extractions and precipitation/evaporation measuring stations in the scope area.



D

FIGURE D.2: Locations of considered piezometers (grey), Vitens' drinking water extractions (blue), and measuring stations for precipitation (green) and evaporation (orange) (Artesia, 2023).

D.2. Methodology Piezometer Time Series Models

Construction of Time Series Models

The TSMs for each piezometer are constructed in a similar fashion (Artesia, 2023):

- 1. Groundwater recharge as an explanatory series:** Groundwater recharge is added as an explanatory series. It consists of the precipitation and evaporation series from the nearest KNMI stations. A linear combination of precipitation minus evaporation is assumed for groundwater recharge and the exponential response function is applied.
- 2. Models with different explanatory series:** 7 models are created for each piezometer series. The first model only includes groundwater recharge as an explanatory series. The drinking water extractions are then added one by one to the time series model. The extractions are included in the "WellModel", where all extractions share a response function that is scaled with the distance between the piezometer and the extraction(s). The average X, Y-coordinate of all pumping wells is used for the location of the extraction and the Hantush and Jacob (1955) function is applied as the response function.
- 3. Noise model:** A noise model is included in the TSMs to account for propagating errors (the error of yesterday affects the error of today).
- 4. Fitting and optimisation:** The model is fitted to piezometer measurements on a 14-day basis. The calculation step of the model is daily (a piezometer level is calculated for each day). Optimization is performed with "LeastSquares". In the first step, optimisation is performed without a noise model, which is an attempt to estimate better start values for the parameters. In the second step, the noise

model is activated and the optimal parameters from the first step are specified as start parameters. Good start parameters contribute to a better final estimate of the parameters and thus ultimately a better fit of the time series model to the measurements.

Model Evaluation Criteria

The evaluation of the TSMs is based on the rules presented in Brakenhoff et al. (2022). In that study, rules were established to test whether a time series model is reliable. In this study, the same requirements are used, except for the requirement regarding the fit, which has been adapted compared to the article:

- The fit of the model, expressed via the R^2 , must be at least greater than 0.6;
- There must be no significant auto-correlation present in the noise. This is tested using the "Runs" test (Wald & Wolfowitz, 1943), which tests a series of numbers (in this case a series of seven correlations) for randomness;
- The length of the responses (t_{95}) must be shorter than half the length of the piezometer series. In the case of extractions, at least one extraction must meet this requirement, the other extractions do not have to meet this requirement;
- The uncertainty of the "gain" (e.g. stationary influence of extractions) must not be smaller than two times the estimated standard deviation.

Based on these four criteria, models are "accepted" or "rejected". The aim of these criteria is to make a quick assessment of whether a model is reliable. These are not strict requirements and it is possible that a rejected model may still be useful depending on the purpose of the study. However, this must be assessed per model and therefore falls outside the scope of this assessment.

Selection of Best Models

If multiple models for a piezometer series meet all the evaluation criteria, the "Akaike Information Criterion" is used to select the best model. The aim is to select the simplest model that gives the best fit. This statistical value therefore says something about the fit of the model, where a penalty is applied for the number of model parameters. This statistic can only be used to compare different model structures for the same measurement point and cannot be used to compare different models for different piezometer series.

D.3. Results Piezometer Time Series Models

Evaluation Time Series Models

A total of 987 TSMs were evaluated for 141 piezometer head time series. Table D.1 shows how many models satisfy each test criterion. Combining the four criteria, this leaves 50 models at 40 unique locations which meet all set criteria. Thus, 29% of the sites has a reliable time series model available. Of these 50 models, the best model for each time series was selected based on the lowest "Akaike Information Criterion" (AIC). This yields 40 models (one per unique location) to which further analysis was applied.

TABLE D.1: Results of evaluation criteria for piezometer time series models (Artesia, 2023).

Evaluation criterion	Accepted models (total = 987)	Unique locations (total = 141)
$R^2 > 0.6$	380 (39%)	65 (45%)
No significant auto-correlation	642 (66%)	108 (77%)
$t_{95} < \text{half of head time series}$	722 (74%)	138 (98%)
gain $> 2\sigma$	263 (27%)	130 (92%)
Total	50 (5%)	40 (29%)

Of the 40 sites with a reliable model, 28 included an extraction as a significant influence. Significant here means that the model with extraction(s) meets all criteria and scores better according to the AIC statistic. At 12 sites, Groenekan is included as a significant influence in the time series model, which has been further analysed.

Example Time Series Model

Figure D.3 shows an example of the results of the time series model of the piezometer B32C0003-001 from 1968 to 2005. See Figure D.2 for the location of this piezometer. This model includes the Bilthoven and Groenekan extractions, at 2.6 and 3.4 km from the piezometer respectively. Historical extraction discharges jointly cause a lowering of approximately 25 to 70 cm, resulting in a head lowering varying between 5 and 35 cm.

In the top left of Figure D.3, the model simulation is compared with the actual measurements and the R^2 shows the correlation between the measurements and the model. Below that, the residuals and noise are presented. Next, the contributions of groundwater recharge and extraction to the head dynamics are given, where the contributions from Bilthoven and Groenekan are summed. On the top right, the optimal model parameters are presented, including the estimated uncertainty. Lastly, the step responses of groundwater recharge and extraction are presented below the model parameters.

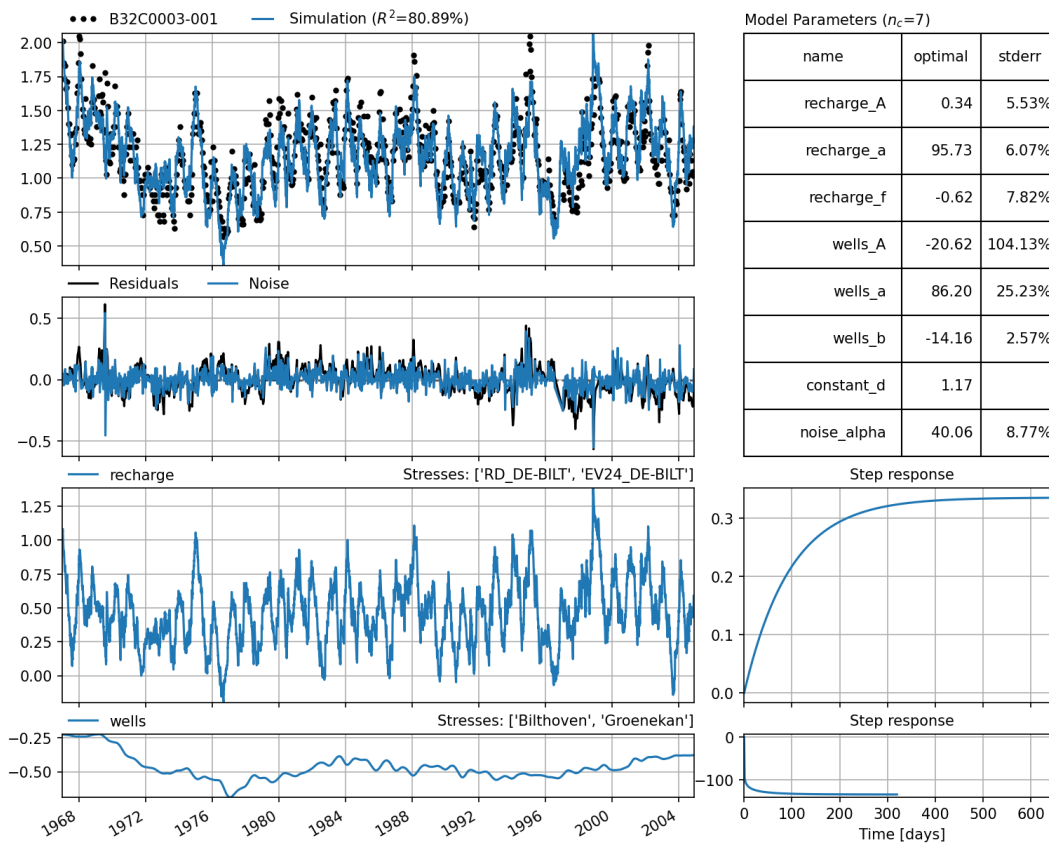


FIGURE D.3: Time series model results for piezometer B32C0003-001 from 1968 till 2005 (Artesia, 2023).

Estimated Influence on Heads due to Groenekan Extraction

The estimated influence of Groenekan extraction on the head lowerings is shown in Figure D.4 with the twelve best TSMs. For each model, the calculated contribution of Groenekan extraction over time is shown. The head lowering graph covers the same time period as the head measurements for that concerning piezometer, hence the graphs do not all extend over the same period.

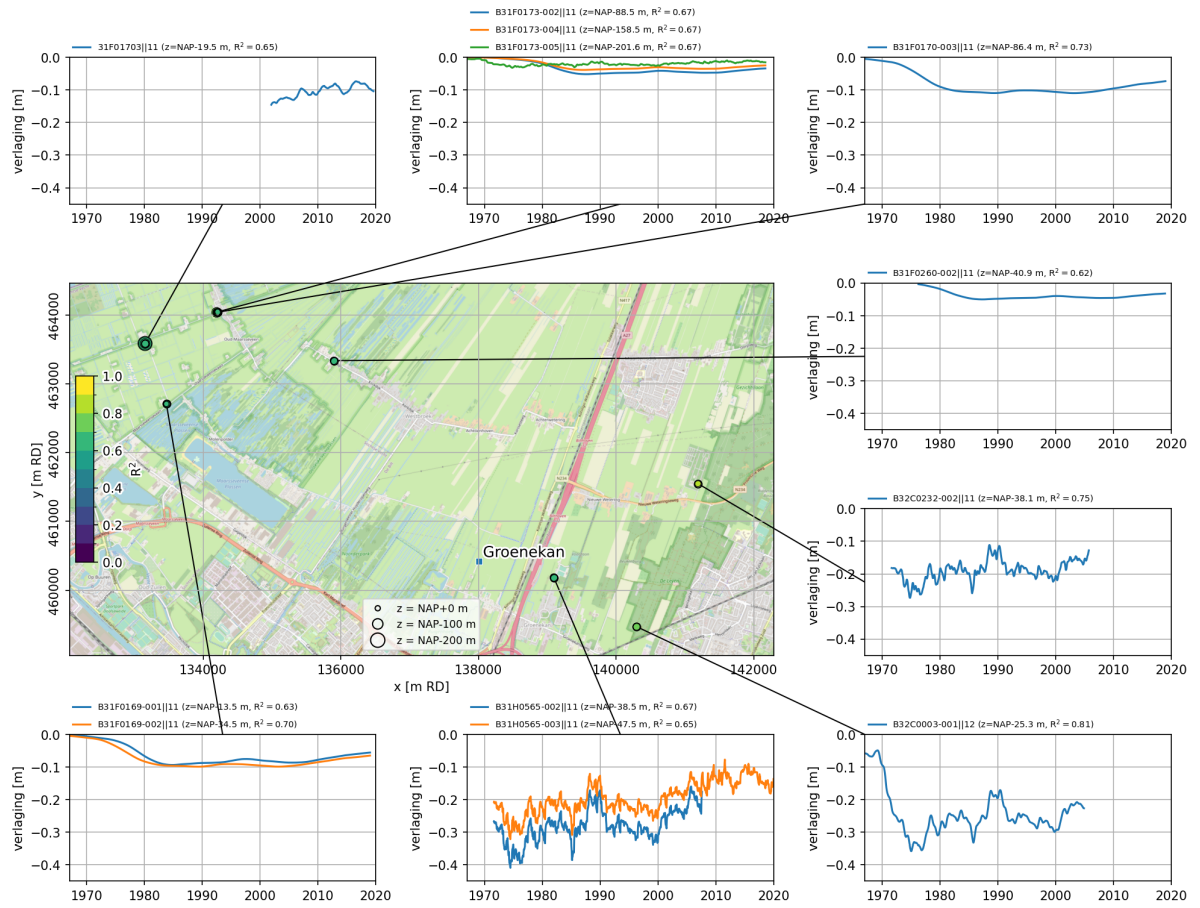


FIGURE D.4: The estimated head lowering due to Groenekan extraction of twelve Pastas time series models (Artesia, 2023). The size of the dots on the map represents the depth of the filter.

From Figure D.4, three key insights are observed:

- Western TSMs result in head lowerings of 5 to 10 cm in either the first or second aquifer (-13 to -200 m NAP). These piezometers are located between 3.6 and 5.8 km from Groenekan;
- Eastern TSMs show head lowerings of 10 to 40 cm, all from piezometers in the first aquifer (-25 to -48 m NAP). The piezometers are located between 1.1 and 3.4 km from the extraction;
- The speed of response, shown by faster dynamics and flashy peaks in the graphs, is greater in the east. All TSMs show similar dynamics with a recognisable decrease in lowering around 1990, a period when the extraction discharge from Groenekan was also lower compared to the period 1980-1990 (Figure 3.6).

Other Historical Subsidence Data Analyses

Sections E.1 and E.2 give the methodologies and results for the comparison of MD to AHN4 data and the analysis of peat oxidation maps. For the two methods in the following paragraphs, the NAP revision in 2005 was taken into account for Groenekan (map sheet 31H), which was lowered by 8 mm compared to the previous NAP level (Rijkswaterstaat, 2005, 2023b).

E.1. Meetkundige Dienst vs. Actueel Hoogtebestand Nederland Methodology MD vs. AHN4

Until 2003, the MD was the geographic information centre of Rijkswaterstaat. Since then, the height maps were digitalised into the online viewer AHN. There is a possibility to compare manual height measurements of the MD, from the period 1954 to 1969, with different AHN maps (AHN1 (1998-2000), AHN2 (2008-2010), AHN3 (2014-2018), AHN4 (2020-2023)) of Utrecht to deduct an annual subsidence rate. However, it needs to be noted that Ten Bosch (2020) investigated this comparison method and concluded it is subject to large uncertainties. Nonetheless, the uncertainties may not be as large as the total subsidence over the period 1961 to 2023.

Namely, all measurement points from the MD and AHN viewers have a certain error, the total error for each point includes both a random error (stochastic error) and a systematic error (standard deviation). The error of the MD measurements is not documented properly, since they are done between 1954 and 1969 with manual devices which measure surface elevation. Rijkswaterstaat (2023a) declares that MD data is rounded to 10 cm, so an error of ± 5 cm may be present. Also, AHN (2023) documented their error ranges and states 95,4% (two standard deviations) of the AHN2, 3 and 4 height measurement points fall within an uncertainty margin of 15cm. This is the sum of 5 cm of stochastic error and two standard deviation errors of 2×5 cm = 10 cm. On the contrary, AHN1 has an even larger uncertainty margin of 35 cm due to a larger systematic error of 15 cm per standard deviation (AHN, 2023). Therefore, it is chosen to compare the MD and AHN4 points to have the largest possible time frame and obtain the most reliable results.

Maps MD vs. AHN4

1,489 available MD and AHN data points have been compared and analysed in GIS. Figure E.1 presents a histogram, which includes 17 bins and their count, on the distribution of subsidence or uplift around Groenekan. The mean μ of all points is -2.6 cm/10yrs and the standard deviation σ is 2.6.

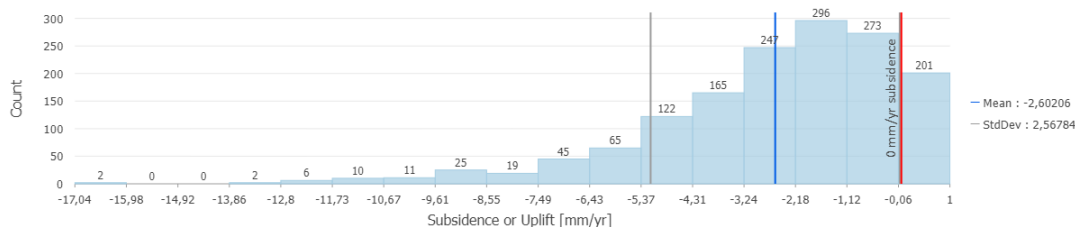


FIGURE E.1: Distribution histogram of subsidence or uplift rates around Groenekan, divided over 17 bins. 0-subsidence line is plotted in red, mean μ in blue and the standard deviation σ in grey.

In Figure E.2, the data points are plotted around Groenekan. In ArcGIS, the data points are categorised in six legend classes, from dark red for high subsidence rates to bright green for high uplift rates in [mm/yr]. Points with higher subsidence rates are mainly located around extraction locations Bethunepolder and Groenekan. The green uplift points are scattered throughout the area.

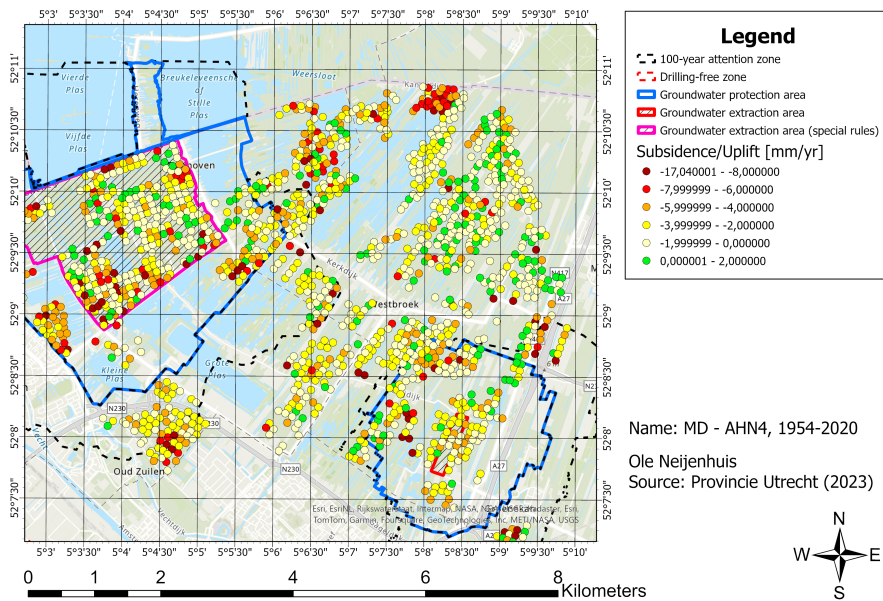


FIGURE E.2: Subsidence or uplift data points [mm/yr] obtained by comparing MD with AHN4 data points around Groenekan and Bethunepolder from 1954 to 2020 (AHN, 2023; Mankor, 2023).

It needs to be noted that the Bethunepolder extraction most likely plays a large factor in influencing the average subsidence in this map, due to its high extraction rate and the peat-rich top layer which is vulnerable to BDOM. Therefore, the map in Figure E.3 excludes the Bethunepolder and isolate the data points surrounding Groenekan only, so that conclusions can be drawn. The Groenekan groundwater protection area and three circles with 1, 2, and 3 km radii (purple, orange, and blue dashed circles respectively) have been plotted within the map and the data within the four distances to Groenekan are analysed.

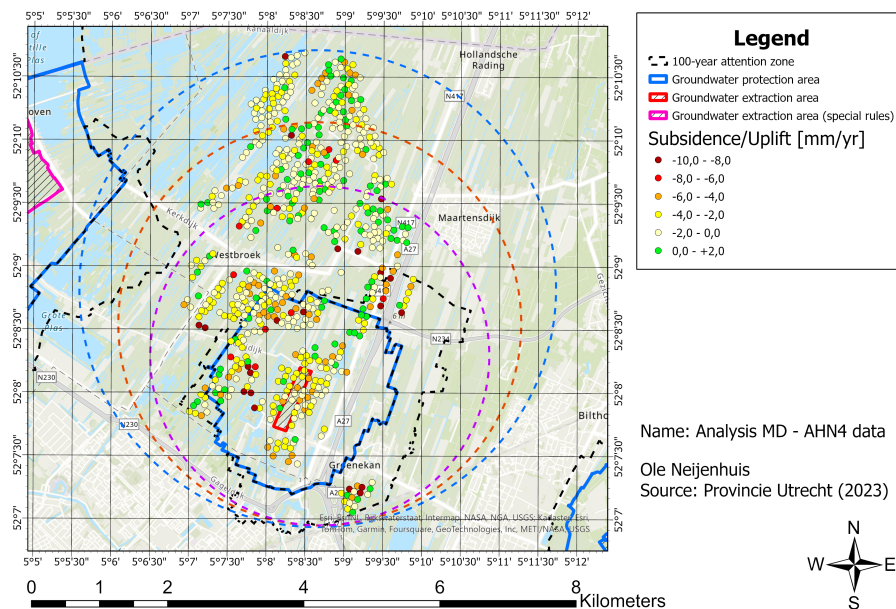


FIGURE E.3: Subsidence or uplift data points [mm/yr] within three circles with 1, 2, and 3 km radii (AHN, 2023; Mankor, 2023).

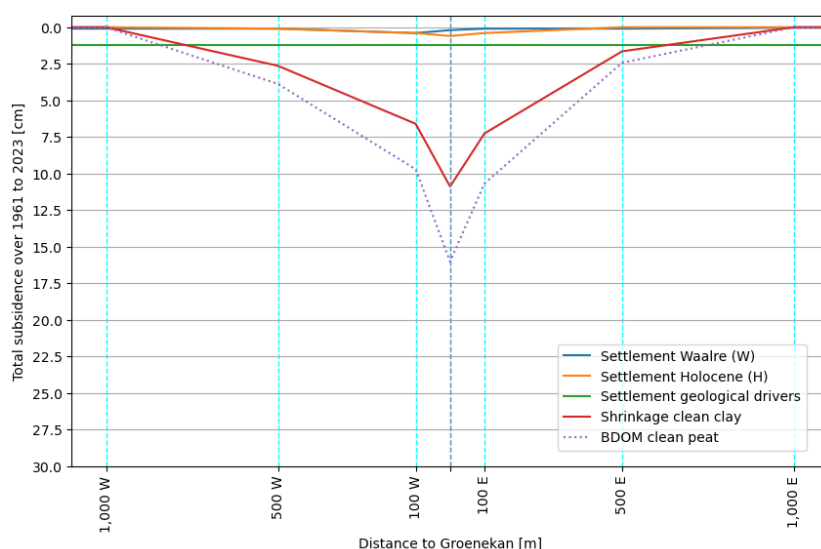
Table E.1 compares the data points within each area, so it can be investigated if the subsidence fades over a further distance from Groenekan. The decrease in mean subsidence further away from Groenekan is an interesting finding, but it should also be noted that the standard deviation decreases for each step. Thus, the overall error margin of the data points within the protection area is larger than the points within the 3 km radius.

TABLE E.1: MD vs. AHN4 data analysis on four different distances from Groenekan (GK) extraction.

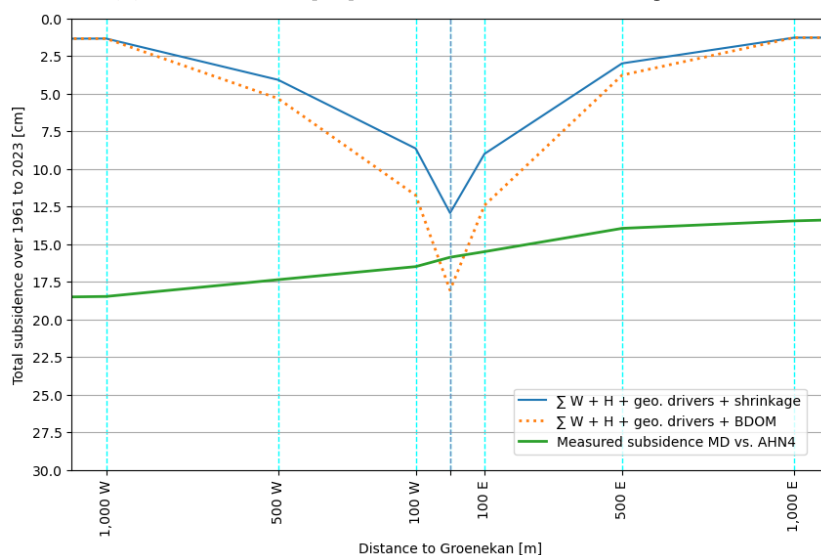
Distance	No. of data points	Mean subsidence [cm/10yrs]	Standard Deviation
Protection area GK	223	-2.6	2.6
1 km radius	399	-2.4	2.5
2 km radius	505	-2.2	2.4
3 km radius	663	-2.0	2.3

Results Overview 1961 to 2023: Comparison with MD vs. AHN4

Figure E.4 shows the total modelled **SGE** around Groenekan for each individual subsidence process. Subsequently, the sums of all subsidence processes are compared to the **MD** vs. **AHN4** data. The sum which includes shrinkage of clay is deemed most likely around Groenekan, whereas the sum with **BDOM** of peat is deemed the least likely. Therefore, the sums are plotted with solid and dotted graphs respectively.



(A) Total subsidence [cm] for each individual subsidence process.



(B) Sum of all subsidence processes compared to MD vs. AHN4 data. Blue solid graph includes shrinkage of clean clay and the orange dotted graph includes BDOM of clean peat.

FIGURE E.4: Results overview for base scenario of Groenekan over the period 1961 to 2023 with a 2 km west to east cross-section.

E.2. Historical Peat Oxidation in Province of Utrecht

Methodology Historical Peat Oxidation

There are open-source [GIS](#) maps available of historical subsidence due to peat oxidation ([BDOM](#)) in the Province of Utrecht based on height data collected in the years between 1955 and 1975 by [MD](#) and height data from [AHN2](#) between 2008 and 2010 (Provincie Utrecht, 2008, 2022b). Only points located in actual peatlands are considered, excluding built-up areas, roads, and excavations to isolate subsidence related to peat oxidation.

The analysis involves several steps (Provincie Utrecht, 2022b):

1. **Elevation change:** The difference in elevation between [MD](#) and [AHN2](#) data reveals the subsidence occurring over the period of 33 to 55 years;
2. **Sub-area delineation:** The analysed area is divided into subareas based on:
 - (a) [TLS](#)'s: Administrative water management units under responsibility of the water boards;
 - (b) Ground composition: Categorised, using the Dutch GeoTOP map (BRO, 2023a) into five types: clay; clay on peat; peat with clay cover; clayey peat; thin peat.
3. **Vulnerability to oxidation:** From the distinguished five types of top layers, a map with vulnerability to oxidation (Figure E.5) is made and used in assessing the historical subsidence (Provincie Utrecht, 2008).
4. **Average subsidence:** Within each sub-area, the average subsidence of all included [MD](#) points is calculated, representing the overall subsidence for that specific region. Sub-areas with fewer than 10 [MD](#) points are excluded due to insufficient data.

The extended time frame between data sources ensures that measured subsidence significantly exceeds potential measurement errors, leading to reliable findings. This method provides detailed estimates of [BDOM](#)-related subsidence across various areas in the Province of Utrecht, considering both temporal changes and spatial variations in ground composition.

Figure E.5 illustrates the vulnerability to peat oxidation (or [BDOM](#)) around Groenekan (Mankor, 2023; Provincie Utrecht, 2008). Around Groenekan some vulnerable areas are shown, but this is relatively innocent compared to the peat-rich top layer of the Bethunepolder.

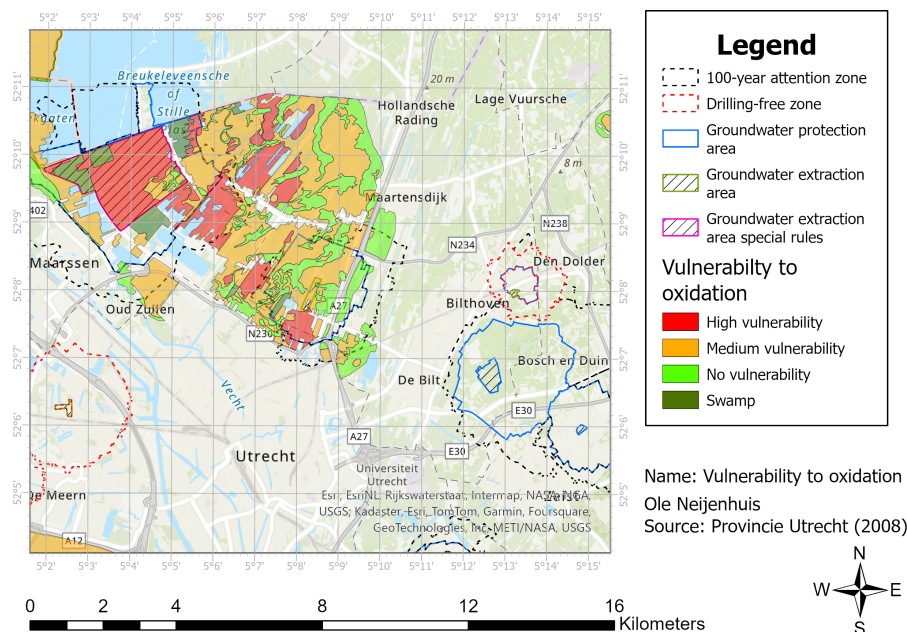


FIGURE E.5: Vulnerability to peat oxidation around Groenekan extraction (Provincie Utrecht, 2008).

Maps Historical Peat Oxidation

Next, the vulnerability map is translated into Figure E.6, which shows the historical peat oxidation. This analysis is done based on height data collected in the years between 1955 and 1975 by the MD and height data from the AHN2 (2010) (Mankor, 2023; Provincie Utrecht, 2022b). Thus, subsidence by oxidation is calculated in mm/yr over a maximum period of 55 years.

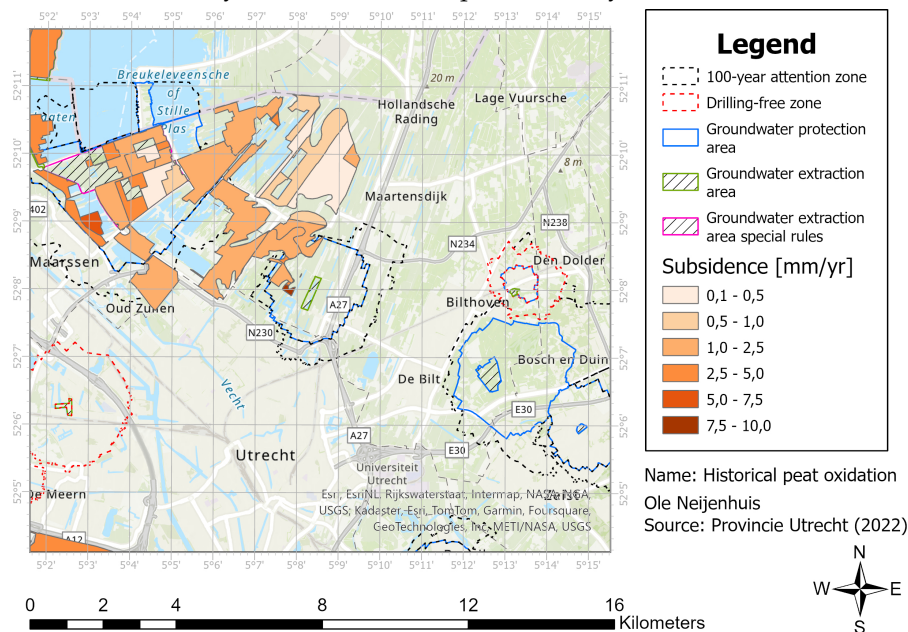


FIGURE E.6: Historical peat oxidation around Groenekan extraction (Provincie Utrecht, 2022b).

Subsequently, the historical peat oxidation is compared to the phreatic GLG results from L1 in AZURE (Figure 2.1), which creates Figure E.7:

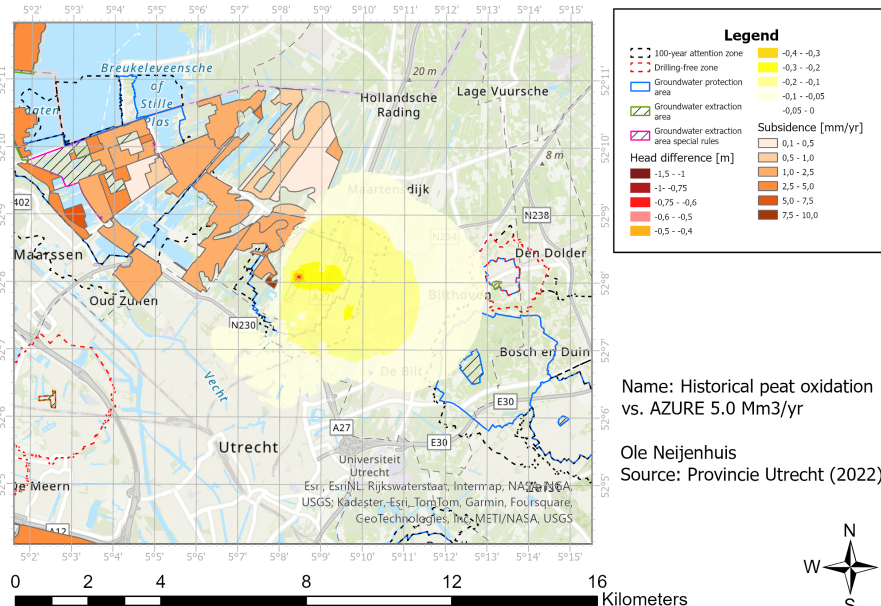


FIGURE E.7: Historical peat oxidation around Groenekan extraction vs. AZURE 5.0 Mm³/yr in L1 (phreatic) (Provincie Utrecht, 2022b).

Figure E.7 clearly shows no real overlap with the historical peat oxidation and the AZURE model results for 5.0 Mm³/yr in L1 (phreatic layer). This may indicate that Groenekan extraction did not have a significant influence on historical peat oxidation in the scope area.

F.1. AZURE Packages & Layers

TABLE F.1: Active packages for each layer in the AZURE model.

Package	Unit	Meaning
BND	-	AZURE model boundaries
CHD	m+NAP	Heads at the model boundaries
SHD	m+NAP	Starting heads
KDW	m ² /day	Transmissivity (kD-values)
VCW	days	Vertical resistance (c-values)
STO	-	Storativity
ANI	-	Anisotropy
RIV	-	Spatial flux for rivers with varying water levels & surface area
WEL	-	Point fluxes of water extractions from groundwater
DRN	-	Drainage or waterways, represents the surface water
OLF	-	Overland flow, only functional if precipitation > infiltration
RCH	-	Recharge (stationary model only)
CAP	-	MetaSWAP capillary zone (non-stationary model only)

TABLE F.2: REGIS II.2 layers linked to formations, soil types, and AZURE model layers (Arcadis, 2019; BRO, 2023b).

REGIS II layer	Formation	Soil type	AZURE model layer
hlc	Holocene deposits	Peat/clay	1
bxz	Boxtel	Sand	1-3
krz	Kreftenheye	Sand	2-4
drz	Drente	Sand	4-6
urz	Urk	Sand	6-7
dtc	Propagated ¹ complex deposits	Sand	7
stz	Sterksel	Sand	7
stk	Sterksel	Clay	8
wak1	Waalre layer 1	Clay	10
pzwaz	Peize & Waalre	Sand	11-14
msk1	Maassluis layer 1	Clay	14
msz2	Maassluis layer 2	Sand	15
msk2	Maassluis layer 2	Clay	15
msz3	Maassluis layer 3	Sand	16
ooc	Oosterhout complex unit	Clay	17
ooz	Oosterhout	Sand	18

¹dtc are the propagated (NL: *gestuwde*) deposits from the Utrechtse Heuvelrug during the Ice Age.

F.2. AZURE Assumptions & Conditions

- The **AZURE** model is first tested in multiple stationary runs to check the resulting heads for 0.0, 5.0, 7.5, and 10.0 Mm³/yr scenarios for Groenekan. Thereafter, four transient runs with a 25x25 m grid resolution were performed to investigate the effects of the extraction over time and space for a model extent that is similar to Figure 3.1;
- **AZURE** model period is from 2004 to 2016. **KNMI** precipitation and evaporation data are used for the same period. **AZURE** includes three years of warm-up time, so 2007-2016 = 10 years model run time. The system needs this time to warm-up before results become reliable (Arcadis, 2019);
- The resistances of the Waalre and Sterksel clays are modelled in **AZURE** with **DINOloket** data in Figures 3.4 and A.8 respectively;
- Effects on the groundwater level and head are determined with an accuracy of 5 cm. Effects smaller than 5 cm fall within the measurement and calculation uncertainty and are considered insignificant. Effects smaller than 5 cm are therefore not presented to avoid creating a sense of "false accuracy".

F.3. AZURE Result Tables

TABLE F.3: AZURE groundwater level and head lowerings [m] (drawdown cones) in the phreatic aquifer (Holocene) and second aquifer (Waalre) for six westward distances to Groenekan and three different extraction scenarios.

Aquifer	Groenekan			Groenekan + 100 m			Groenekan + 500 m		
	5.0 vs 0	7.5 vs 0	10.0 vs 0	5.0 vs 0	7.5 vs 0	10.0 vs 0	5.0 vs 0	7.5 vs 0	10.0 vs 0
Holocene	-0.33	-0.47	-0.60	-0.22	-0.32	-0.42	-0.08	-0.10	-0.12
Waalre	-1.44	-2.17	-2.88	-1.10	-1.65	-1.98	-0.70	-1.06	-1.32

Aquifer	Groenekan + 1,000 m			Groenekan + 2,500 m			Groenekan + 5,000 m		
	5.0 vs 0	7.5 vs 0	10.0 vs 0	5.0 vs 0	7.5 vs 0	10.0 vs 0	5.0 vs 0	7.5 vs 0	10.0 vs 0
Holocene	0.00	0.00	0.00	0.00	0.00	0.00	0.00	0.00	0.00
Waalre	-0.35	-0.60	-1.10	-0.13	-0.20	-0.24	-0.05	-0.06	-0.08

TABLE F.4: AZURE groundwater level and head lowerings [m] (drawdown cones) in the phreatic aquifer (Holocene) and second aquifer (Waalre) for six eastward distances to Groenekan and three different extraction scenarios.

Aquifer	Groenekan			Groenekan + 100 m			Groenekan + 500 m		
	5.0 vs 0	7.5 vs 0	10.0 vs 0	5.0 vs 0	7.5 vs 0	10.0 vs 0	5.0 vs 0	7.5 vs 0	10.0 vs 0
Holocene	-0.33	-0.47	-0.60	-0.20	-0.32	-0.42	-0.19	-0.30	-0.34
Waalre	-1.44	-2.17	-2.88	-1.10	-1.65	-1.98	-0.70	-1.06	-1.32

Aquifer	Groenekan + 1,000 m			Groenekan + 2,500 m			Groenekan + 5,000 m		
	5.0 vs 0	7.5 vs 0	10.0 vs 0	5.0 vs 0	7.5 vs 0	10.0 vs 0	5.0 vs 0	7.5 vs 0	10.0 vs 0
Holocene	-0.13	-0.20	-0.22	-0.05	-0.06	-0.08	-0.02	-0.03	-0.04
Waalre	-0.35	-0.60	-1.10	-0.13	-0.20	-0.24	-0.05	-0.06	-0.08

F.4. AZURE Maps

This Appendix shows the created maps in [AZURE](#) and processed in [GIS](#).

Influence Areas of 7.5 and 10.0 vs. 0.0 Mm³/yr Extraction Discharges

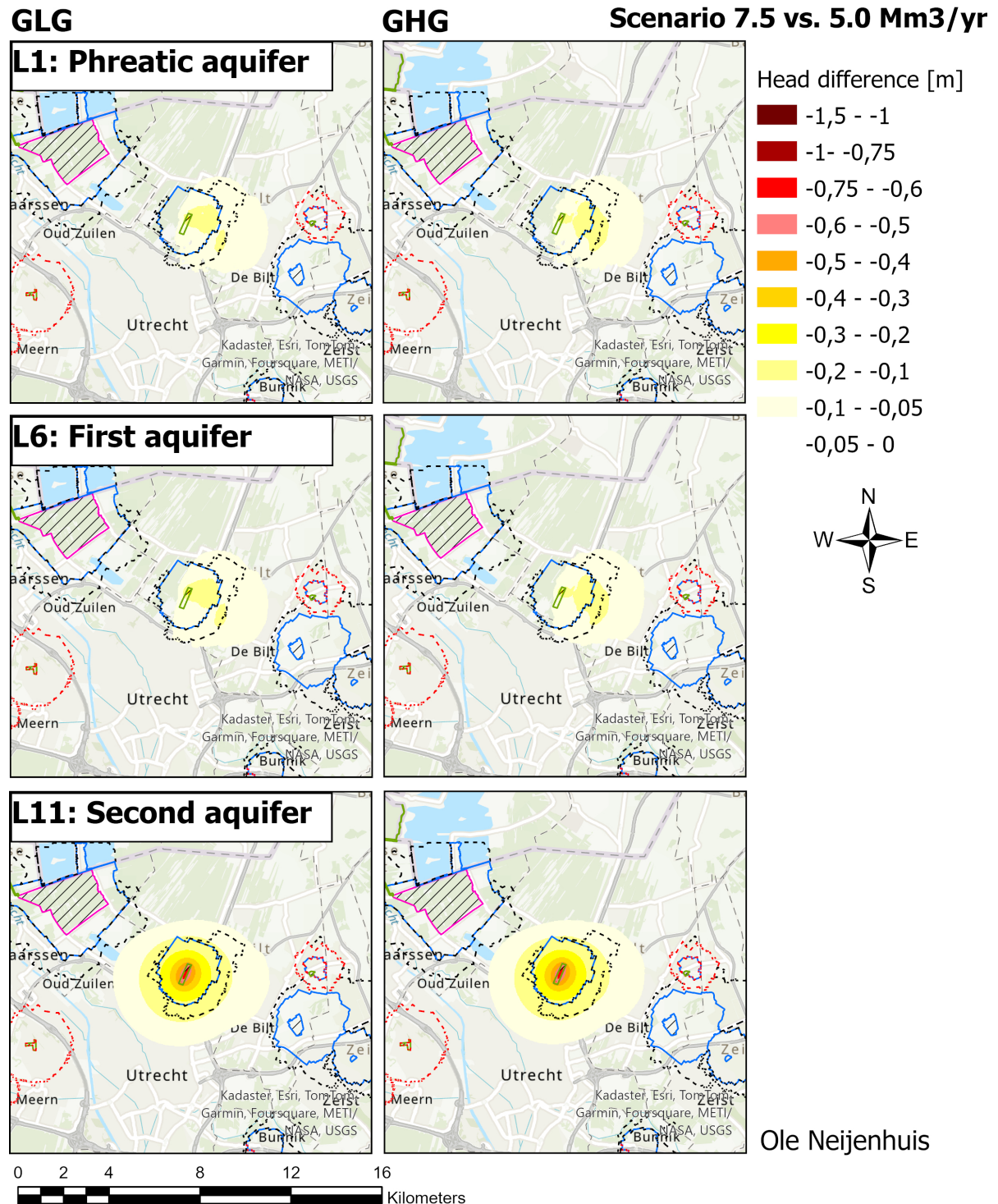


FIGURE F.1: 7.5 vs. 5.0 Mm³/yr extraction: Differences in head for the GLG & GHG in AZURE model layers 1, 6, and 11.

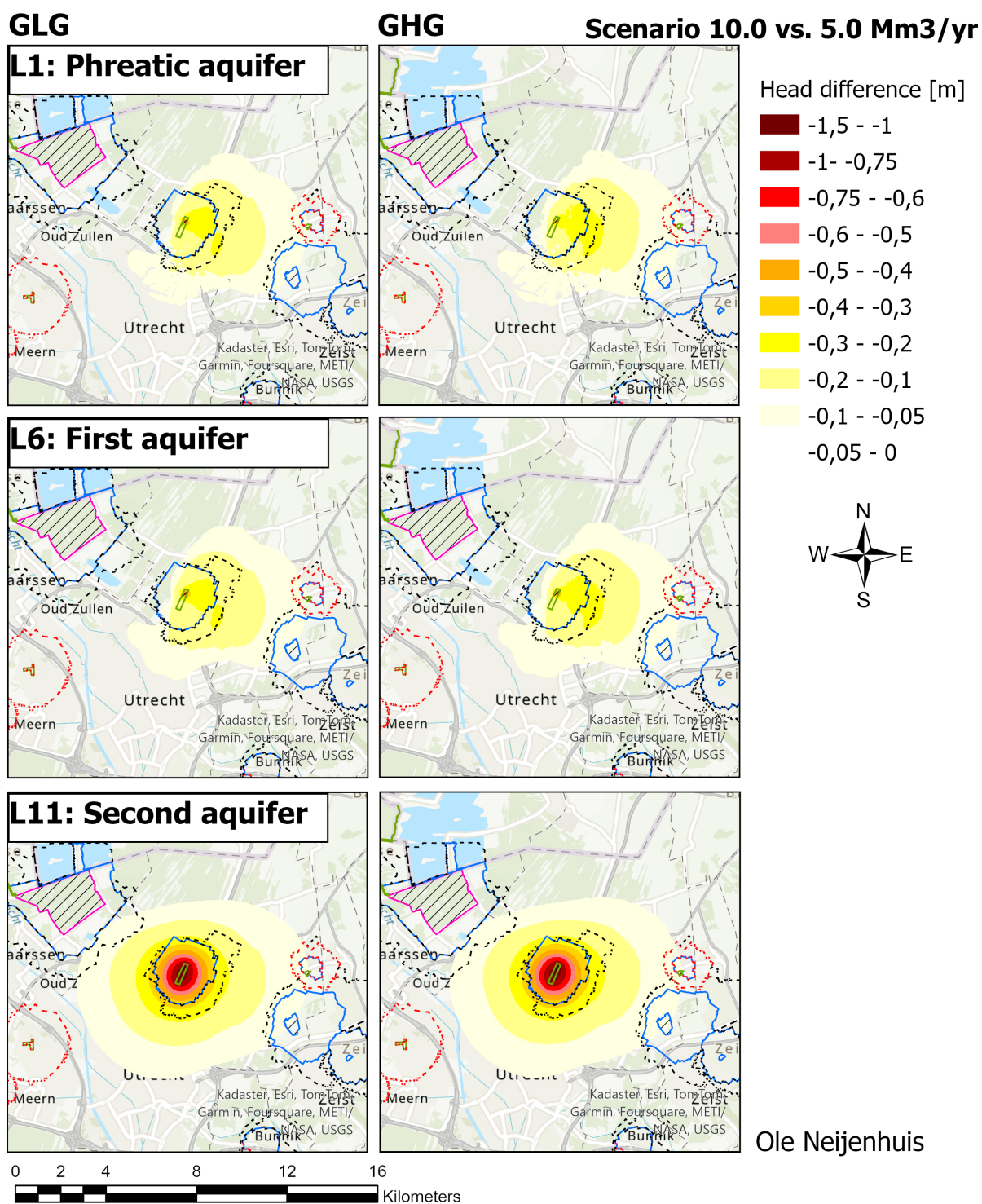


FIGURE F.2: 10.0 vs. 5.0 Mm³/yr extraction: Differences in head for the GLG & GHG in AZURE model layers 1, 6, and 11.

BDOM & Shrinkage

G.1. BDOM & Shrinkage Parameterisation & Assumptions

- Similarly to Section 4.4, surface level is at 0 m **NAP** and similar Holocene dimensions to the west and east of Groenekan are assumed;
- Timescales of 1961 to 2023 and 1961 to 2100 are used;
- Either a clean peat (**BDOM**), clean clay, or organic clay (shrinkage) top layer is assumed;
- Groundwater level lowerings from **AZURE** are used to calculate the additional exposed Holocene compared to the original groundwater level of -0.50 m **NAP** (Table F.3 for west Groenekan and Table F.4 for east Groenekan);
- Crucially west of Groenekan, the effect of the extraction on the phreatic groundwater level fades to zero at 1,000 from Groenekan. Also, it is observed that to the east of Groenekan, the Holocene layer gradually decreases to zero thickness at 1,000m from Groenekan.

G.2. BDOM & Shrinkage Result Tables

TABLE G.1: Aerobic BDOM of clean peat results west (W) and (E) of Groenekan (GK) for periods 1961 to 2023 and 1961 to 2100.

Period	Distance to GK [m]	Exposed Holocene [cm]		Total BDOM [cm]		BDOM rate [cm/10yrs]	
1961-2023	0	33.0		-16.02		-2.584	
1961-2023	100	20.0 (W)	22.0 (E)	-9.71 (W)	-10.68 (E)	-1.566 (W)	-1.723 (E)
1961-2023	500	8.0 (W)	5.0 (E)	-3.88 (W)	-2.43 (E)	-0.626 (W)	-0.392 (E)
1961-2023	>1,000	0.0		0.0		0.0	
1961-2100	0	33.0		-24.60		-1.770	
1961-2100	100	20.0 (W)	22.0 (E)	-14.91 (W)	-16.40 (E)	-1.072 (W)	-1.180 (E)
1961-2100	500	8.0 (W)	5.0 (E)	-5.96 (W)	-3.73 (E)	-0.429 (W)	-0.268 (E)
1961-2100	>1,000	0.0		0.0		0.0	

TABLE G.2: Clean clay and organic clay shrinkage results west (W) and (E) of Groenekan (GK) for period 1961 to 2023.

Soil Type	Distance to GK [m]	Exposed Holocene [cm]		Total shrinkage [cm]		Shrinkage rate [cm/10yrs]	
Clean clay	0	33.0		-10.89		-1.756	
Clean clay	100	20.0 (W)	22.0 (E)	-6.60 (W)	-7.26 (E)	-1.065 (W)	-1.171 (E)
Clean clay	500	8.0 (W)	5.0 (E)	-2.64 (W)	-1.65 (E)	-0.426 (W)	-0.266 (E)
Clean clay	>1,000	0.0		0.0		0.0	
Organic clay	0	33.0		-17.52		-2.826	
Organic clay	100	20.0 (W)	22.0 (E)	-10.62 (W)	-11.68 (E)	-1.713 (W)	-1.884 (E)
Organic clay	500	8.0 (W)	5.0 (E)	-4.25 (W)	-2.65 (E)	-0.685 (W)	-0.428 (E)
Organic clay	>1,000	0.0		0.0		0.0	

D-Settlement

H.1. D-Settlement Structure of Western and Eastern Models

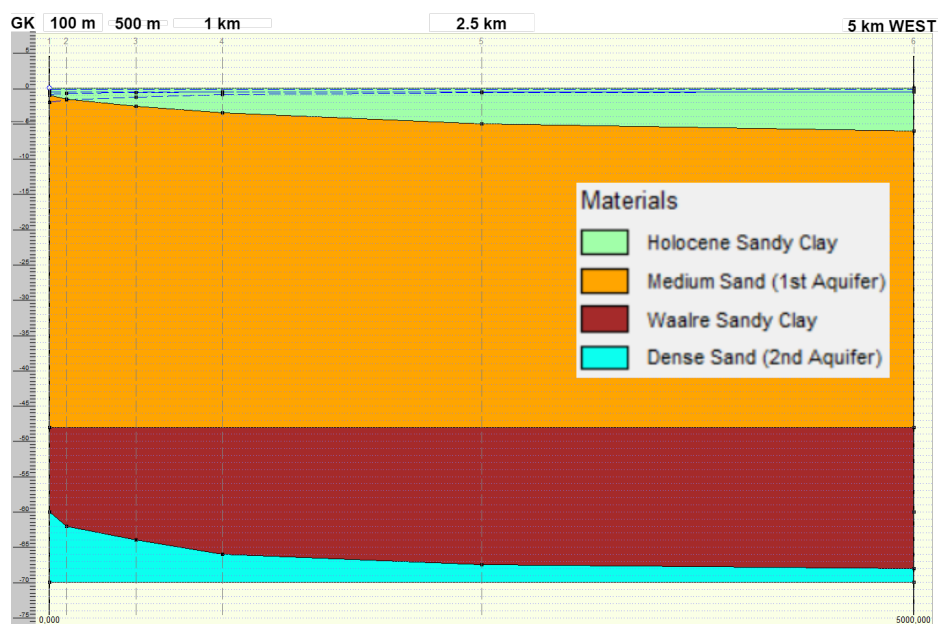


FIGURE H.1: Visualisation of the westward D-Settlement model structure.

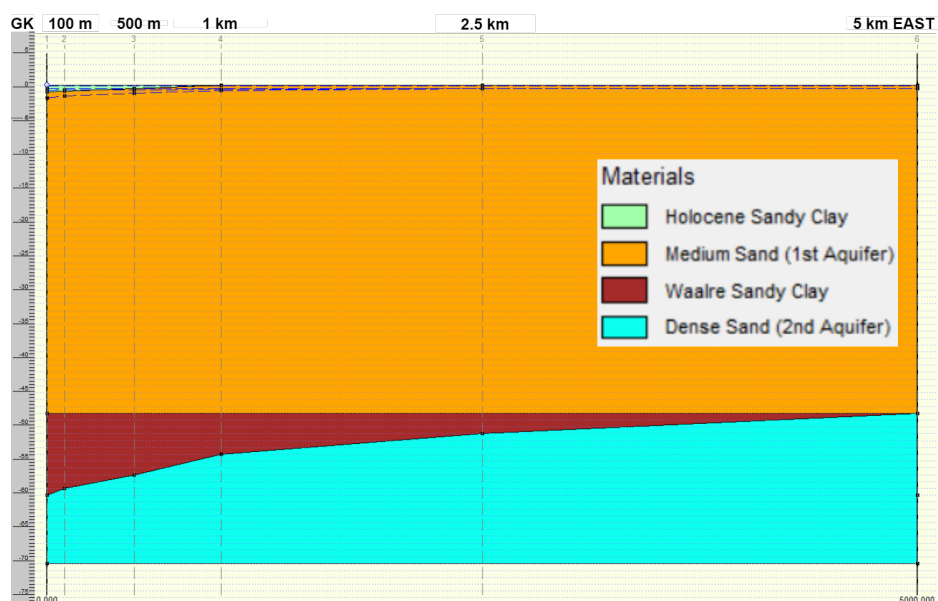


FIGURE H.2: Visualisation of the eastward D-Settlement model structure.

H.2. D-Settlement Layer Parameterisation

TABLE H.1: D-Settlement model parameter values for the four soil layers in base scenario. (U) = undrained, (D) = drained.

Layer	Soil type	Unit weight [kN/m ³]	k_v [m/s]	OCR [-]	RR [-]	CR [-]	C_α [-]
Holocene (U)	Sandy clay	15.0	$5.0e^{10}$	2.16	0.0767	0.2300	0.0092
First aquifer (D)	Medium dense sand	20.0	N/A	1.10	0.0080	0.0023	0.0000
Waalre aquitard (U)	Sandy clay	20.0	$5.0e^{10}$	3.18	0.0110	0.0329	0.0013
Second aquifer (D)	Dense sand	21.0	N/A	N/A	N/A	N/A	N/A

Parameterisation Holocene Top Layer

- Thickness $D_{Holocene}$ is assumed to be 1 metre (Figure 3.3);
- Holocene formation originates from the early Middle Stone Age (Mesolithic, ca. 8800 BC-present). An equivalent age t_{age} of 1,000 years old is assumed, which results in a t_{age} of 365,000 days (Ten Bosch, 2020; TNO, 2023a);
- Top layer is undrained in D-Settlement, which means the water is unable to flow out of the system quickly via ditches or deeper laterally;
- Two independent CPTs show cone resistances q_c (NL: *Conusweerstand*) of 0.1 to 0.7 MPa at 0 to -3 m NAP. The tests were executed at locations Wittevrouwen and Haarrijnseplas in Utrecht, 3.0 km south and 8.5 km west from Groenekan respectively (Figure A.7);
- Five potential Holocene soil types (NEN, 2017):
 1. Soft, clean peat (NL: *slap, schoon veen*);
 2. Organic clay (NL: *organische klei*);
 3. Soft, clean clay (NL: *slappe, schone klei*);
 4. Soft, weakly sandy clay (NL: *slappe, zwak zandige klei*);
 5. Medium dense, clean sand (NL: *matig vast, schoon zand*).

Values of the NEN-Bjerrum isotach parameters of the possible Holocene soil types are listed in Table H.2.

TABLE H.2: Holocene top layer NEN-Bjerrum isotach parameter values for clay soil types (NEN, 2017).

Soil type	Consistency	Cone resistance q_c [MPa]	RR [-]	CR [-]	C_α [-]	k_v [m/d]
Peat: clean	Soft	0.1	0.1533	0.4600	0.0230	$1.8 \cdot 10^{-4}$
Clay: organic	Soft	0.2	0.1022	0.3067	0.0153	$1.8 \cdot 10^{-4}$
Clay: clean	Soft	0.5	0.1095	0.3286	0.0131	$1.8 \cdot 10^{-6}$
Clay: weakly sandy	Soft	0.7	0.0767	0.2300	0.0092	$1.8 \cdot 10^{-6}$
Sand: clean	Medium dense	15.0	0.0013	0.0038	0.0000	$1.8 \cdot 10^{-2}$

Equation H.1 gives an example in determining the OCR for weakly sandy clay by rewriting Equation 2.17 and filling in the NEN-Bjerrum isotach parameters from Table H.2:

$$\text{OCR}^{\left(\frac{\text{CR}-\text{RR}}{C_\alpha}\right)} = \frac{t_{age}}{\tau_0} \Rightarrow \text{OCR}^{\left(\frac{0.2300-0.0767}{0.0092}\right)} = \frac{365,000}{1} \Rightarrow \text{OCR} = \sqrt[16.66]{365,000} \approx 2.16 \quad (\text{H.1})$$

The OCRs of the clean peat, organic clay, clean clay, and clean sand soil types are 2.61, 2.61, 2.16, and 1.12 respectively.

Parameterisation Waalre Clay

- Thickness D_{Waalre} is assumed to be 12 metres (Figure 3.2);
- Waalre clay is assumed to be an early Pleistocene (Menapian) formation and with an equivalent age t_{age} of 1,000,000 years old, which results in a t_{age} of 365,000,000 days (TNO, 2023a);
- Waalre clay is undrained in D-Settlement. This means the water is unable to flow out of the system instantly;

- The same CPTs give cone resistances q_c of 2.5 to 3.0 MPa at -48 to -60 m NAP (Figure A.7);
- Either a soil type of solid, weakly sandy loam (NL: *vaste, zwak zandige leem*) or solid, weakly sandy clay (NL: *vaste, zwak zandige klei*) (NEN, 2017).

Values of the NEN-Bjerrum isotach parameters of the possible Waalre aquitard soil type are listed in Table H.3.

TABLE H.3: Waalre aquitard NEN-Bjerrum isotach parameter values for loam and clay soil types (NEN, 2017).

Soil type	Consistency	Cone resistance q_c [MPa]	RR [-]	CR [-]	C_α [-]	k_v [m/d]
Loam: weakly sandy	Solid	3.0	0.0077	0.0230	0.0009	0.004
Clay: weakly sandy	Solid	2.5	0.0153	0.0460	0.0018	0.004

Following, the OCR can be determined by rewriting Equation 2.17 and filling in the NEN-Bjerrum isotach parameters from Table H.3:

$$\text{OCR}^{\left(\frac{\text{CR}-\text{RR}}{C_\alpha}\right)} = \frac{t_{\text{age}}}{\tau_0} \Rightarrow \text{OCR}^{\left(\frac{0.0230-0.0077}{0.0009}\right)} = \frac{365,000,000}{1} \Rightarrow \text{OCR} = \sqrt[17.06]{365,000,000} \approx 3.18 \quad (\text{H.2})$$

Note: Since the clay parameters are twice the value of the loam parameters, the OCR result is 3.18 for both weakly sandy clay and loam. The higher the OCR, the more stress is necessary to reach the pre-consolidation stress σ'_p and let the concerning soil "collapse" and reach the plastic strain regime (Figure 2.11). Thus, a high OCR generally results in a smaller amount of subsidence, since the σ'_p is never reached and only the recompression (RR) and creep (C_α) isotach parameters influence the subsidence rate.

H

H.3. D-Settlement Base Scenario Assumptions & Conditions

In Visschedijk et al. (2009), it is stated that the D-Settlement package includes a number of key assumptions and simplifications that address aspects of scale:

- 1 metre of head drop equals 9.81 kPa of pressure loss (Crombaghs et al., 2002);
- Initial intrinsic time τ_0 is assumed to be 1 day;
- Influences of horizontal components of stress and strain are neglected;
- (Vertical) effective stress is determined from pore pressure and the vertical component of geostatic stress;
- Effective stress σ' is taken in the middle of each model layer.

Experiments

Assumptions and decisions made for the base scenario D-Settlement experiments are listed here:

- Original groundwater level in the phreatic aquifer (Holocene) and the hydraulic head in the Waalre clay are assumed to be -0.5 and -0.1 m NAP respectively. These values are taken from Geologische Dienst Nederland (2023) (Figure A.4) and the 0.0 Mm³/yr scenario AZURE output respectively;
- Model period is from 1961 to 2023 (62 years or ~23,000 days) with a maximum distance r of 5,000 m to the extraction, resulting in a 2D-calculation. The value of r is chosen based on the AZURE output, where the influence circle of the groundwater lowering is negligible beyond 5,000 metres;
- Both the Holocene and Waalre layers are assumed to be sandy clay, since this is the most common soil type around Groenekan (TNO, 2023a). Tables H.2 and H.3 give the respective NEN-Bjerrum parameters which are used in the D-Settlement model;
- The AZURE GLGs for the phreatic and second aquifer are used (Tables F.3 and F.4).

Assumptions & Conditions Future Scenarios in D-Settlement

Assumptions and decisions made for the [D-Settlement](#) future scenario experiments are listed here:

- The base scenario [D-Settlement](#) model structure from Section 4.4 is used;
- Tables [F.3](#) and [F.4](#) list the groundwater level and head lowerings over western and eastern distance from Groenekan for extraction scenarios 5.0, 7.5, and 10.0 Mm³/yr;
- Model period is from 1961 to 2100. 139 years (app. 50,000 days) is taken as total time frame;
- Real extraction discharge (Figure 3.6) is used for the period 1961 to 2023 and is then exchanged for one of the eight future scenarios for the period 2023 to 2100;
- Settlement in the Holocene top layer and Waalre aquitard is calculated at Groenekan.

H.4. Consolidation & Creep in Holocene and Waalre Result Tables

In the tables below, all underlying settlement (denoted as S) results from Section 5.4 graphs are given.

Base Scenario

TABLE H.4: Settlement (S) results: Base scenario over western distance to Groenekan (GK) in period 1961 to 2023.

Scenario	S Holocene [cm]	S Waalre [cm]	Total S [cm]	S rate [cm/10yrs]
Groenekan (GK)	~ 0.6	~ 0.2	0.790	0.127
GK + 100 m	~ 0.6	~ 0.4	1.021	0.165
GK + 500 m	~ 0.5	~ 0.1	0.633	0.102
GK + 1,000 m	~ 0.0	~ 0.1	0.135	0.022
GK + 2,500 m	~ 0.1	~ 0.1	0.155	0.025
GK + 5,000 m	~ 0.1	~ 0.1	0.170	0.027

TABLE H.5: Settlement (S) results: Base scenario over eastern distance to Groenekan (GK) in period 1961 to 2023.

Scenario	S Holocene [cm]	S Waalre [cm]	Total S [cm]	S rate [cm/10yrs]
Groenekan (GK)	~ 0.6	~ 0.2	0.790	0.127
GK + 100 m	~ 0.4	~ 0.1	0.467	0.075
GK + 500 m	~ 0.0	~ 0.1	0.094	0.015
GK + 1,000 m	~ 0.0	~ 0.04	0.044	0.007
GK + 2,500 m	~ 0.0	~ 0.02	0.016	0.003
GK + 5,000 m	~ 0.0	~ 0.01	0.006	0.001

Sensitivity Analyses

Groundwater Level and Head Lowerings

TABLE H.6: Settlement (S) results of sensitivity analysis: Groundwater level (GWL) and head lowerings at Groenekan in period 1961 to 2023. Base scenario highlighted in cyan and a settlement difference (ΔS) in percentages is given.

GWL & head lowering	S Holocene [cm]	S Waalre [cm]	Total S [cm]	ΔS [%]	S rate [cm/10yrs]
0 m GWL & 0 m head	0.0	0.0	0.000	-100.00	0.000
-0.17m GWL & -0.5m head	~ 0.3	~ 0.1	0.439	-44.18	0.071
-0.17m GWL & -1.5m head	~ 0.4	~ 0.1	0.492	-37.47	0.079
-0.17m GWL & -2.5m head	~ 0.3	~ 0.2	0.544	-31.14	0.088
-0.33m GWL & -0.5m head	~ 0.6	~ 0.1	0.741	-6.20	0.120
-0.33m GWL & -1.5m head	~ 0.6	~ 0.2	0.790		0.127
-0.33m GWL & -2.5m head	~ 0.6	~ 0.2	0.845	+6.96	0.136
-0.50m GWL & -0.5m head	~ 0.8	~ 0.1	0.881	+11.52	0.142
-0.50m GWL & -1.5m head	~ 0.8	~ 0.1	0.934	+18.23	0.151
-0.50m GWL & -2.5m head	~ 0.8	~ 0.2	0.986	+24.81	0.159

Thickness of Holocene and Waalre Layers

TABLE H.7: Settlement (S) results of sensitivity analysis: Holocene (H) and Waalre (W) layer thicknesses at Groenekan in period 1961 to 2023. Base scenario highlighted in cyan and a settlement difference (ΔS) in percentages is given.

Layer thicknesses	S Holocene [cm]	S Waalre [cm]	Total S [cm]	ΔS [%]	S rate [cm/10yrs]
0 m H & 0 m W	0.0	0.0	0.000	-100.00	0.000
0.5 m H & 6 m W	0.0	~ 0.1	0.130	-83.54	0.021
0.5 m H & 12 m W	0.0	~ 0.2	0.176	-77.72	0.028
1 m H & 6 m W	~ 0.6	~ 0.1	0.744	-5.82	0.120
1 m H & 12 m W	~ 0.6	~ 0.2	0.790		0.127
1 m H & 24 m W	~ 0.6	~ 0.3	0.870	+10.13	0.140
2 m H & 12 m W	~ 1.8	~ 0.2	2.054	+159.75	0.331
2 m H & 24 m W	~ 1.8	~ 0.3	2.132	+170.13	0.344

Soil Type of Holocene Top Layer

TABLE H.8: Settlement (S) results of sensitivity analysis: Five different Holocene soil types at Groenekan in period 1961 to 2023. The Holocene settlement excludes 0.16 cm of Waalre settlement. Base scenario highlighted in cyan and a settlement difference (ΔS) in percentages is given.

Soil type	Unit weight [kN/m ³]	S Holocene [cm]	ΔS [%]	S rate [cm/10yrs]
Medium dense sand	20.0	0.000	-100.00	0.000
Sandy clay	15.0	0.630		0.102
Organic clay	13.0	0.984	+56.19	0.159
Clean clay	14.0	1.016	+61.27	0.164
Clean peat	11.0	1.977	+213.81	0.319

H

Future Scenarios

Table H.9 displays the settlement results of the eight future scenarios from Section 4.5.

TABLE H.9: Settlement (S) results: Eight future scenarios at Groenekan (GK) in period 1961 to 2100. Base scenario is highlighted in cyan as a reference and a settlement difference (ΔS) in percentages is given.

Future scenario	S Holocene [cm]	S Waalre [cm]	Total S [cm]	ΔS [%]	S rate [cm/10yrs]
0.0 Mm ³ /yr + LW	~ 0.3	~ 0.1	0.367	-59.69	0.026
0.0 Mm ³ /yr + HD	~ 0.5	~ 0.2	0.654	-28.23	0.047
Base scenario GK	~ 0.7	~ 0.2	0.911		0.066
5.0 Mm ³ /yr + LW	~ 0.5	~ 0.2	0.943	+3.51	0.068
5.0 Mm ³ /yr + HD	~ 0.5	~ 0.2	1.040	+14.15	0.075
7.5 Mm ³ /yr + LW	~ 0.7	~ 0.3	1.070	+17.47	0.077
7.5 Mm ³ /yr + HD	~ 0.8	~ 0.3	1.113	+22.20	0.080
10.0 Mm ³ /yr + LW	~ 0.8	~ 0.3	1.139	+24.98	0.082
10.0 Mm ³ /yr + HD	~ 0.9	~ 0.3	1.182	+29.87	0.085

Python Scripts

I.1. Analytical Groundwater Flow Calculations: Glee & Hantush

The following Python code is used for calculating and plotting Equations 2.1 and 2.3 for Groenekan:

```

1 from pylab import *
2 from scipy import *
3 from scipy import special
4 from scipy.special import kn as BesselK
5
6 from math import sqrt as sqrt
7 from math import cosh as cosh
8 from math import log as ln # in python: log(x)=Ln(x)
9 import matplotlib.ticker as ticker
10 %matplotlib qt
11
12 def DeGlee(r,Q0,kD,c):
13     labda = sqrt(kD*c)
14     s = Q0/(2*pi*kD)*BesselK(0,r/labda)
15     q = Q0*r/labda*BesselK(1,r/labda)
16     return s,q,labda
17
18 def Hantush(r,t,Q0,kD,c,S):
19     labda = sqrt(kD*c)
20     rho = r/labda
21     tau = ln(2*labda/r*t/(c*S))
22     F = func_F(rho,tau)
23     s = Q0/(4*pi*kD)*F
24     return s
25
26 def ExpInt(n,u):
27
28     # n wordt niet gebruikt
29
30     # Fast approximation for Wu according to equation 7a and 7b from Srivastava(1998)
31     gamma = 0.5772 # Euler-Macheroni constant
32
33     # Wu for u<1
34     u0 = where(u<1.0,u,1) # u=1 is just a dummy to make ln() work on all values
35     Wu0 = log(exp(-gamma)/u0) + 0.9653*u - 0.1690*u**2
36
37     #Wu for u>=1
38     u1 = where(u>=1.0,u,1) # u=1 is just a dummy to make ln() work on all values
39     Wu1 = 1/(u1*exp(u1))*(u1+0.3575)/(u1+1.280)
40
41     # combine Wu0 and Wu1
42     Wu = where(u<1.0,Wu0,Wu1)
43     return Wu
44
45 def func_F(rho,tau):
46 # func_F is a fast approximation of Hantush well function W
47
48     # Calculate parameter w
49     w = (ExpInt(1,rho)-BesselK(0,rho))/(ExpInt(1,rho)-ExpInt(1,rho/2))
50
51     # Calculate F(rho,tau)
52     if tau <= 0:
53         F = w*ExpInt(1,rho/2*e**(-tau))-(w-1)*ExpInt(1,rho*cosh(tau))
54     else:
55         F = 2*BesselK(0,rho) - w*ExpInt(1,rho/2*e**tau) + (w-1)*ExpInt(1,rho*cosh(tau))

```

```

56
57     # return calculated value of F(rho,tau)
58     return F
59
60 def plot_s(r,t,s_stat,s):
61
62     # Define colors
63     orange = '#FF9900'
64     blue   = '#2F64B2'
65
66     # Create plots
67     graph = subplot(111)
68
69     # Set ticklines
70     xticklines = graph.get_xticklines()
71     yticklines = graph.get_yticklines()
72
73     for line in xticklines+yticklines:
74         line.set_linewidth(3)
75
76     for line in xticklines:
77         line.set_visible(False)
78
79     # Set gridlines
80     gridlines = graph.get_xgridlines()
81     gridlines.extend( graph.get_ygridlines() )
82     for line in gridlines:
83         line.set_linestyle('-')
84     grid(True)
85
86     # Set ticklabels
87     xticklabels = graph.get_xticklabels()
88     yticklabels = graph.get_yticklabels()
89
90     for label in xticklabels+yticklabels:
91         label.set_color('k')
92         label.set_fontsize('medium')
93         label.set_visible(True)
94
95     # Create annotation
96     ylabel('Groundwater lowering [m]')
97     xlabel('Distance to well [m]')
98
99     # Plot lowering in time (Hantush)
100    for ti in range(len(t)):
101        si = s[ti,:]
102        graph.plot(r, -si, color=blue, lw=1.0)
103
104    # Plot stationary lowering s_stat (De Glee)
105    graph.plot(r, -s_stat, color=orange, lw=2.0)
106
107    # Set axes limits
108    # If you see a plot without lines, delete or comment next line:
109    graph.set_ylim(-10, 0)
110
111    # Filename
112    filename = "Hantush_GK.png"
113
114    # Save figure to file
115    fig = figure(1)
116    mydpi = 100.0
117    fig.set_dpi(mydpi)
118    fig.set_size_inches(6.0,4.0)
119    fig.savefig(filename,dpi=mydpi, facecolor='w', edgecolor='w')
120
121    # Show the plot on screen
122    show()
123
124    if __name__ == '__main__': #XXXXXXX 5.0 Mm3/yr extraction
125
126    r = arange(0.1, 5000.0, 0.1) # r is a numpy array

```

```

127     day = 365.0
128     t = array([10.0 / day, 60 / day, 180 / day, 1, 2])
129     Q0 = 5000000.0 / 365.0 # 5.0 Mm3/yr
130     k = 50 # m/d
131     D = 80 # m
132     kD = k * D # m2/d
133     c = 2500.0 # days
134     S = 0.001
135
136
137     # Calculate stationary lowering (De Glee)
138     s_stat, q_stat, labda = DeGlee(r, Q0, kD, c)
139
140     # Calculate lowering in time (Hantush)
141     print("Calculation Hantush well function started...")
142     s = zeros((len(t), len(r)))
143     for ti in range(len(t)):
144         for ri in range(len(r)):
145             s[ti, ri] = Hantush(r[ri], t[ti], Q0, kD, c, S)
146     print("Calculation Hantush well function finished...")
147
148     # Define labels for each curve in the plot
149     labels = ["10_days", "60_days", "180_days", "1_year", "2_years"]
150
151     # Plot lowering of groundwater and add a legend
152     import matplotlib.pyplot as plt
153
154     plt.figure(figsize=(10, 6))
155
156     # Reverse the order for drawdown cone and plot
157     for i in range(len(t)):
158         plt.plot(r[::-1], s[i, ::-1], label=labels[i])
159     plt.plot(r[::-1], s_stat[::-1], label="Stationary lowering (De Glee)", color='blue',
160             linewidth=1)
161
162     # # Format y-axis labels with one decimal place
163     # y_formatter = matplotlib.ticker.ScalarFormatter(useOffset=False, format="%1.1f")
164     # plt.gca().yaxis.set_major_formatter(y_formatter)
165
166     plt.xlabel("Distance to well [m]")
167     plt.ylabel("Groundwater level lowering [m]")
168     # plt.title("Lowering of Groundwater")
169     plt.legend()
170     plt.grid(True)
171     plt.gca().invert_yaxis() # Invert y-axis to display drawdown
172     plt.gca().yaxis.set_major_formatter(ticker.FormatStrFormatter('%1.1f'))
173
174     # Add extra grid lines (optional, you can keep this or remove)
175     plt.minorticks_on()
176     plt.grid(which='both', linestyle='--', linewidth=0.5, color='gray')
177     plt.show()

```

I.2. Aerobic BDOM Calculation

The following Python code from Ten Bosch (2020) is adjusted and used for calculating aerobic BDOM:

```

1 import numpy as np
2 #import temperaturecalculation as tempcalc
3 import matplotlib.pyplot as plt
4 from collections import namedtuple
5 from IPython import get_ipython
6 get_ipython().run_line_magic('matplotlib', 'qt5')
7
8 ### Input parameters
9 startyr = 1961 #startyear
10 years = 62 #nr of years being evaluated, 62 for 2023 and 138 for 2100!
11 dt = 1 #timestep in years
12 htopini = 0 #initial top of surface level
13

```

```

14 waterlevels = np.array([-0.5, -0.7])          #m NAP
15 yearsGWL = np.array([startyr, startyr+years]) #years water level lowerings
16
17 %%% check water level lowerings setup
18
19 if len(waterlevels)==len(yearsGWL):
20     print('water_levels_okay')
21 else:
22     print('error_in_waterlevels')
23
24 %%% set up time discretisation
25
26 t = np.linspace(0, years, int(years/dt)+1)
27 t1 = t + startyr
28
29 timeDis = namedtuple('timeDis', ['startyr', 'years', 't', 'dt'])
30 tDis = timeDis(startyr = startyr,
31                years = years,
32                t = t,
33                dt = dt)
34
35 %%% set up space discretisation
36
37 #work with top level that can change over time and fixed bottom level
38
39 #top level
40 htop = np.zeros(len(t))
41 htop[0] = htopini
42
43 #bottom level = based on thickness embankment, NOTE: introduces uncertainty because ripening
44   field situation is now not represented properly
45 hbot = np.ones(len(t))*-0.2 ## 1m Holocene thickness
46
47 modDim = namedtuple('ModDim', ['htop', 'hbot'])
48 mDim = modDim(htop = htop,
49               hbot = hbot)
50
51 %%% Soil parameters
52
53 V_ox = 0.0123          #paper Fokker    V_ox peat NB estimate
54 lambda_r_ox = 0.090    #paper Fokker    lambda_r_ox peat NB estimate
55
56 soilPar = namedtuple('soilPar', ['lambda_r_ox', 'V_ox'])
57 sPar = soilPar(lambda_r_ox = lambda_r_ox,
58                V_ox = V_ox)
59
60 %%% FOKKER
61 def aerobic_oxidation_fokker(tDis, mDim, sPar):
62     t = tDis.t
63     dt = tDis.dt
64     years = tDis.years
65     # hlayers = mDim.hlayers[:,i]
66     # hlayers0 = mDim.hlayers[:,0]
67     # hwat = mDim.hwat[i]
68     # array2 = mDim.array2
69     V_ox = sPar.V_ox
70     lambda_r_ox = sPar.lambda_r_ox
71     hbot = mDim.hbot
72     htop = mDim.htop
73
74     dh0 = np.zeros(len(t))
75     for i in range(len(t)):
76         dh0[i] = (1-np.exp(-V_ox*dt))*((htop[i]-hbot[i])-lambda_r_ox*(htop[0]-hbot[0]))
77
78         if i == int(years/dt):
79             break
80         else:
81             htop[i+1] = htop[i] - dh0[i]
82
83     d0total = np.sum(dh0)

```

```

84         return htop, d0total
85
86
87 ### CALCULATION
88 fokker_ae_ox = aerobic_oxidation_fokker(tDis, mDim, sPar)[0]*100 # to obtain centimeter
89 total_ae_ox = aerobic_oxidation_fokker(tDis, mDim, sPar)[1]*100
90
91 ### Plot results
92 plt.figure()
93 plt.plot(t+startyr, fokker_ae_ox, label = 'Aerobic_BDOM_Fokker')
94 #plt.title('Subsidence by aerobic oxidation in unsaturated zone, Fokker model')
95 plt.xlabel('Time[years]')
96 plt.ylabel('Aerobic_BDOM[cm]')
97 plt.legend(loc='best')
98
99 print('Aerobic_oxidation_expected_in_total_time_period', years, 'years=', np.round(
100      total_ae_ox, 3), 'cm')
101 print('Annual_aerobic_oxidation_expected', np.round(total_ae_ox/years, 3), 'cm/yr')

```

I.3. Shrinkage Calculation

The following Python code from Ten Bosch (2020) is adjusted and used for calculating shrinkage:

```

1 import numpy as np
2 import matplotlib.pyplot as plt
3 from collections import namedtuple
4 from IPython import get_ipython
5 get_ipython().run_line_magic('matplotlib', 'qt5')
6
7 ### Input parameters
8 startyr = 1961          #startyear
9 years = 62              #nr of years being evaluated
10 dt = 1                  #timestep in years
11 htopini = 0             #initial top of surface level
12
13 waterlevels = np.array([0])      #m NAP
14 yearsGWL = np.array([startyr])  #years water level lowerings
15
16 ### check water level lowerings setup
17
18 if len(waterlevels)==len(yearsGWL):
19     print('water_levels_okay')
20 else:
21     print('error_in_waterlevels')
22
23 ### set up time discretisation
24
25 t = np.linspace(0, years, int(years/dt)+1)
26 t1 = t + startyr
27
28 timeDis = namedtuple('timeDis', ['startyr', 'years', 't', 'dt'])
29 tDis = timeDis(startyr = startyr,
30               years = years,
31               t = t,
32               dt = dt)
33 #top level clay
34 h_top_clay = np.zeros(len(t))
35 h_top_clay[0] = htopini
36
37 #bottom level clay = based on GWL decrease modelled in AZURE
38 hbot_clay = np.ones(len(t))*-0.2 ## 1m Holocene thickness
39
40 modDim_clay = namedtuple('ModDim', ['h_top_clay', 'hbot_clay'])
41 mDim_clay = modDim_clay(h_top_clay = h_top_clay,
42                        hbot_clay = hbot_clay)
43
44 #####
45
46 #top level organic clay
47 h_top_organic_clay = np.zeros(len(t))

```

```

48 h_top_organic_clay[0] = htopini
49
50 #bottom level organic clay = ased on GWL decrease modelled in AZURE
51 hbot_organic_clay = np.ones(len(t))*-0.2 ## 1m Holocene thickness
52
53 modDim_organic_clay = namedtuple('ModDim', ['h_top_organic_clay', 'hbot_organic_clay'])
54 mDim_organic_clay = modDim_organic_clay(h_top_organic_clay = h_top_organic_clay,
55                                         hbot_organic_clay = hbot_organic_clay)
56
57 ### Soil parameters
58 V_sh = [0.270, 0.138]          #paper Fokker    V_sh clay & organic clay NB estimate
59 lambda_r_sh = [0.670,0.469]    #paper Fokker    lambda_r_sh clay & organic clay NB estimate
60
61 soilPar = namedtuple('soilPar', ['lambda_r_sh', 'V_sh'])
62 sPar = soilPar(lambda_r_sh = lambda_r_sh,
63                V_sh = V_sh)
64
65 ### Clay Shrinkage Fokker
66 def ShrFokkerClay(tDis, mDim, sPar):
67     t = tDis.t
68     dt = tDis.dt
69     years = tDis.years
70     lambda_r_sh = sPar.lambda_r_sh
71     V_sh = sPar.V_sh
72     hbot_clay = mDim_clay.hbot_clay
73     htop_clay = mDim_clay.h_top_clay
74
75     dhS_clay = np.zeros(len(t))
76
77     for i in range(len(t)):
78         dhS_clay[i] = (1-np.exp(-V_sh[0]*dt))*((h_top_clay[i]-hbot_clay[i])-lambda_r_sh[0]*(
79             h_top_clay[0]-hbot_clay[0]))
80
81         if i == int(years/dt):
82             break
83         else:
84             h_top_clay[i+1] = h_top_clay[i] - dhS_clay[i]
85
86     dS_clay_total = np.sum(dhS_clay)
87
88     return htop_clay, dS_clay_total
89
90 ### CALCULATION
91 fokkershrink_clay = ShrFokkerClay(tDis, mDim_clay, sPar)[0]*100
92 totalshrink_clay = ShrFokkerClay(tDis, mDim_clay, sPar)[1]*100
93
94 ### Organic Clay Shrinkage Fokker
95 def ShrFokkerOrganicClay(tDis, mDim, sPar):
96     t = tDis.t
97     dt = tDis.dt
98     years = tDis.years
99     lambda_r_sh = sPar.lambda_r_sh
100     V_sh = sPar.V_sh
101     hbot_organic_clay = mDim_organic_clay.hbot_organic_clay
102     htop_organic_clay = mDim_organic_clay.h_top_organic_clay
103
104     dhS_organic_clay = np.zeros(len(t))
105
106     for i in range(len(t)):
107         dhS_organic_clay[i] = (1-np.exp(-V_sh[1]*dt))*((h_top_organic_clay[i]-
108             hbot_organic_clay[i])-lambda_r_sh[1]*(h_top_organic_clay[0]-hbot_organic_clay[0])
109         )
110
111         if i == int(years/dt):
112             break
113         else:
114             h_top_organic_clay[i+1] = h_top_organic_clay[i] - dhS_organic_clay[i]
115
116     dhS_organic_clay_total = np.sum(dhS_organic_clay)
117
118     return htop_organic_clay, dhS_organic_clay_total

```

```
116
117 %% CALCULATION
118 fokkersshrink_organic_clay = ShrFokkerOrganicClay(tDis, mDim_organic_clay, sPar)[0]*100
119 totalshrink_organic_clay = ShrFokkerOrganicClay(tDis, mDim_organic_clay, sPar)[1]*100
120
121 %% Plot results
122 plt.figure() # Create a figure
123 # Plot for clay shrinkage with orange line and solid style
124 plt.plot(t+startyr, fokkersshrink_clay, label='Clay_Shrinkage_Fokker', color='orange')
125 # Plot for organic clay shrinkage with blue line
126 plt.plot(t+startyr, fokkersshrink_organic_clay, label='Organic_Clay_Shrinkage_Fokker')
127
128 plt.xlabel('Time[years]')
129 plt.ylabel('Shrinkage[cm]')
130 plt.legend(loc='best')
131 plt.show
```

